



Advanced gaseous detectors for heavy-ion experiments and ALICE 3

Saikat Biswas

Bose Institute

e-mail: saikat@jcbosc.ac.in

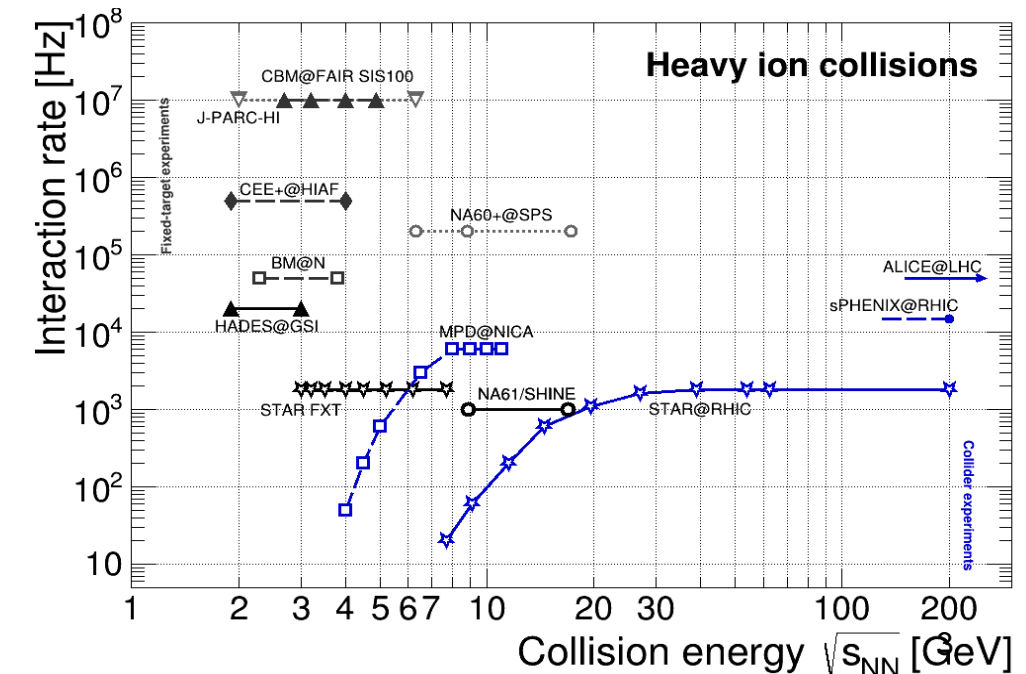
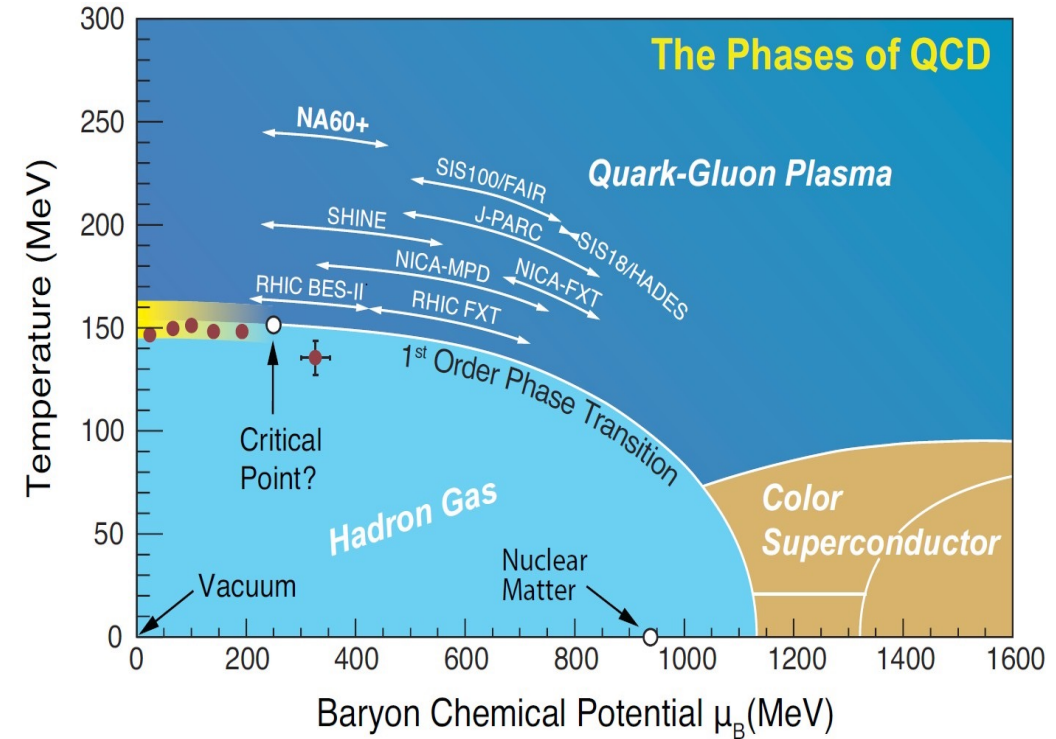
Vth ALICE-STAR India school on Quark-Gluon plasma
01-12 November 2022, Institute of Physics (IOP) Bhubaneswar

Outline

- Present and upcoming heavy-ion experiments
- Physics motivation
- Gaseous detectors for heavy-ion experiments and their characterization
- New development
- ALICE3 - Possible contribution from India

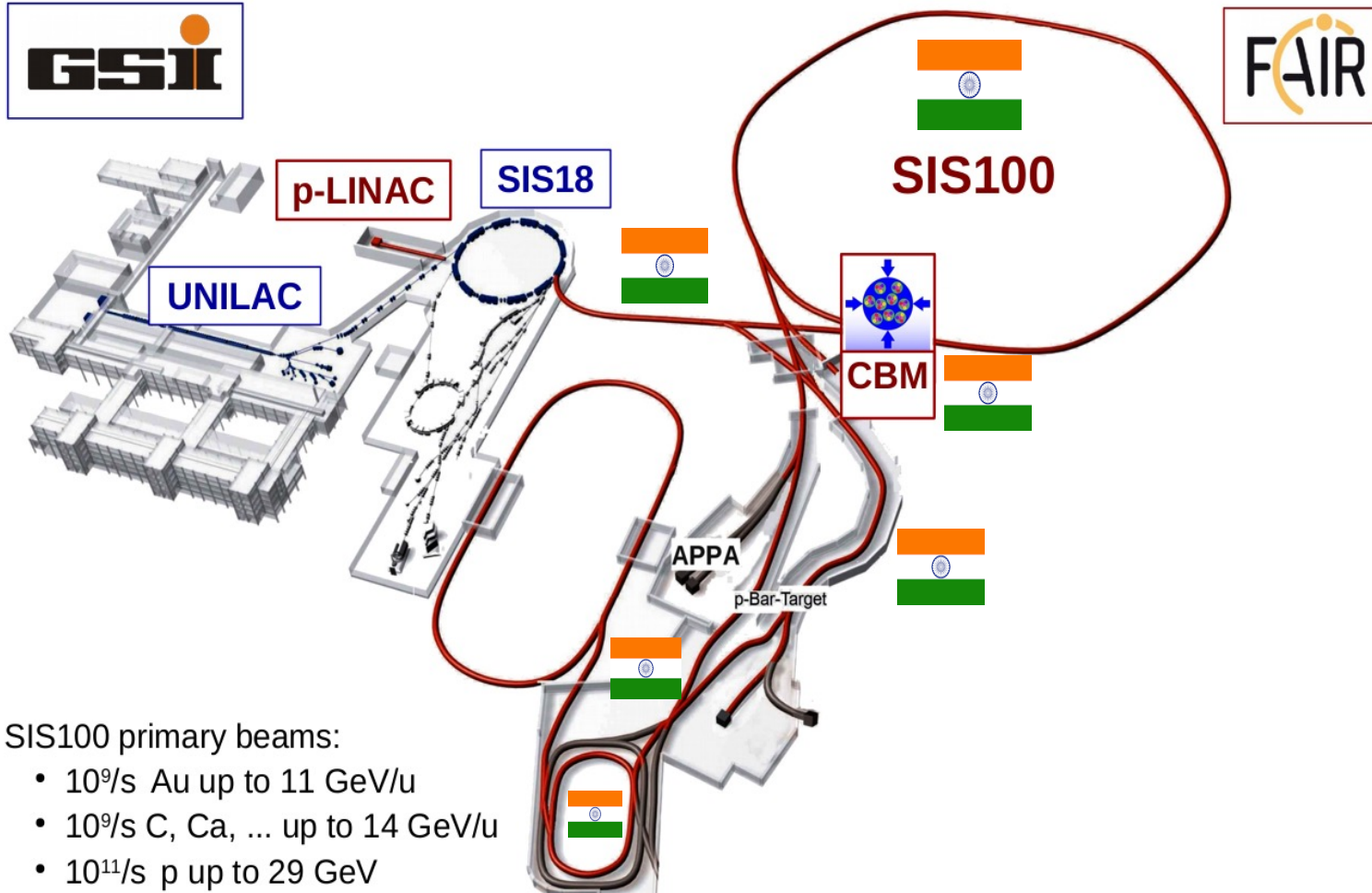
Present and upcoming heavy-ion experiments

- **Systematic exploration of the QCD phase diagram**
 - Low baryon density regime (LHC, RHIC ...)
 - High baryon density regime (RHIC, CERN-SPS, CBM ...)
- **Precise measurement of the physics observables of interest**
 - High luminosity
- **Gaseous detectors with high rate handling capabilities**
 - Micro Pattern Gas Detectors (MPGD)
 - Resistive Plate Chamber (RPC)
- **Innovative technologies for data acquisition**



Eur. Phys. J A53 (2017) 60; CBM Collaboration, EPJA 53 3 (2017) 60;
T.Galatyuk, NPA982 (2019), update (2021)

Facility for Antiproton and Ion Research (FAIR)



SIS100 primary beams:

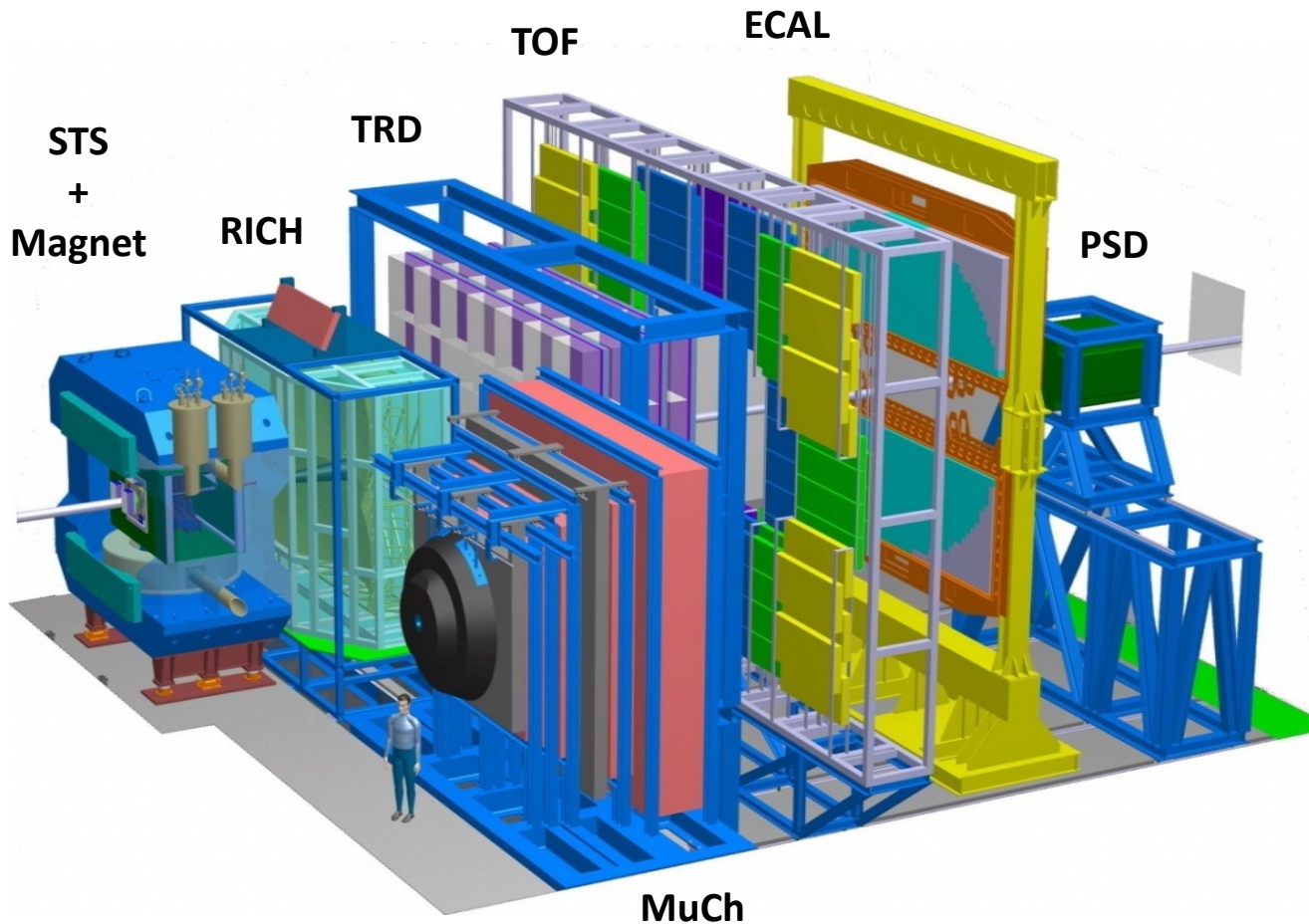
- $10^9/s$ Au up to 11 GeV/u
- $10^9/s$ C, Ca, ... up to 14 GeV/u
- $10^{11}/s$ p up to 29 GeV

Experimental Pillars:

- APPA (Atomic, Plasma Physics and Applications)
- PANDA (antiProton ANnihilation at DArmstadt)
- **CBM (Compressed Baryonic Matter)**
- NuSTAR (Nuclear Structure, Astrophysics and Reactions)

Compressed Baryonic Matter (CBM) experiment at FAIR

Mission: Systematic exploration of the QCD matter at large densities with high precision and rare probes



Physics Goals:

- QCD equation of state at high baryon density
- Location of critical point
- Chiral phase transition
- Charm production and propagation at and below threshold energies

Muon Chamber (MuCh) at CBM

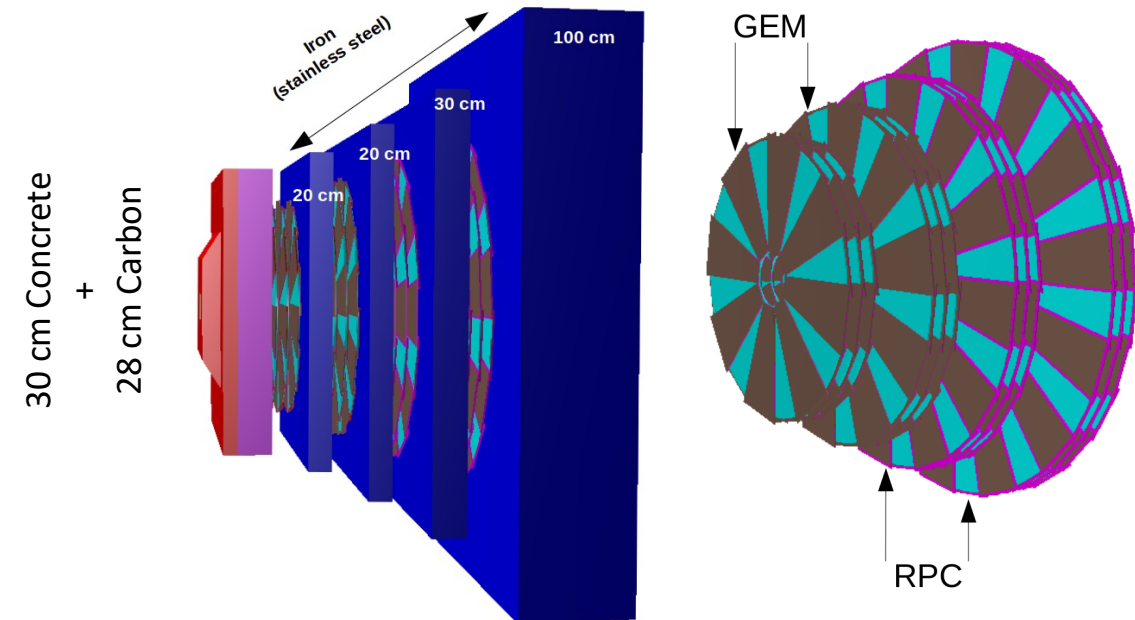
- MuCh is dedicatedly designed to detect the di-muons coming from the decay of low mass vector mesons and J/ψ

Uniqueness & Opportunities of di-muon measurement at CBM

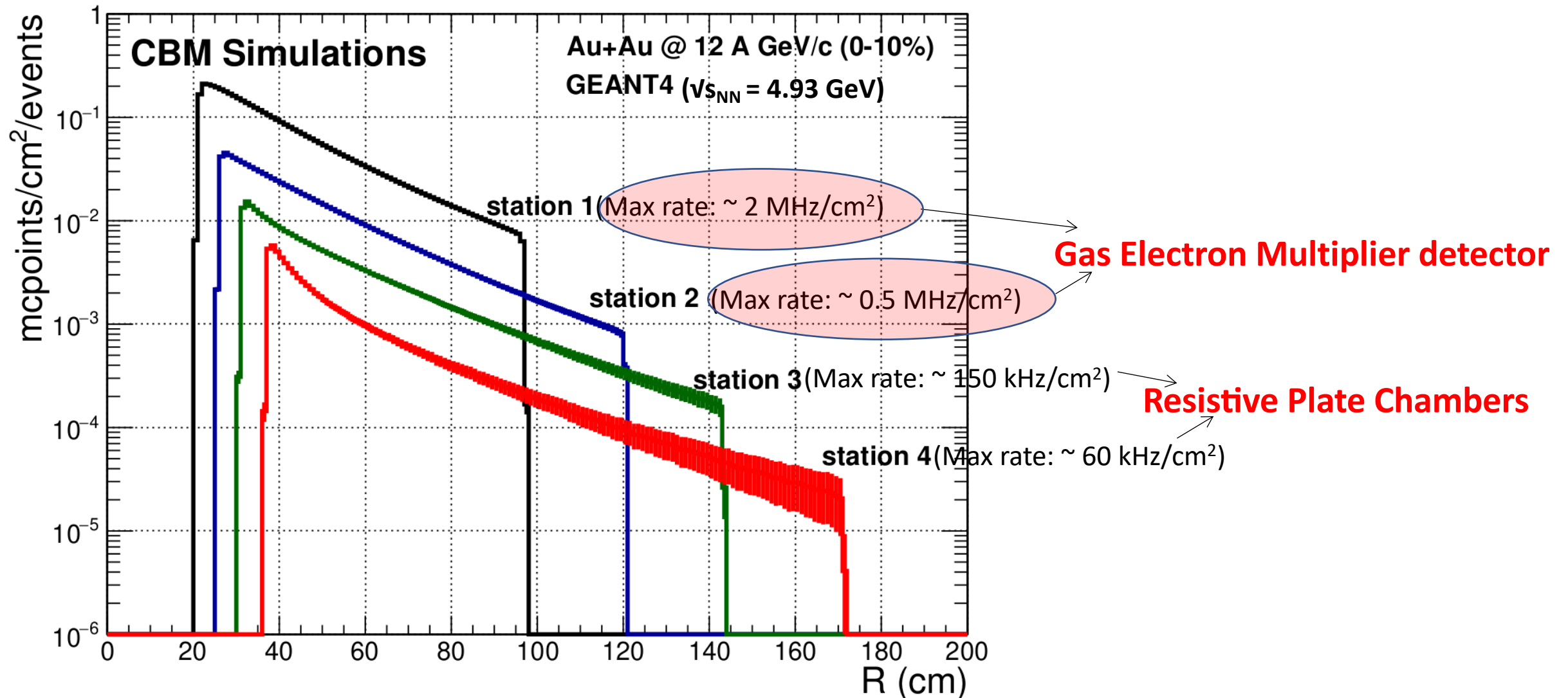
- No di-muon data in the heavy-ion sector between 2 - 11 A GeV (SIS-100)
- High precision measurements
- Effect of baryon densities to in-medium spectral functions
- Di-lepton caloric curve (signal of 1st order phase transition)

Challenges of di-muon measurement at CBM

- Accelerators with unprecedentedly high beam intensities
- Detectors with rate handling capabilities
- Free streaming data

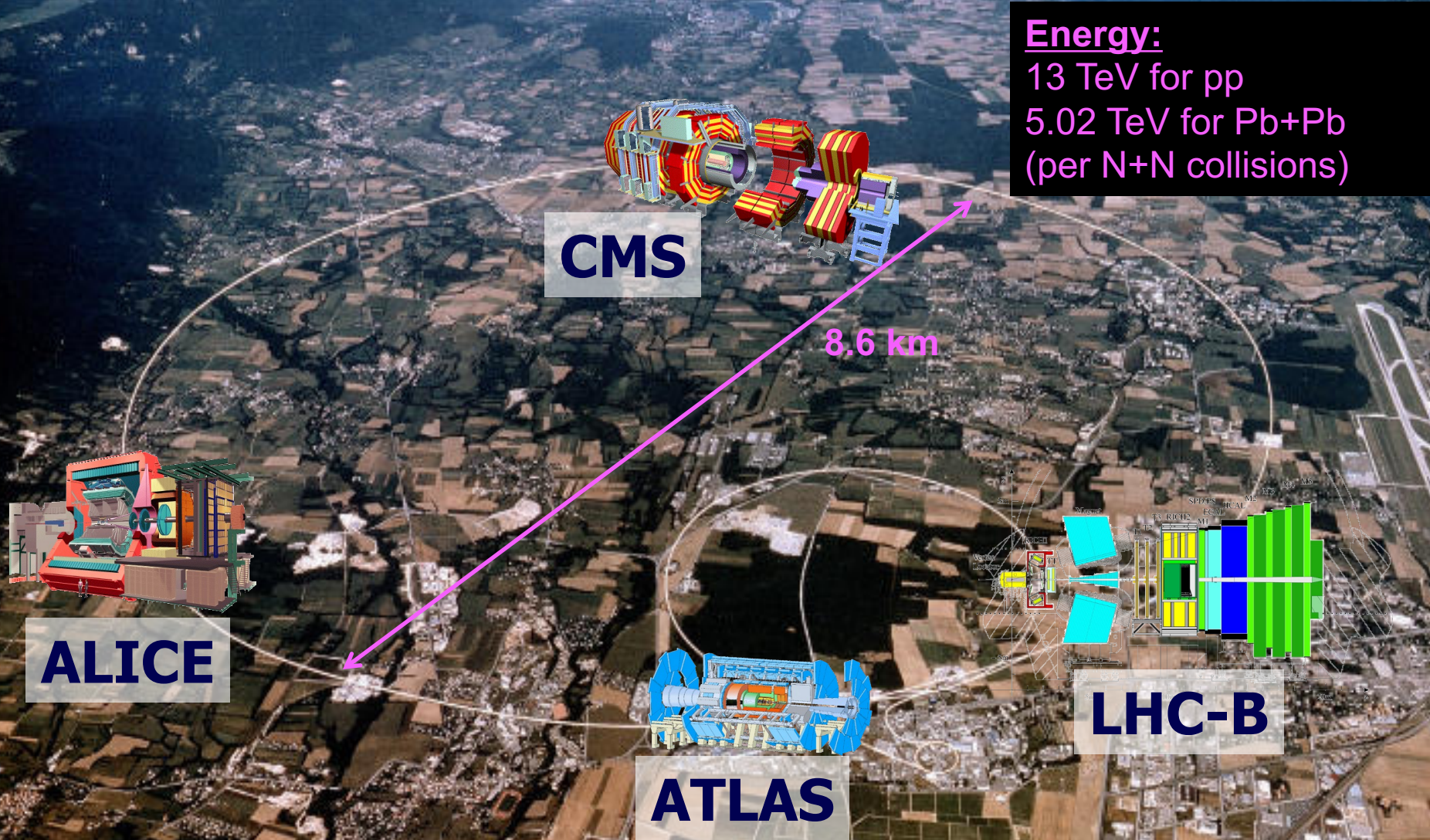


Particle rate in different MuCh stations



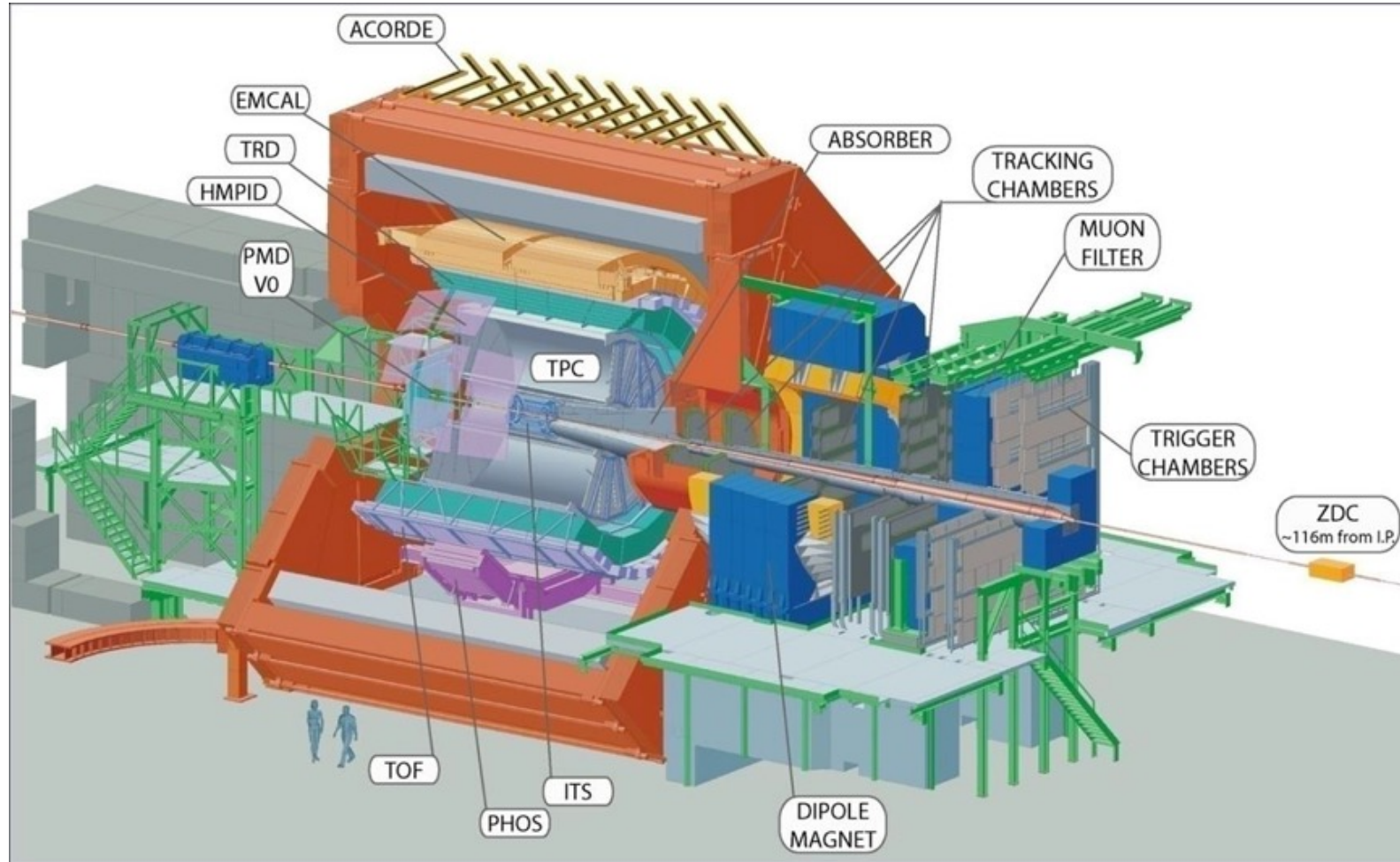
- Gas Electron Multiplier (GEM) is used in the 1st two stations
- Resistive Plate Chamber (RPC) is proposed for the last two tracking stations

The LHC and its experiments ...

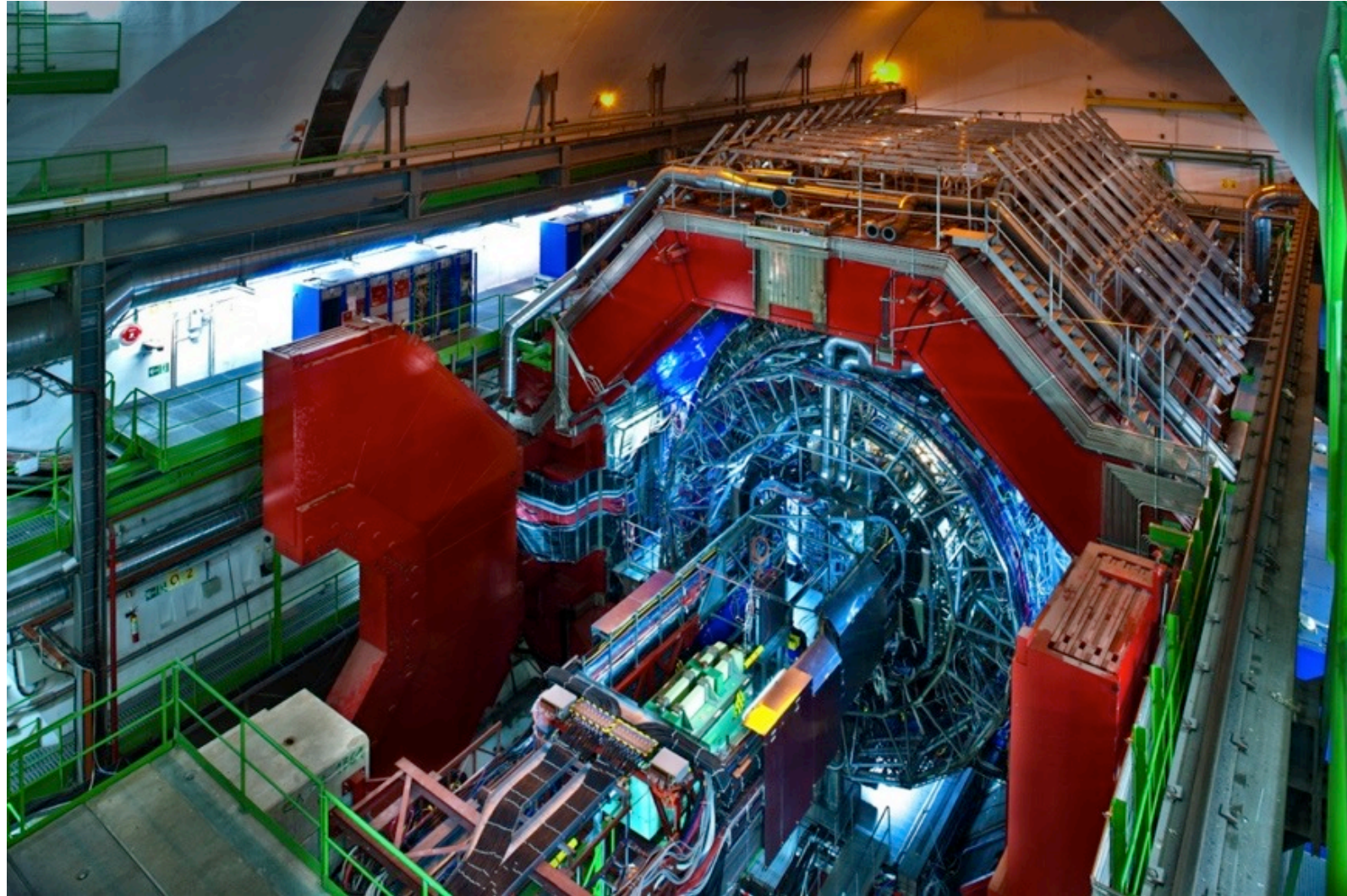


ALICE detector

ALICE detector



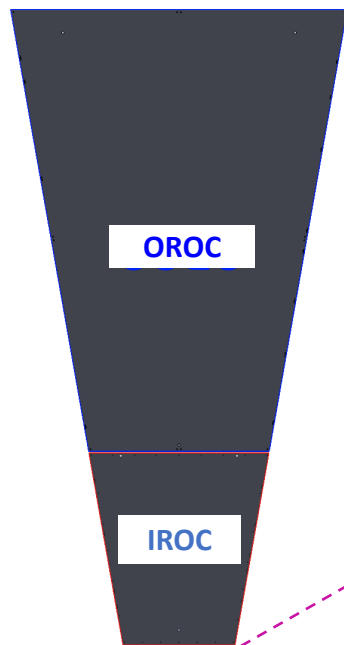
ALICE detector



ALICE TPC

2 x 18

Outer Read Out Chambers

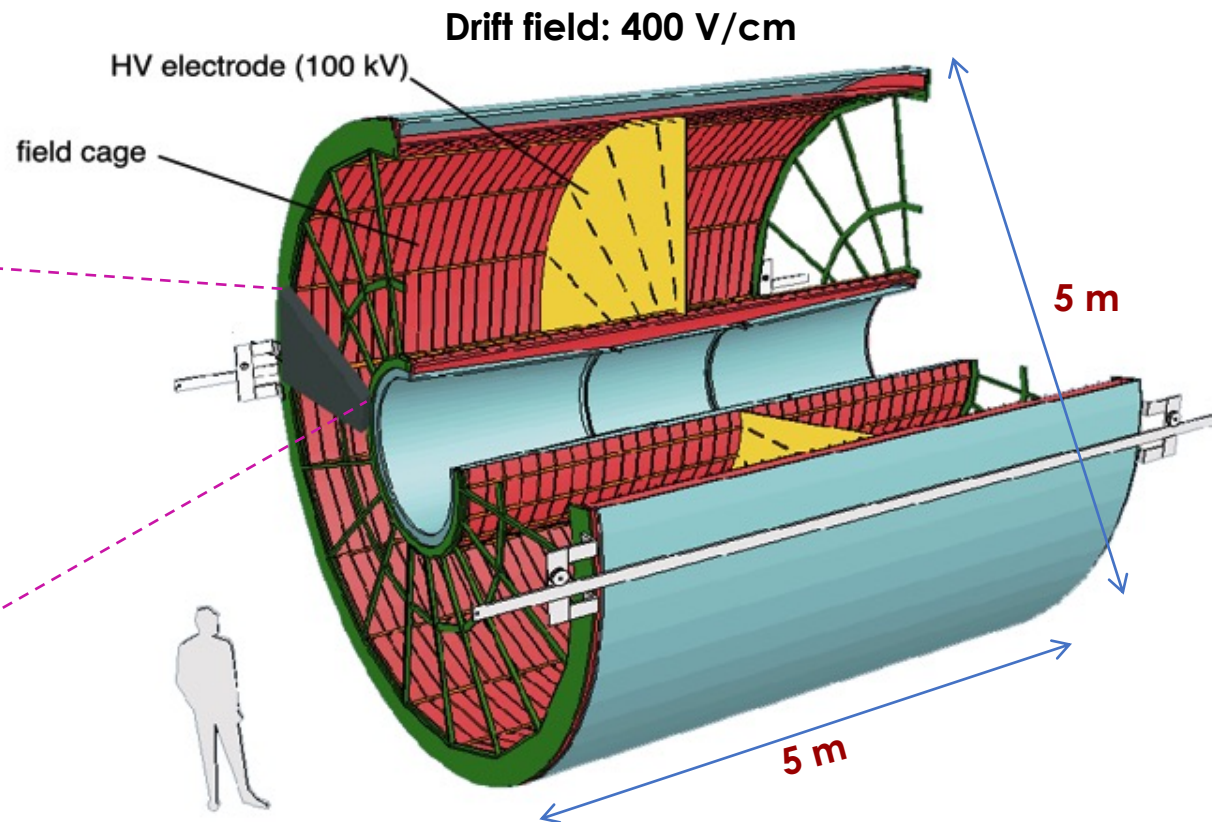


557568 pads

4 x 7.5 mm² (IROC)
6 x 10 mm² (OROC)
6 x 15 mm² (OROC)

2 x 18

Inner Read Out Chambers



GAS:

~90 m³

Ne-CO₂ (90-10) in RUN1

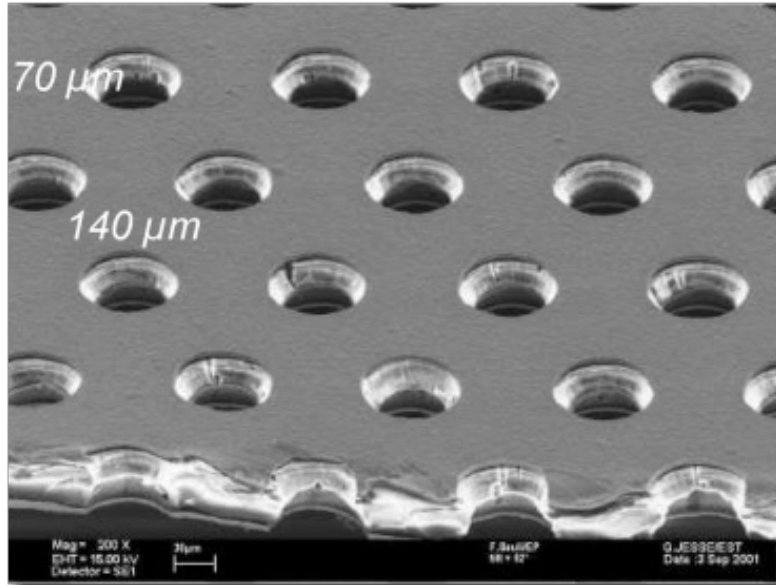
$v_{\text{drift}} = 2.73 \text{ cm}/\mu\text{s}$ (@ 400 V/cm)

Maximum drift time: ~92 μs

- Designed for charged-particle tracking and dE/dx measurement in Pb-Pb collisions with $dN_{\text{ch}}/d\eta=8000$, $\sigma(dE/dx)/(dE/dx)<10\%$

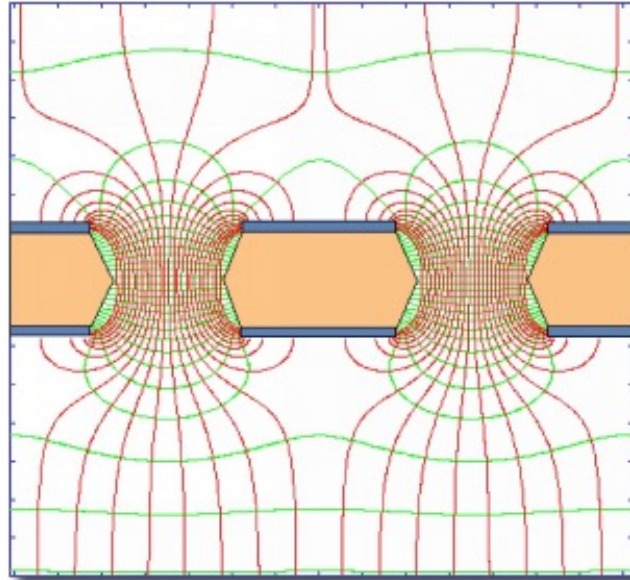
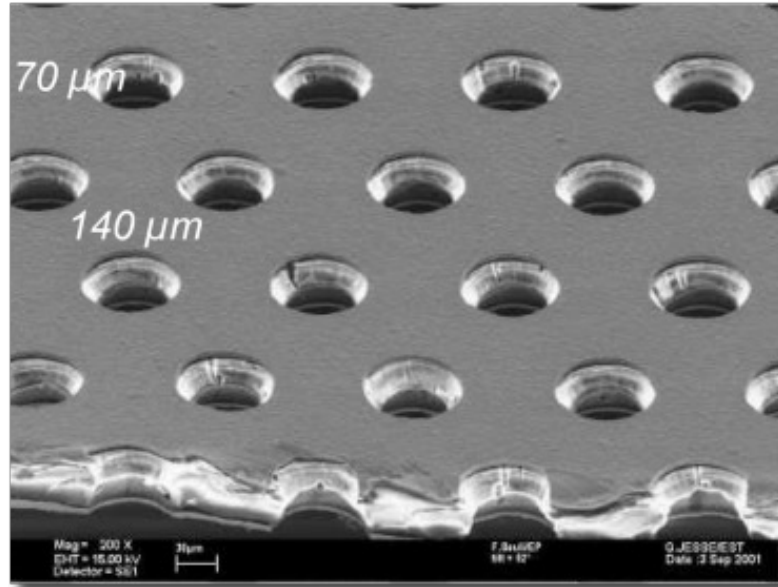
- Employs gating grid to block backdrifting ions
- Rate limitations: < 3.5 kHz (in p-p), ~500 Hz (in Pb-Pb)

Gas Electron Multiplier (GEM)



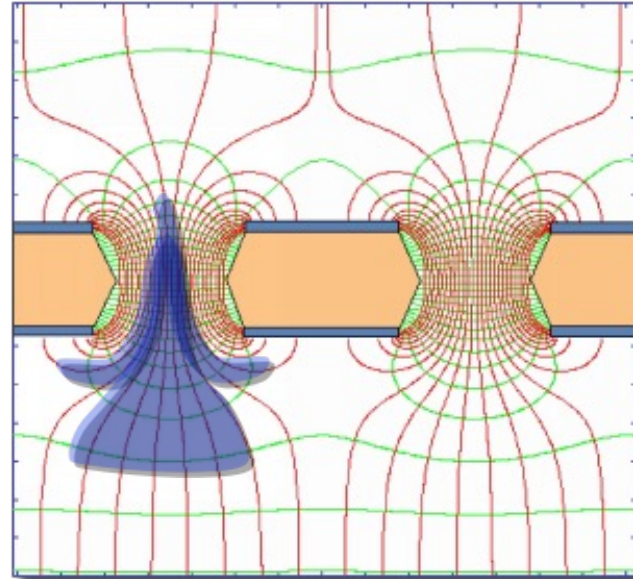
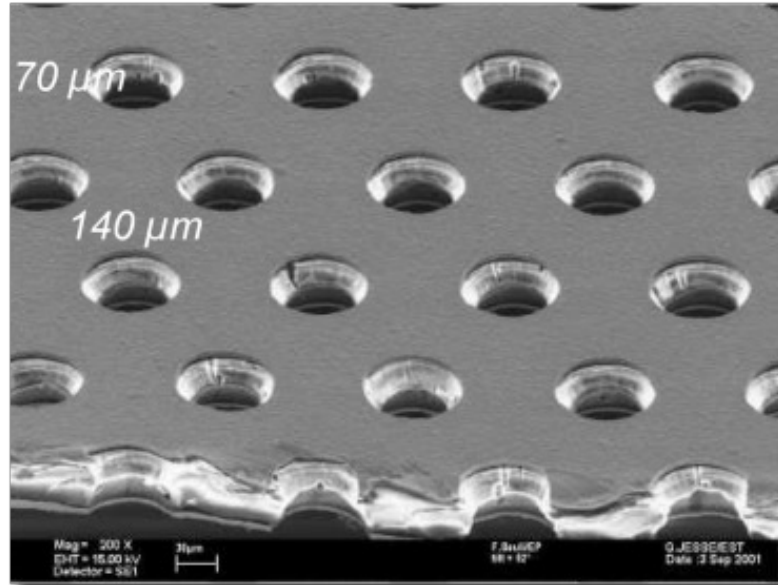
- GEM foil is made of Copper cladded Kapton foil of thickness 60 μm
- Good rate handling capability ($\sim 1 \text{ MHz}/\text{mm}^2$)
- High efficiency ($>95\%$)
- Can be operated in cascaded mode
- Good spatial resolution ($\sim 30 \mu\text{m}$)
- Operated with non-flammable gas mixtures (conventionally Ar-CO₂)
- Depending on the photolithographic techniques used, the GEM foils are classified as Double Mask (DM) or Single Mask (SM) GEM foils

Gas Electron Multiplier (GEM)



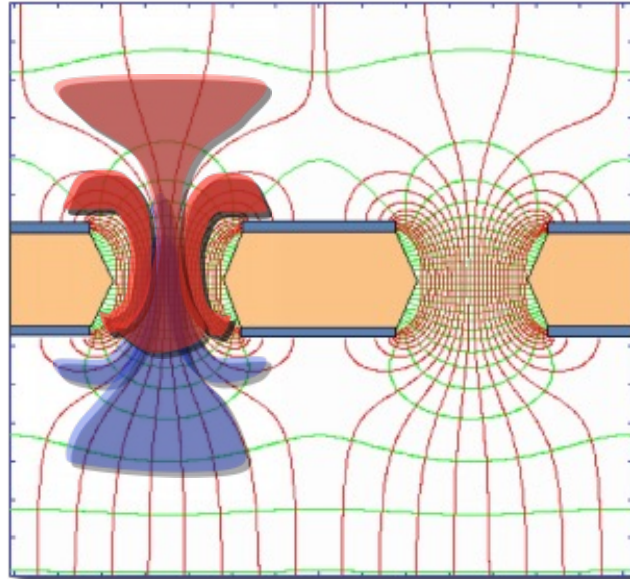
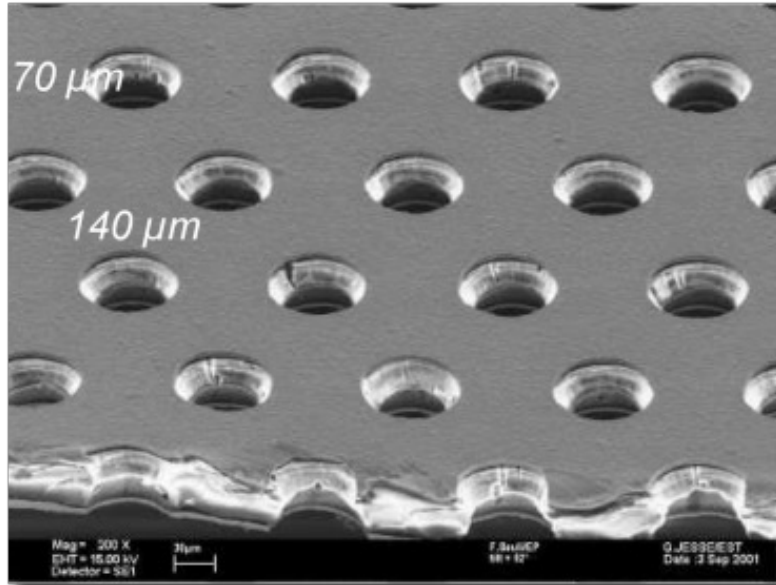
- GEM foil is made of Copper cladded Kapton foil of thickness $60\ \mu\text{m}$
- Good rate handling capability ($\sim 1\ \text{MHz}/\text{mm}^2$)
- High efficiency ($>95\%$)
- Can be operated in cascaded mode
- Good spatial resolution ($\sim 30\ \mu\text{m}$)
- Operated with non-flammable gas mixtures (conventionally Ar-CO₂)
- Depending on the photolithographic techniques used, the GEM foils are classified as Double Mask (DM) or Single Mask (SM) GEM foils

Gas Electron Multiplier (GEM)



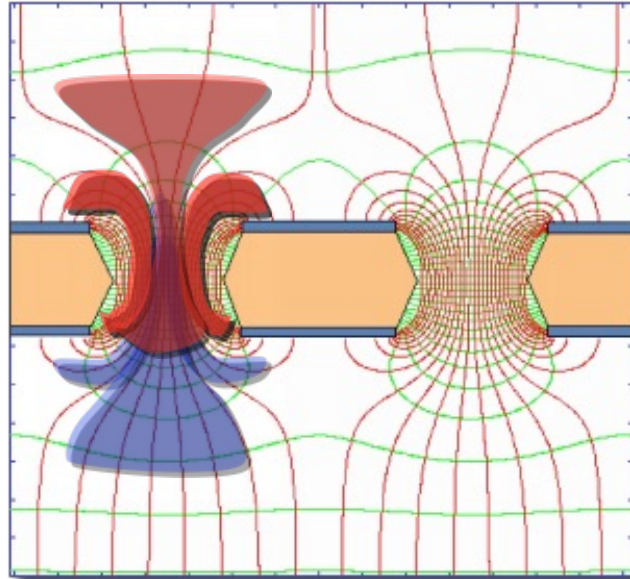
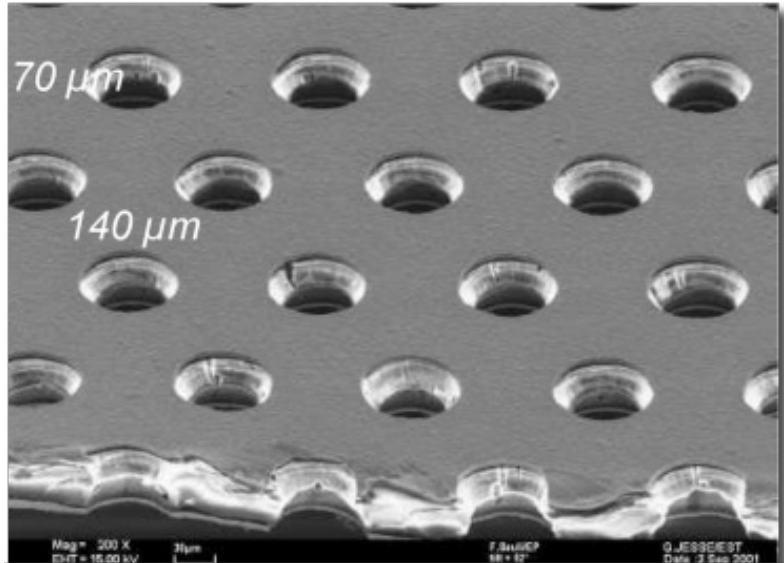
- GEM foil is made of Copper cladded Kapton foil of thickness $60\ \mu\text{m}$
- Good rate handling capability ($\sim 1\ \text{MHz}/\text{mm}^2$)
- High efficiency ($>95\%$)
- Can be operated in cascaded mode
- Good spatial resolution ($\sim 30\ \mu\text{m}$)
- Operated with non-flammable gas mixtures (conventionally Ar-CO₂)
- Depending on the photolithographic techniques used, the GEM foils are classified as Double Mask (DM) or Single Mask (SM) GEM foils

Gas Electron Multiplier (GEM)

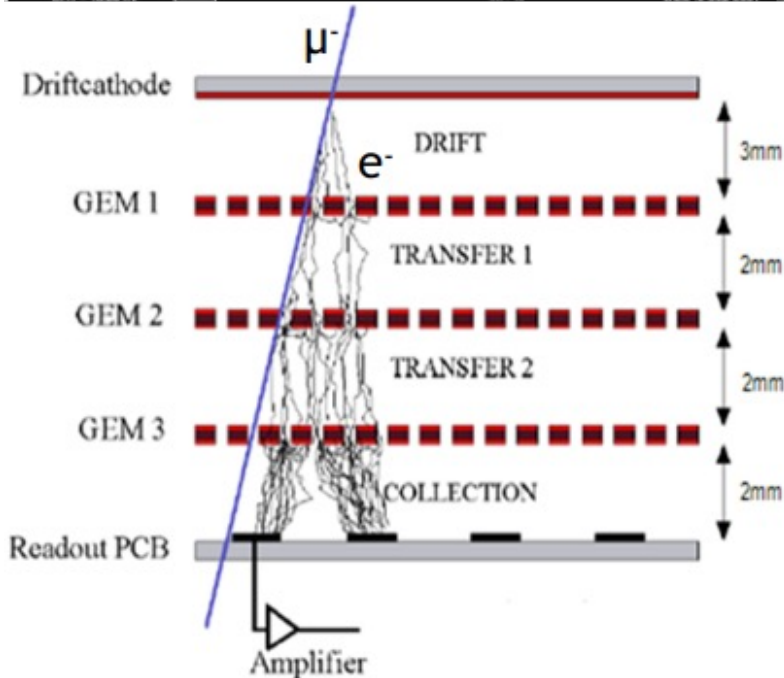


- GEM foil is made of Copper cladded Kapton foil of thickness $60\ \mu\text{m}$
- Good rate handling capability ($\sim 1\ \text{MHz}/\text{mm}^2$)
- High efficiency ($>95\%$)
- Can be operated in cascaded mode
- Good spatial resolution ($\sim 30\ \mu\text{m}$)
- Operated with non-flammable gas mixtures (conventionally Ar-CO₂)
- Depending on the photolithographic techniques used, the GEM foils are classified as Double Mask (DM) or Single Mask (SM) GEM foils

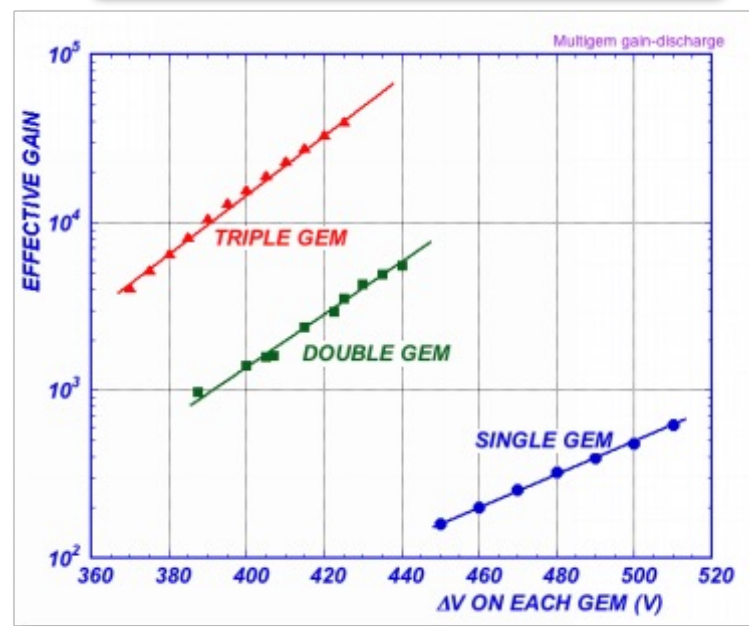
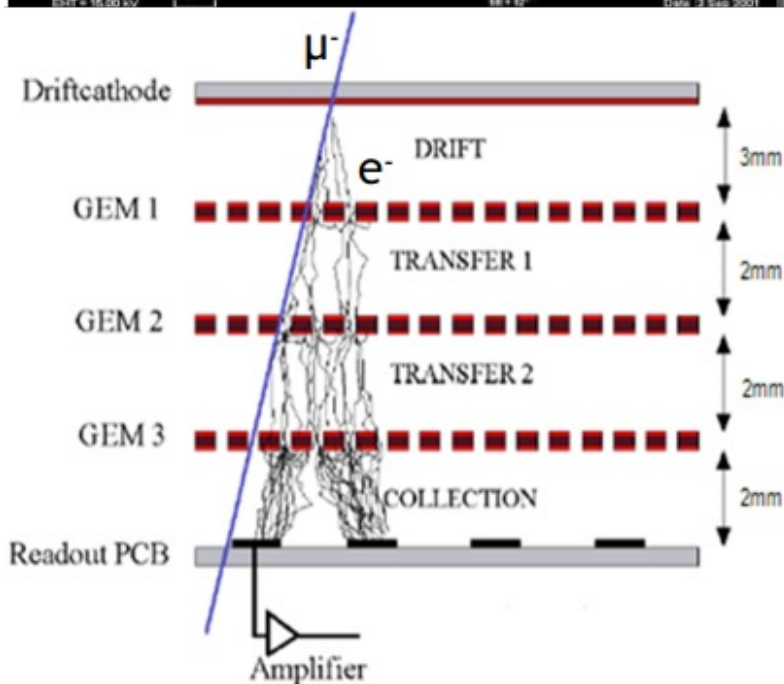
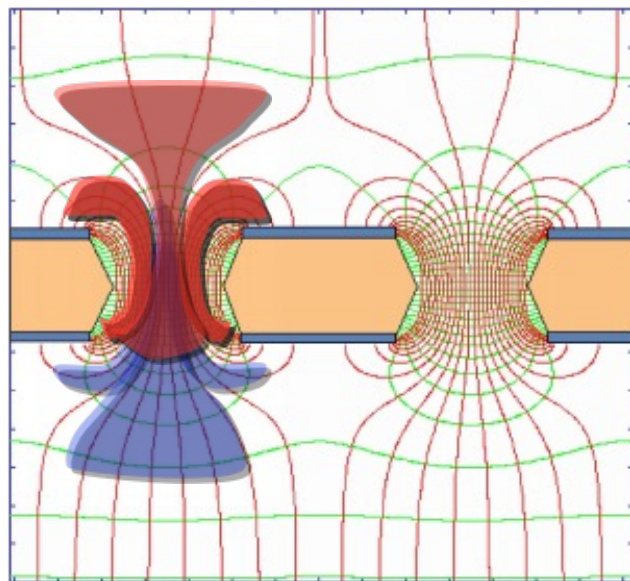
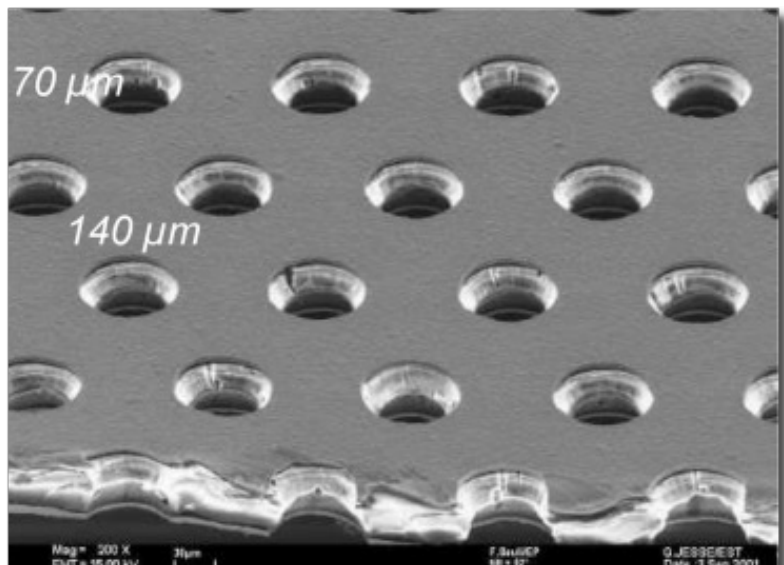
Gas Electron Multiplier (GEM)



- GEM foil is made of Copper cladded Kapton foil of thickness 60 μm
- Good rate handling capability ($\sim 1 \text{ MHz/mm}^2$)
- High efficiency ($>95\%$)
- Can be operated in cascaded mode
- Good spatial resolution ($\sim 30 \mu\text{m}$)
- Operated with non-flammable gas mixtures (conventionally Ar-CO₂)
- Depending on the photolithographic techniques used, the GEM foils are classified as Double Mask (DM) or Single Mask (SM) GEM foils



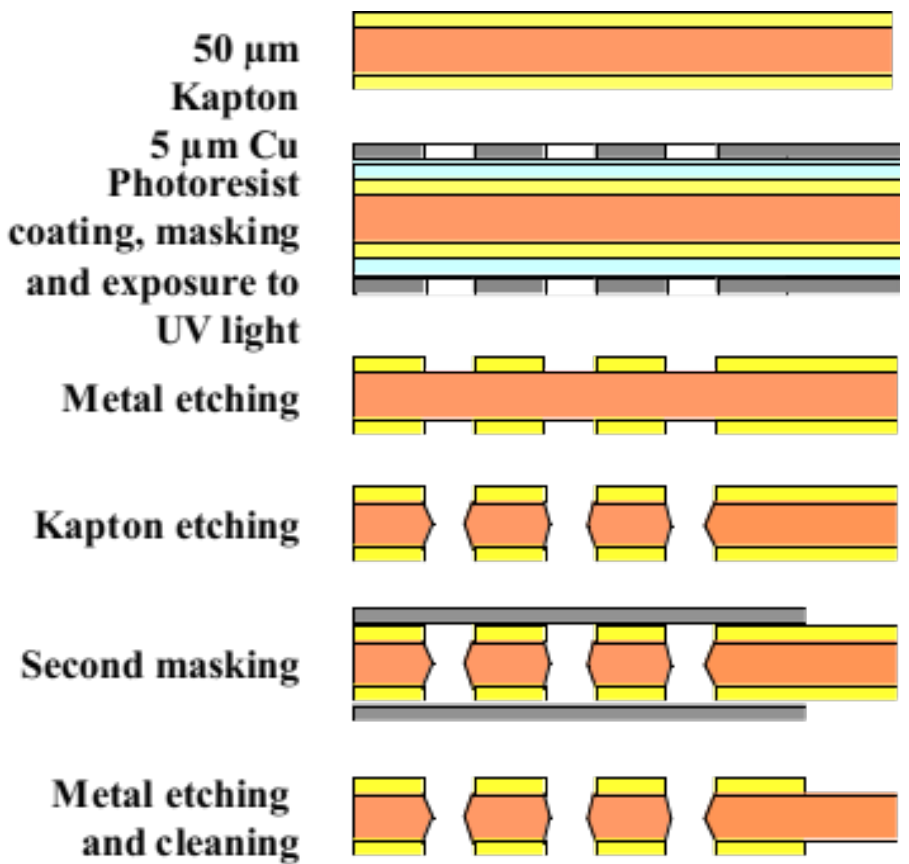
Gas Electron Multiplier (GEM)



- GEM foil is made of Copper cladded Kapton foil of thickness 60 μm
- Good rate handling capability ($\sim 1 \text{ MHz/mm}^2$)
- High efficiency ($>95\%$)
- Can be operated in cascaded mode
- Good spatial resolution ($\sim 30 \mu\text{m}$)
- Operated with non-flammable gas mixtures (conventionally Ar-CO₂)
- Depending on the photolithographic techniques used, the GEM foils are classified as Double Mask (DM) or Single Mask (SM) GEM foils

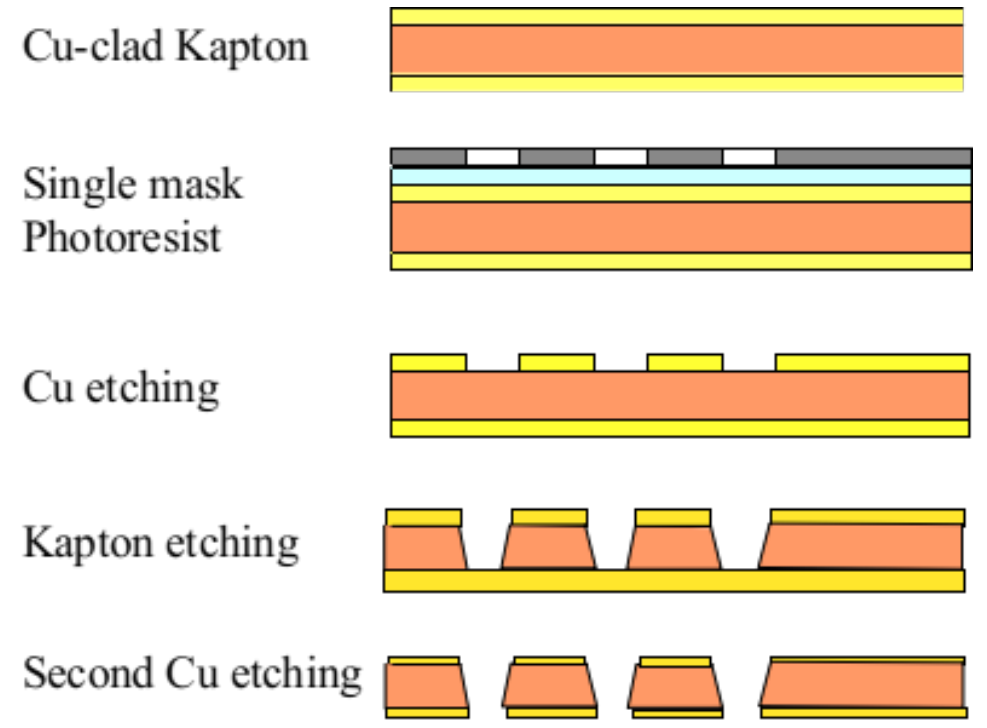
Gas Electron Multiplier (GEM)

Double mask photolithographic technique



Double Mask (DM) GEM foils

Single mask photolithographic techniques



Single Mask (SM) GEM foils

Aspects to be discussed in this talk

- **Uniformity in characteristics**
 - **Gain**
 - **Energy resolution**
 - **Count rate**
- **Long-term stability**
- **Charging-up effect**
 - **Dependency on particle rate**
 - **Dependency on gain**
- **Spark probability measurement**

Triple GEM chamber: Fabrication and prototypes

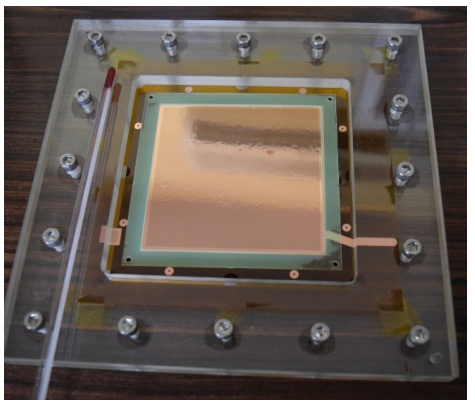
Components used in the fabrication of triple GEM chamber



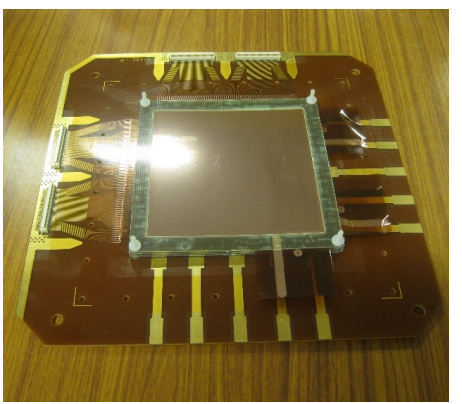
Building of a GEM detector



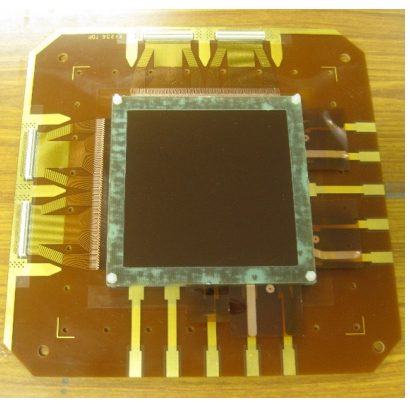
GEM foil



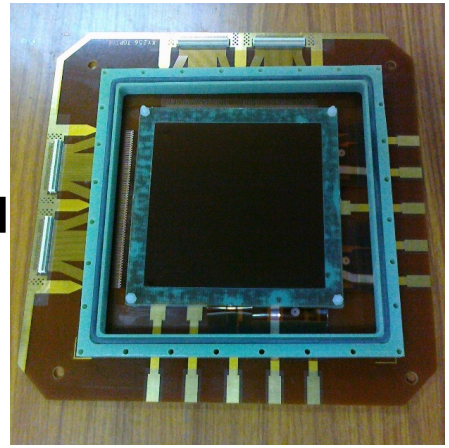
Stretching of the GEM foil



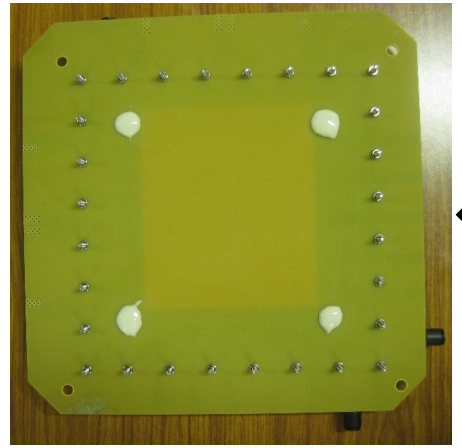
GEM foil on read-out plane



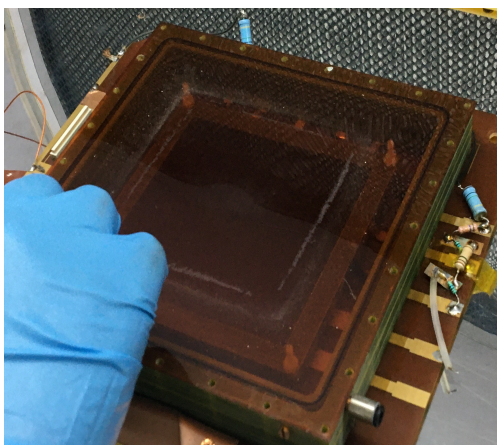
Drift plane is placed



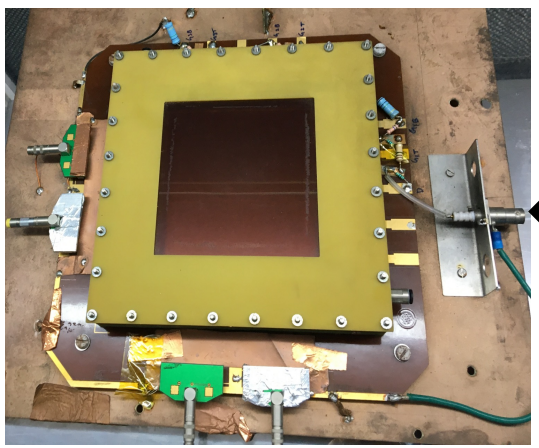
Frame is placed with O-ring



Gluing at the bottom

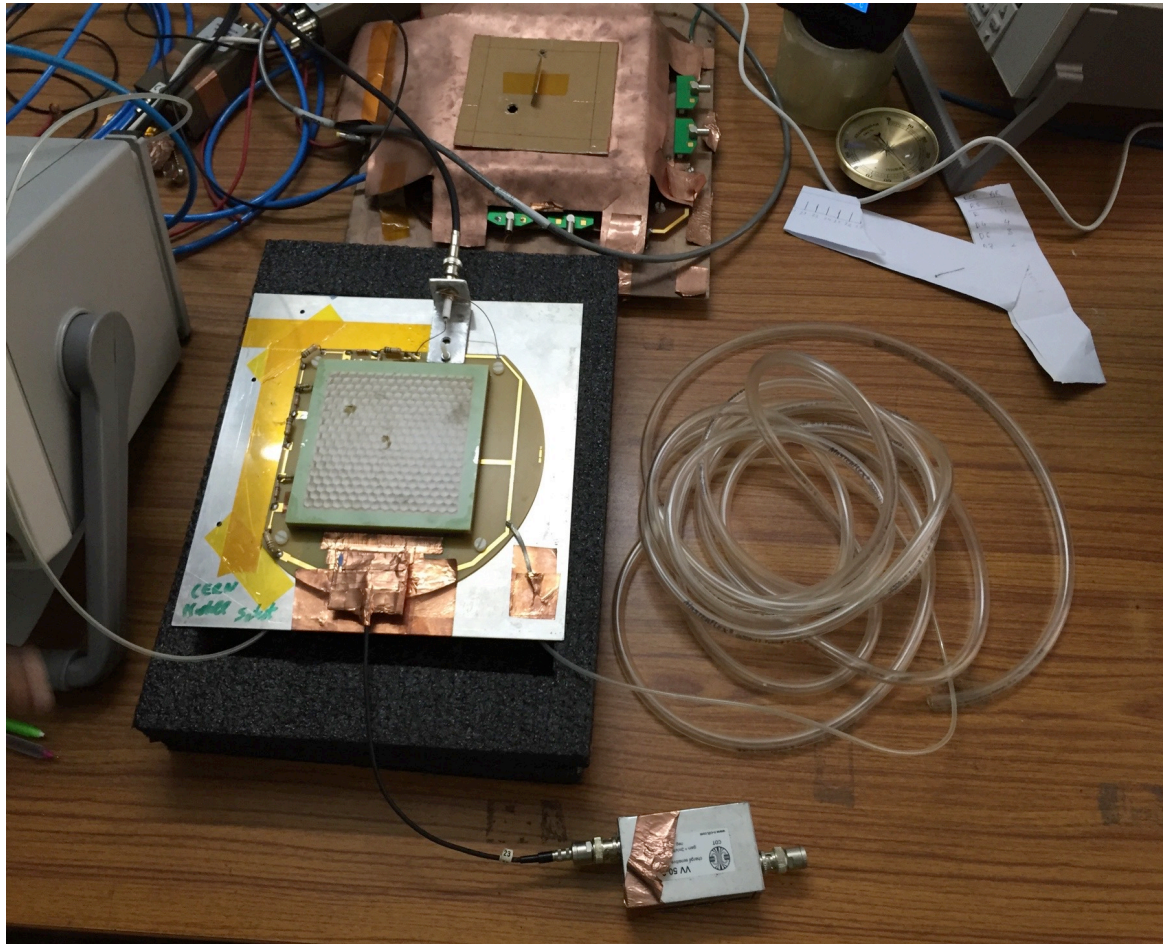


Kapton window is placed

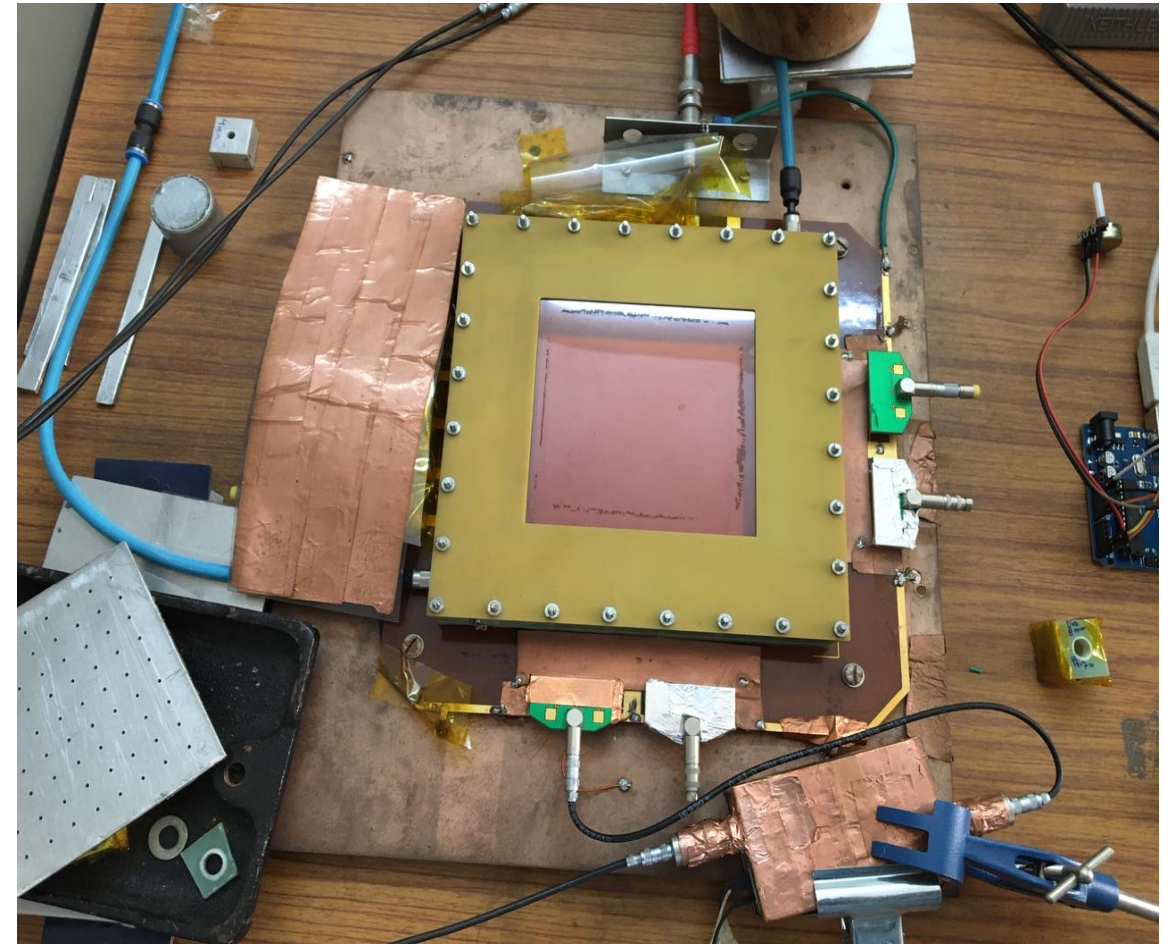


Assembled GEM

Triple GEM chambers prototype under testing at Bose Institute

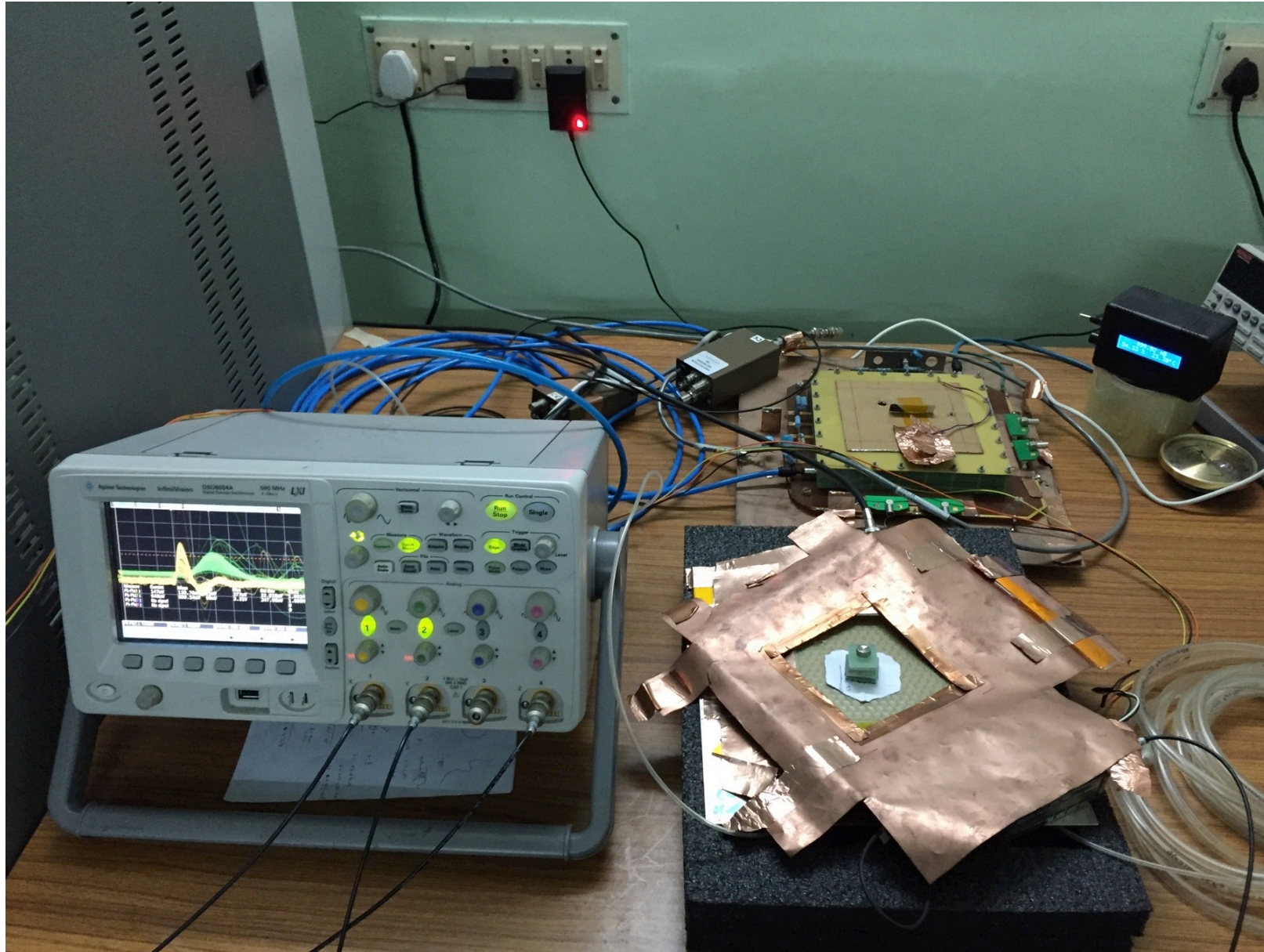


Double Mask (DM) triple GEM chamber



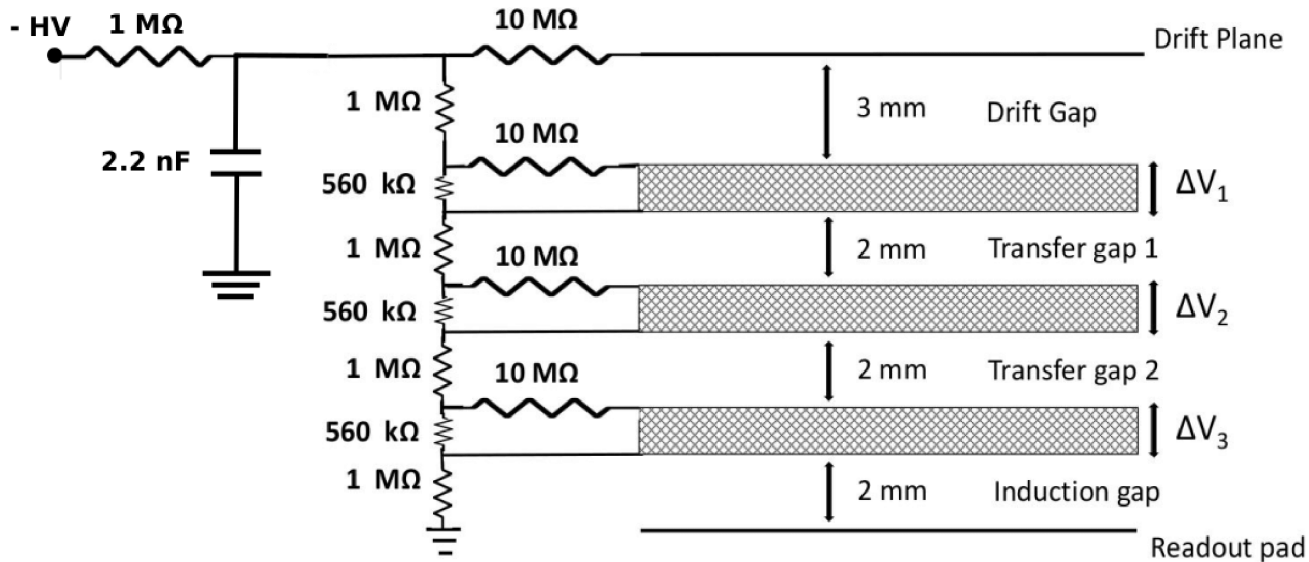
Single Mask (SM) triple GEM chamber

Triple GEM chamber prototype under testing at Bose Institute



Characteristics studies of triple GEM prototypes at Bose Institute

Characteristics studies



Schematic of the High Voltage distribution of the SM mask triple GEM chamber of dimension 10×10 cm²

Dimension of the chamber: 10×10 cm²

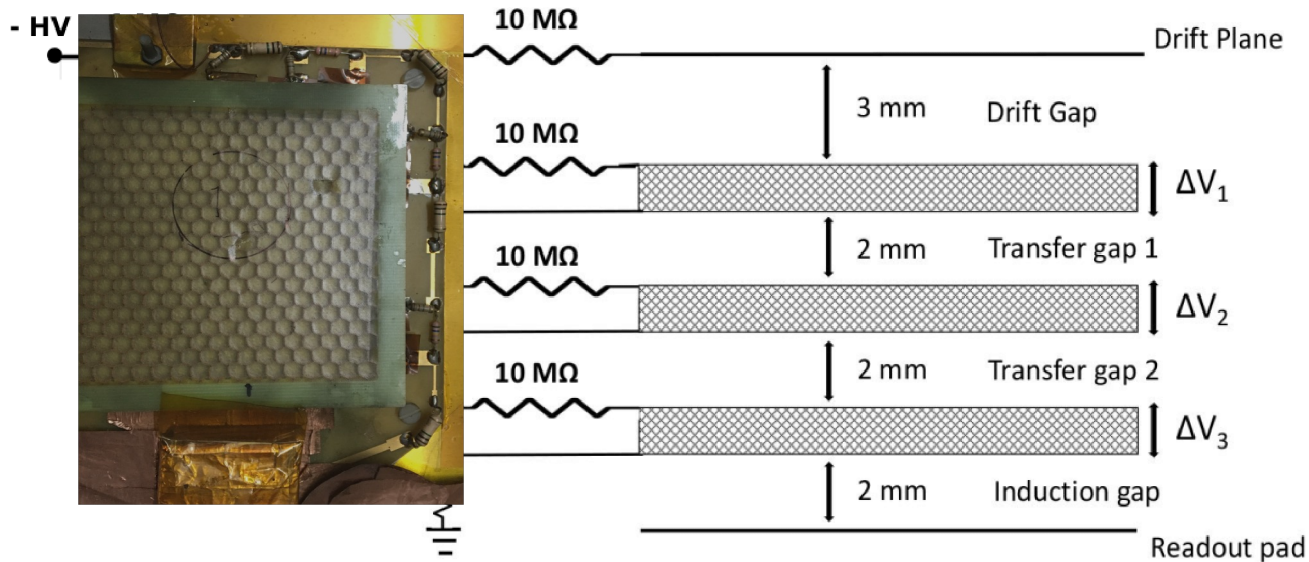
GEM: SM & DM triple GEM chamber

Source: Same Fe⁵⁵ X-ray (5.9 keV) source is used for irradiation and monitoring the spectrum

Gas mixture: Ar/CO₂ (Continuous flow mode)

Preamplifier gain: 2 mV/fC (charge sensitive)

Characteristics studies



Schematic of the High Voltage distribution of the SM mask triple GEM chamber of dimension $10 \times 10 \text{ cm}^2$

Dimension of the chamber: $10 \times 10 \text{ cm}^2$

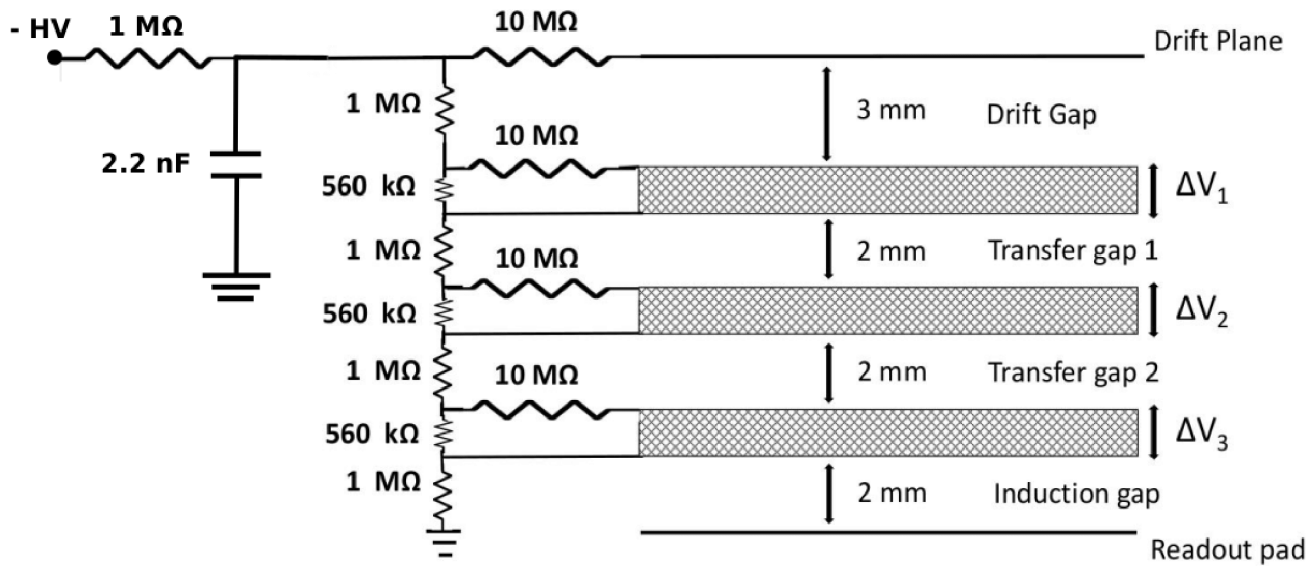
GEM: SM & DM triple GEM chamber

Source: Same Fe^{55} X-ray (5.9 keV) source is used for irradiation and monitoring the spectrum

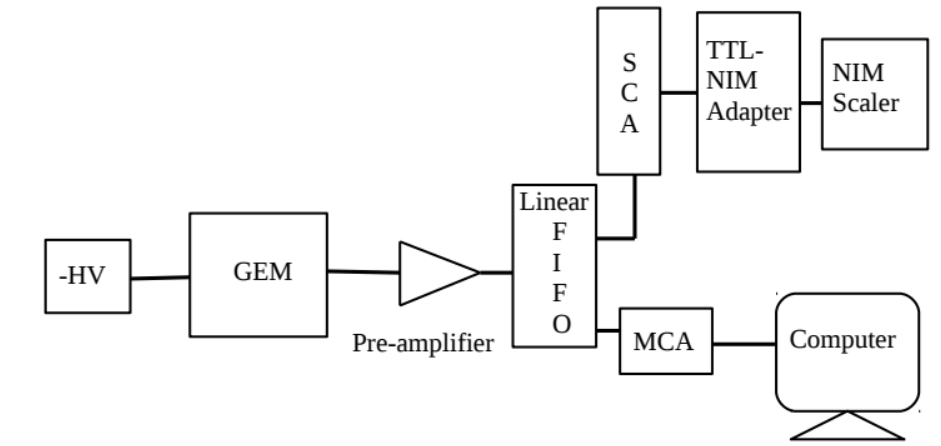
Gas mixture: Ar/ CO_2 (Continuous flow mode)

Preamplifier gain: 2 mV/fC (charge sensitive)

Characteristics studies



Schematic of the High Voltage distribution of the SM mask triple GEM chamber of dimension $10 \times 10 \text{ cm}^2$



Schematic representation of the electronics setup

Dimension of the chamber: $10 \times 10 \text{ cm}^2$

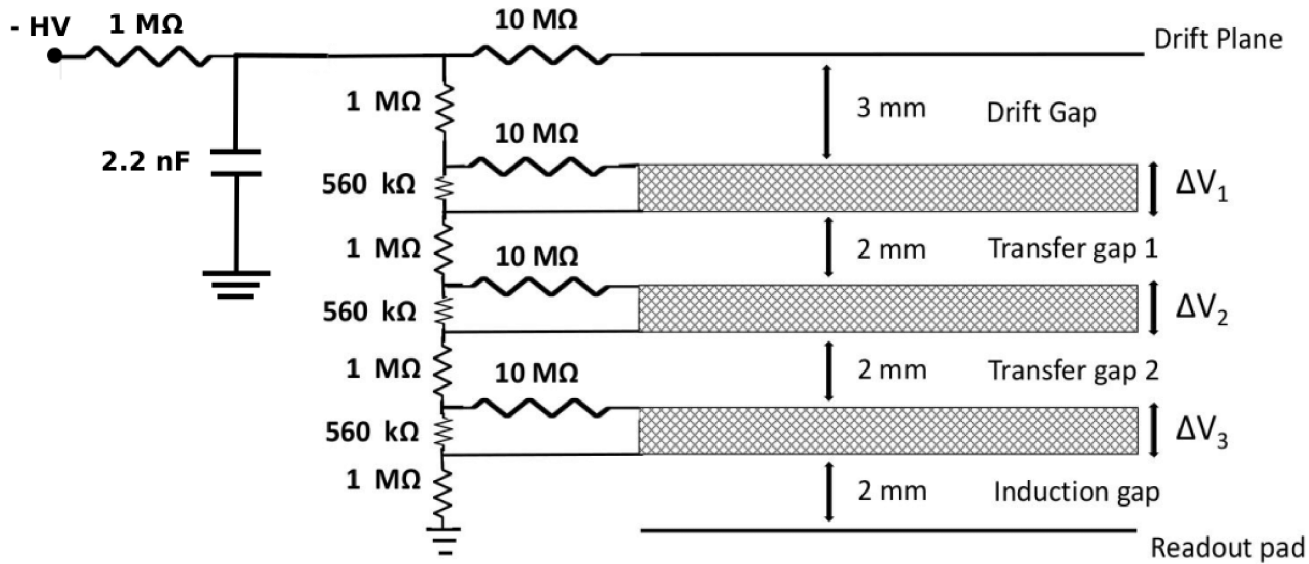
GEM: SM & DM triple GEM chamber

Source: Same Fe^{55} X-ray (5.9 keV) source is used for irradiation and monitoring the spectrum

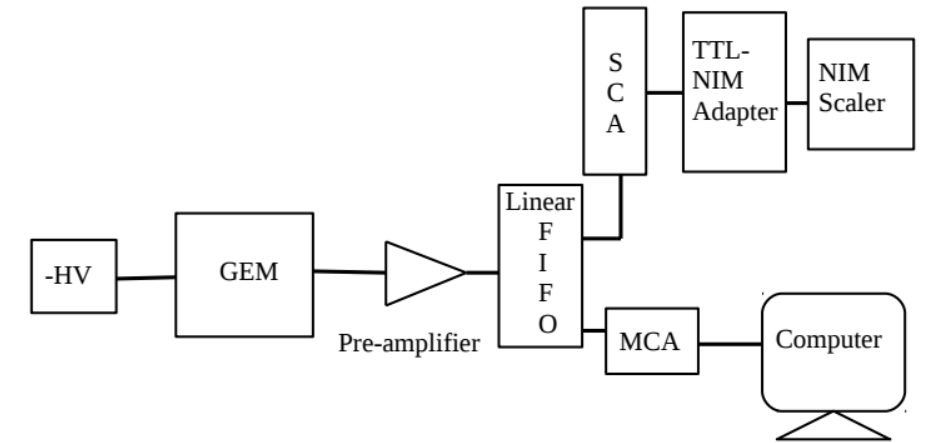
Gas mixture: Ar/CO_2 (Continuous flow mode)

Preamplifier gain: 2 mV/fC (charge sensitive)

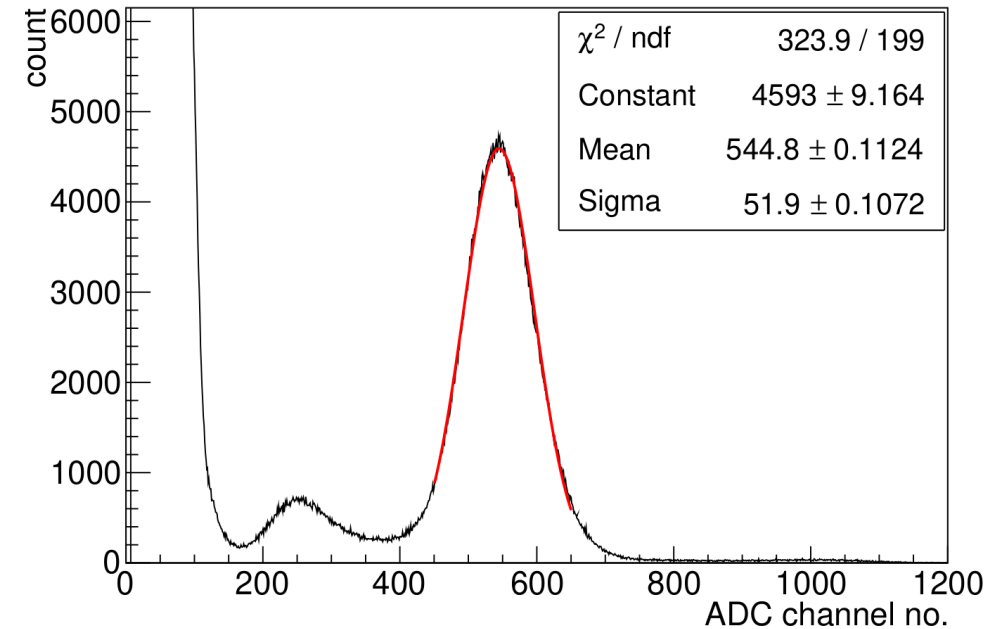
Characteristics studies



Schematic of the High Voltage distribution of the SM mask triple GEM chamber of dimension $10 \times 10 \text{ cm}^2$



Schematic representation of the electronics setup



Fe^{55} spectra at $\Delta V \sim 410 \text{ V}$ and with Ar/CO_2 gas mixture at 70/30 volume ratio

Dimension of the chamber: $10 \times 10 \text{ cm}^2$

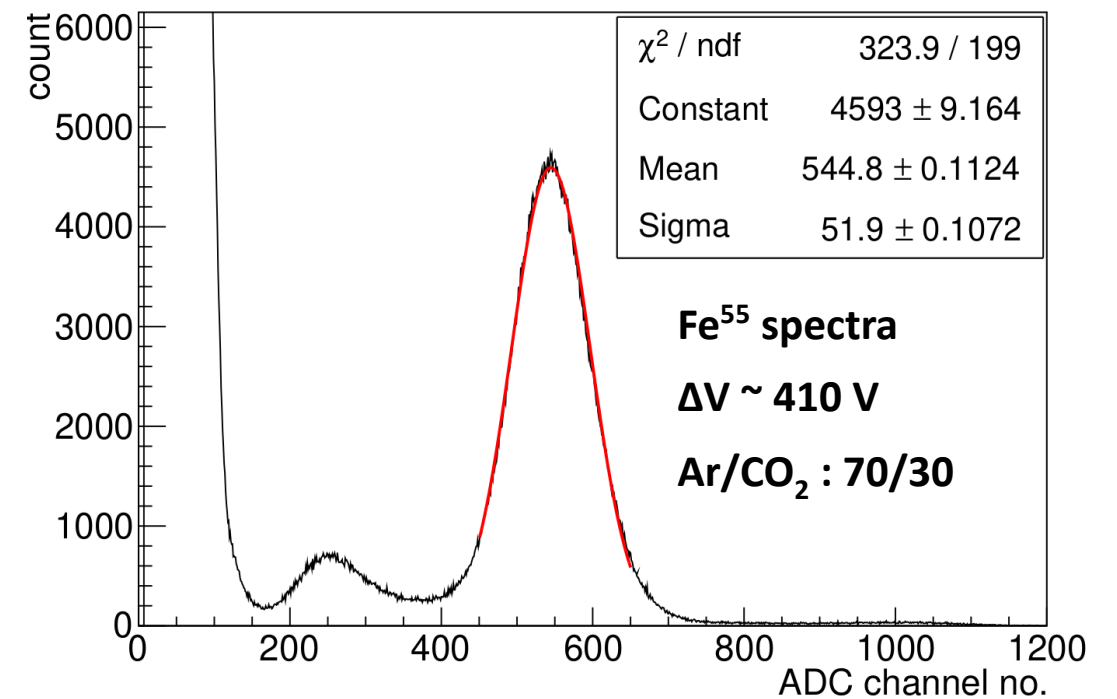
GEM: SM & DM triple GEM chamber

Source: Same Fe^{55} X-ray (5.9 keV) source is used for irradiation and monitoring the spectrum

Gas mixture: Ar/CO_2 (Continuous flow mode)

Preamplifier gain: 2 mV/fC (charge sensitive)

Gain, energy resolution & count rate



$$\text{Gain} = \frac{\text{Output charge}}{\text{Input charge}} = \frac{(\text{Mean pulse height} / 2 \text{ mV}) \text{ fC}}{\text{No of primary electrons} \times e \text{ C}}$$

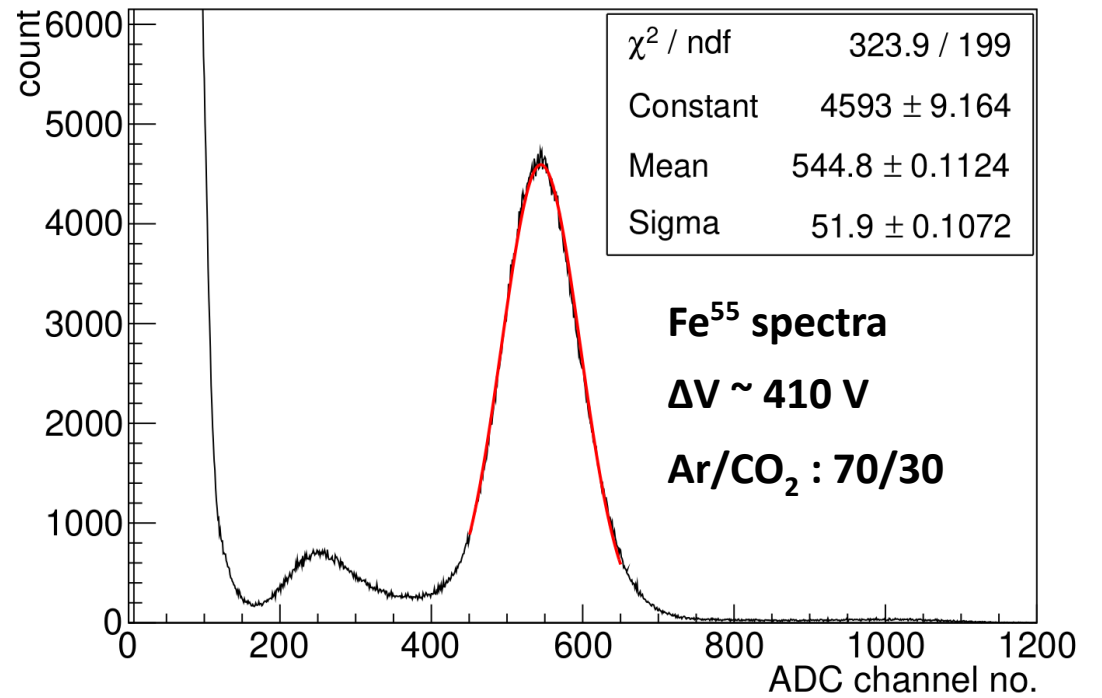
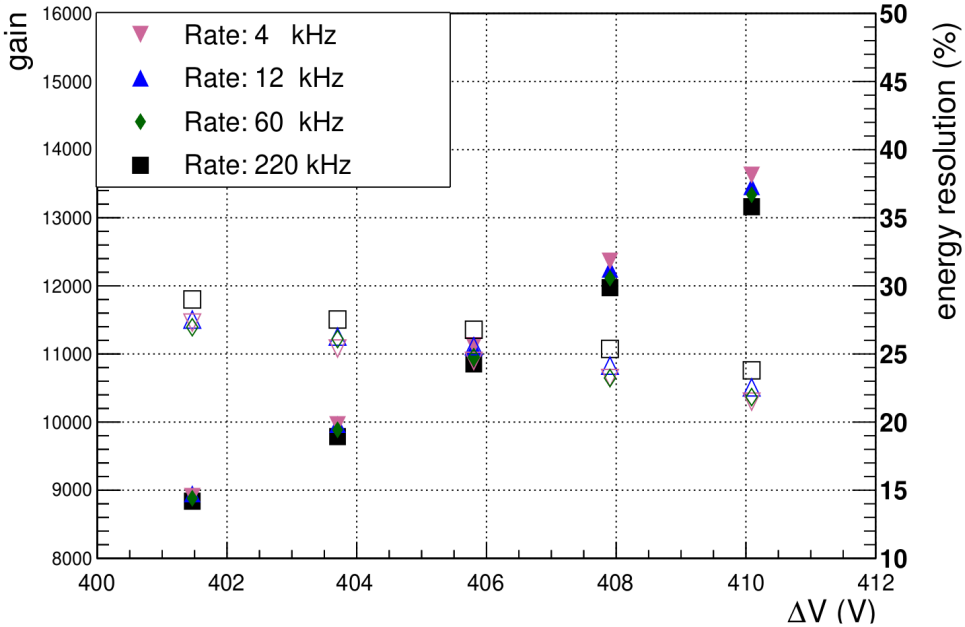
$$\text{Energy resolution} = \frac{\text{Sigma} \times 2.355}{\text{Mean}} \times 100 \%$$

Number of primary electrons (n)

$$n = E_{\text{gamma}} \left(\frac{\% \text{ of Ar}}{W_{\text{Ar}}} + \frac{\% \text{ of CO}_2}{W_{\text{CO}_2}} \right)$$

For Ar/CO₂ in 70/30 volume ratio, the average number of the primary electrons is 212 with the 5.9 keV X-ray source

Gain, energy resolution & count rate



$$\text{Gain} = \frac{\text{Output charge}}{\text{Input charge}} = \frac{(\text{Mean pulse height} / 2 \text{ mV}) \text{ fC}}{\text{No of primary electrons} \times e \text{ C}}$$

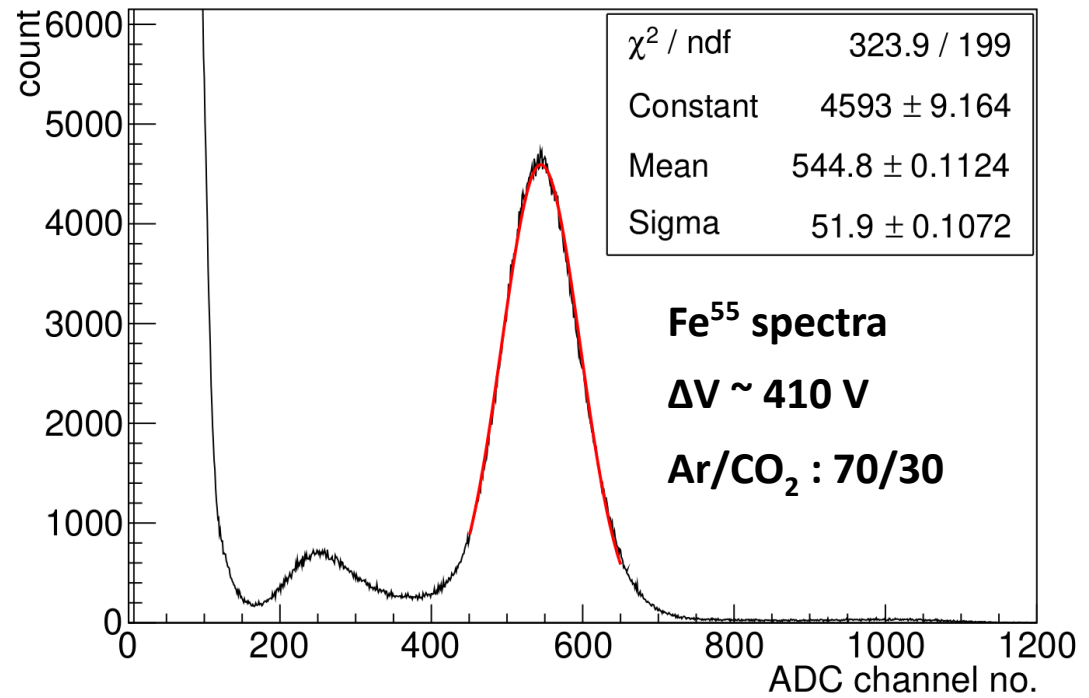
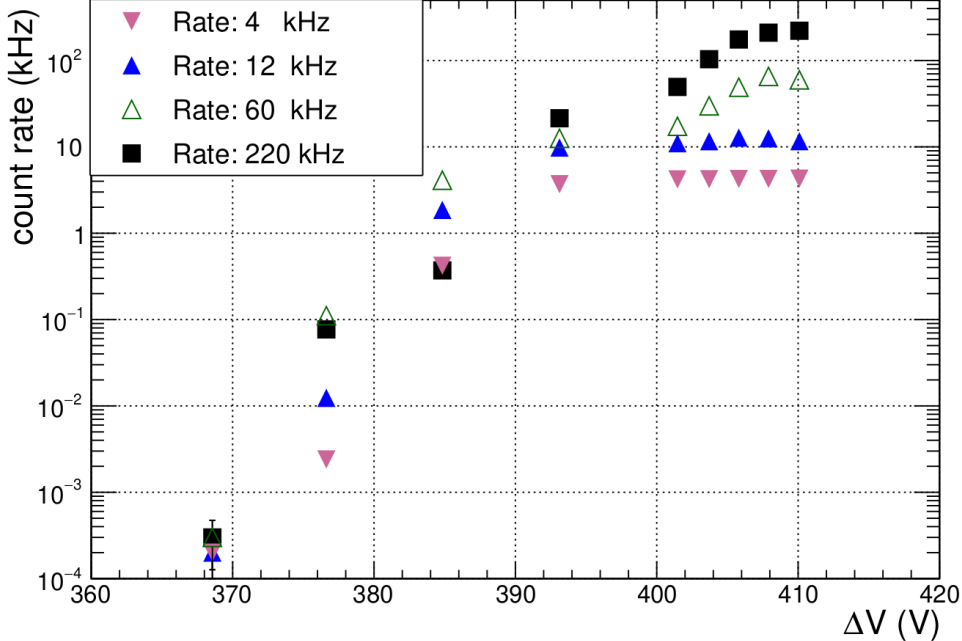
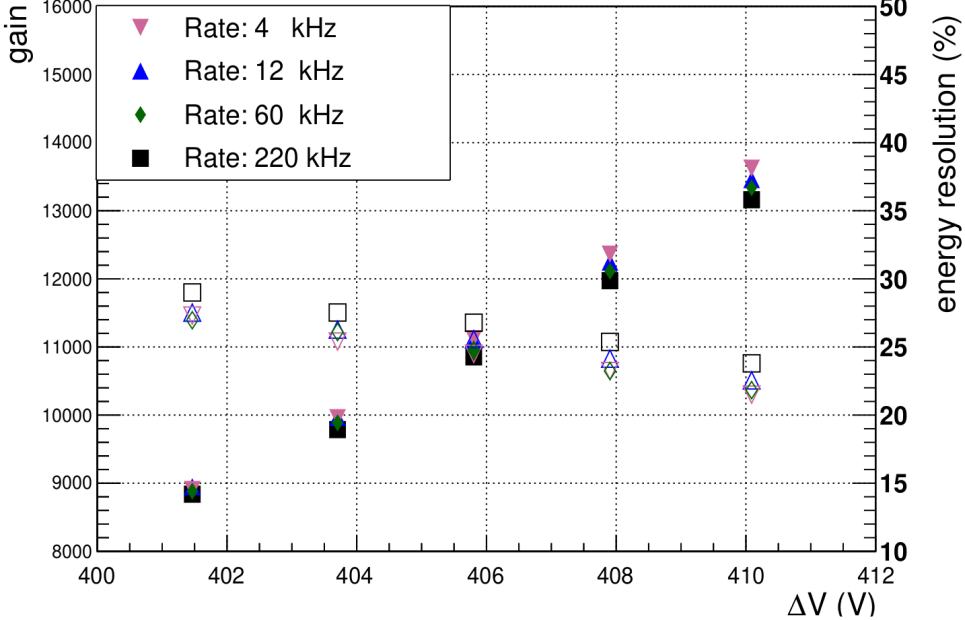
$$\text{Energy resolution} = \frac{\text{Sigma} \times 2.355}{\text{Mean}} \times 100 \%$$

Number of primary electrons (n)

$$n = E_{\text{gamma}} \left(\frac{\% \text{ of Ar}}{W_{\text{Ar}}} + \frac{\% \text{ of CO}_2}{W_{\text{CO}_2}} \right)$$

For Ar/CO₂ in 70/30 volume ratio, the average number of the primary electrons is 212 with the 5.9 keV X-ray source

Gain, energy resolution & count rate



$$\text{Gain} = \frac{\text{Output charge}}{\text{Input charge}} = \frac{(\text{Mean pulse height} / 2 \text{ mV}) \text{ fC}}{\text{No of primary electrons} \times e \text{ C}}$$

$$\text{Energy resolution} = \frac{\text{Sigma} \times 2.355}{\text{Mean}} \times 100 \%$$

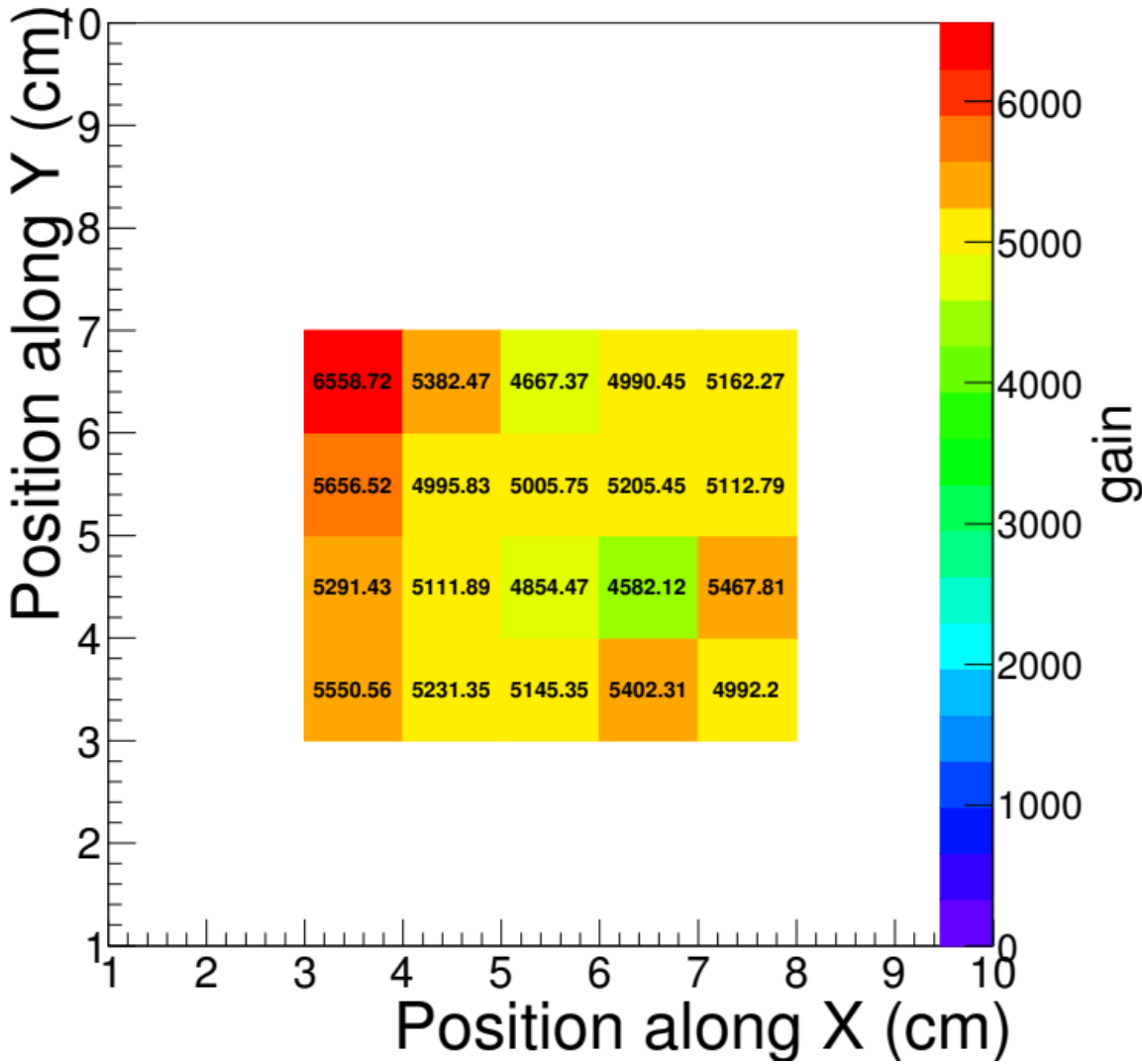
Number of primary electrons (n)

$$n = E_{\text{gamma}} \left(\frac{\% \text{ of Ar}}{W_{\text{Ar}}} + \frac{\% \text{ of CO}_2}{W_{\text{CO}_2}} \right)$$

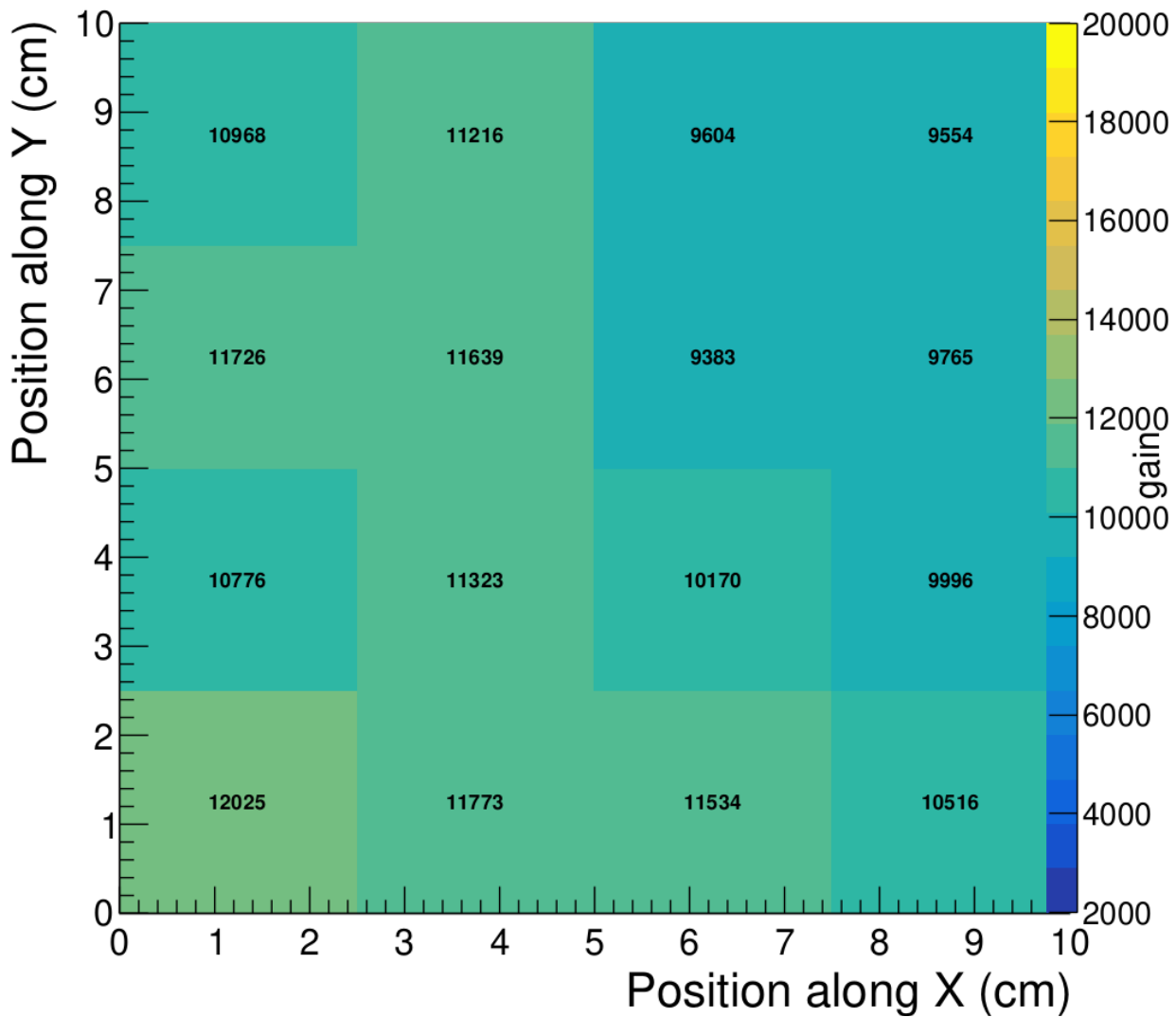
For Ar/CO₂ in 70/30 volume ratio, the average number of the primary electrons is 212 with the 5.9 keV X-ray source

Measurement of uniformity in the characteristics of triple GEM chamber prototypes

Uniformity in gain of a triple GEM chamber

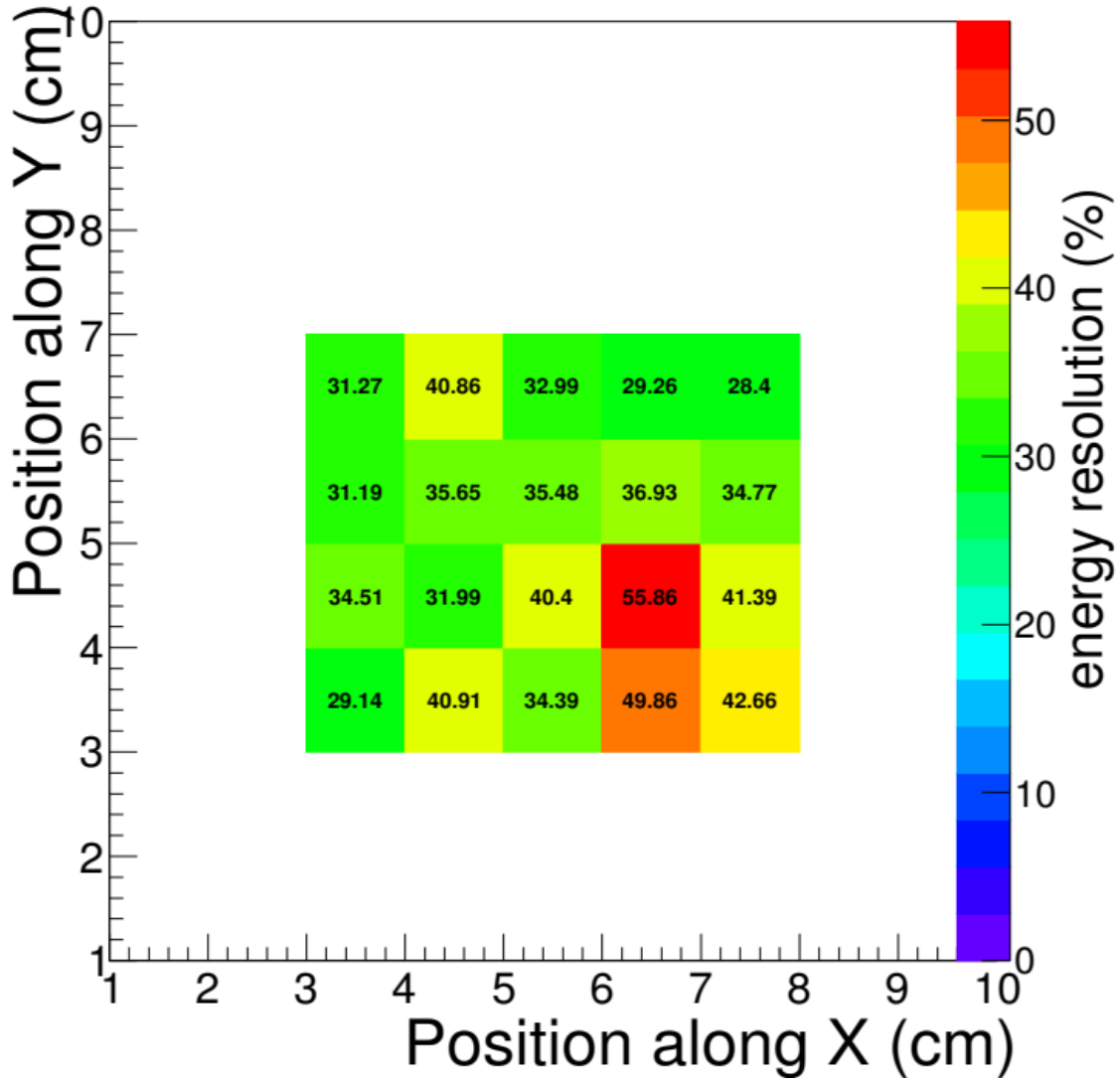


DM GEM; $\Delta V \sim 386$ V; Ar/CO₂ : 70/30
Fluctuation < 10%

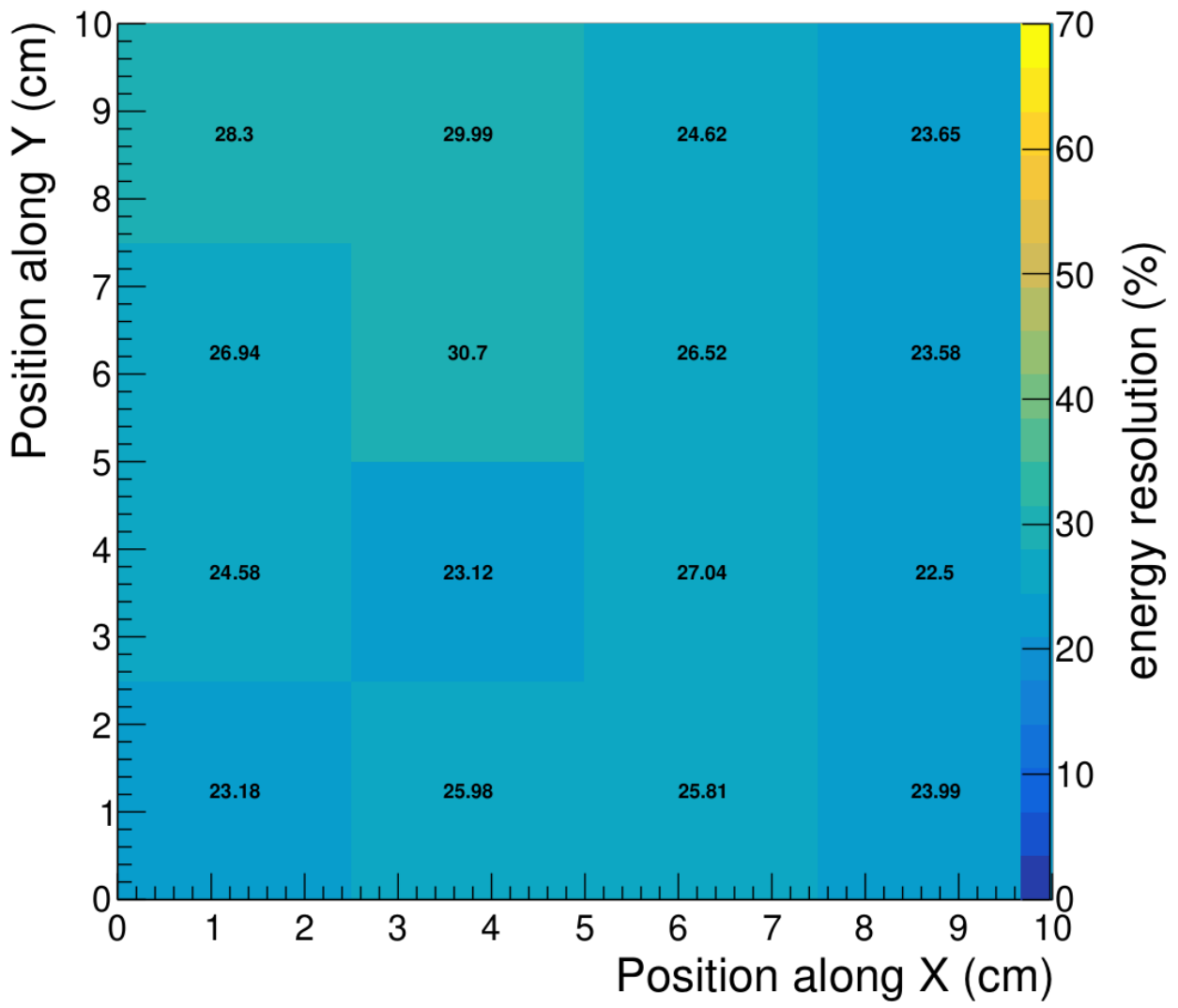


SM GEM; $\Delta V \sim 403$ V; Ar/CO₂ : 70/30
Fluctuation < 10%

Uniformity in energy resolution of a triple GEM chamber

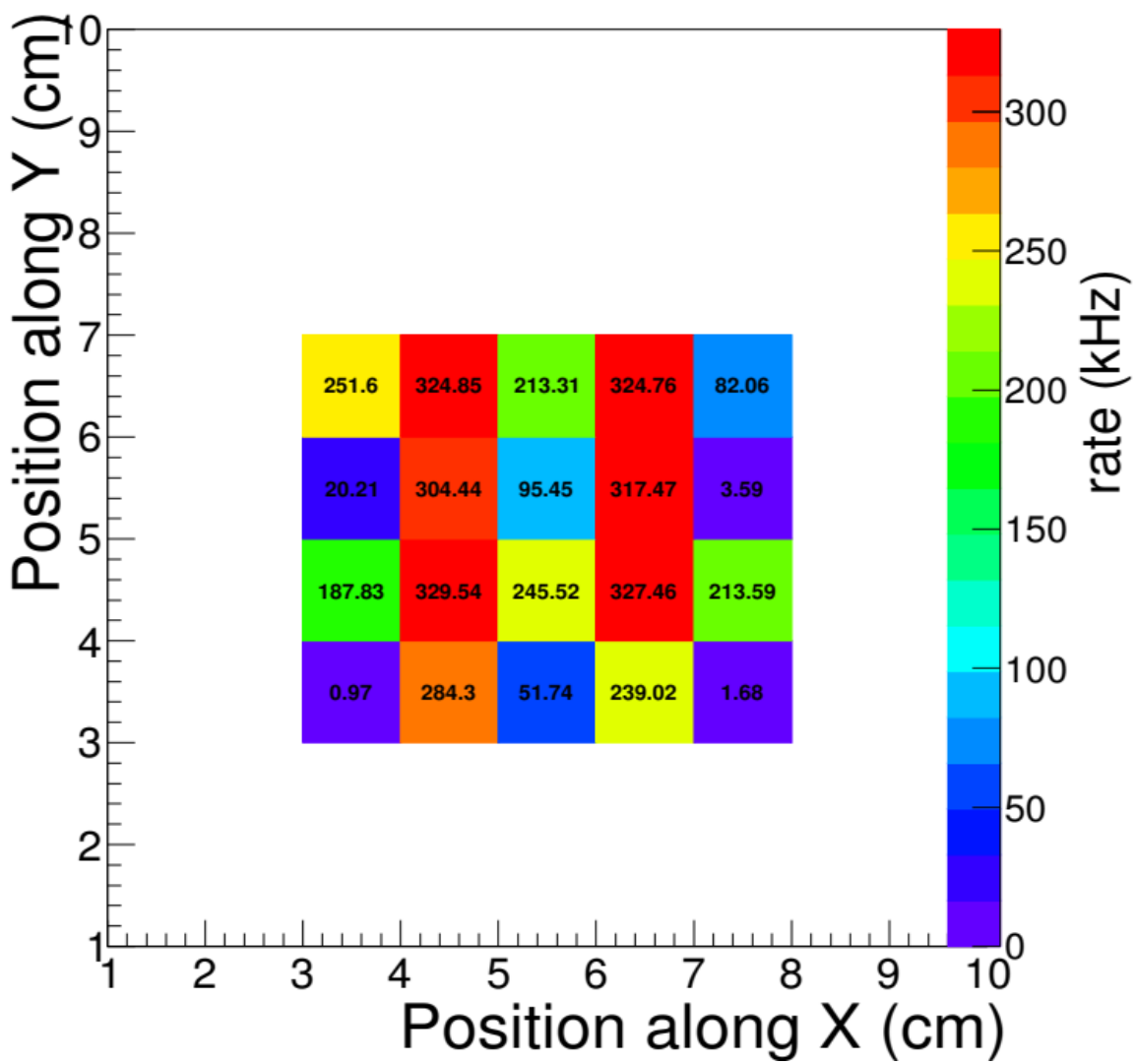


DM GEM; $\Delta V \sim 386$ V; Ar/CO₂ : 70/30
Fluctuation < 20%

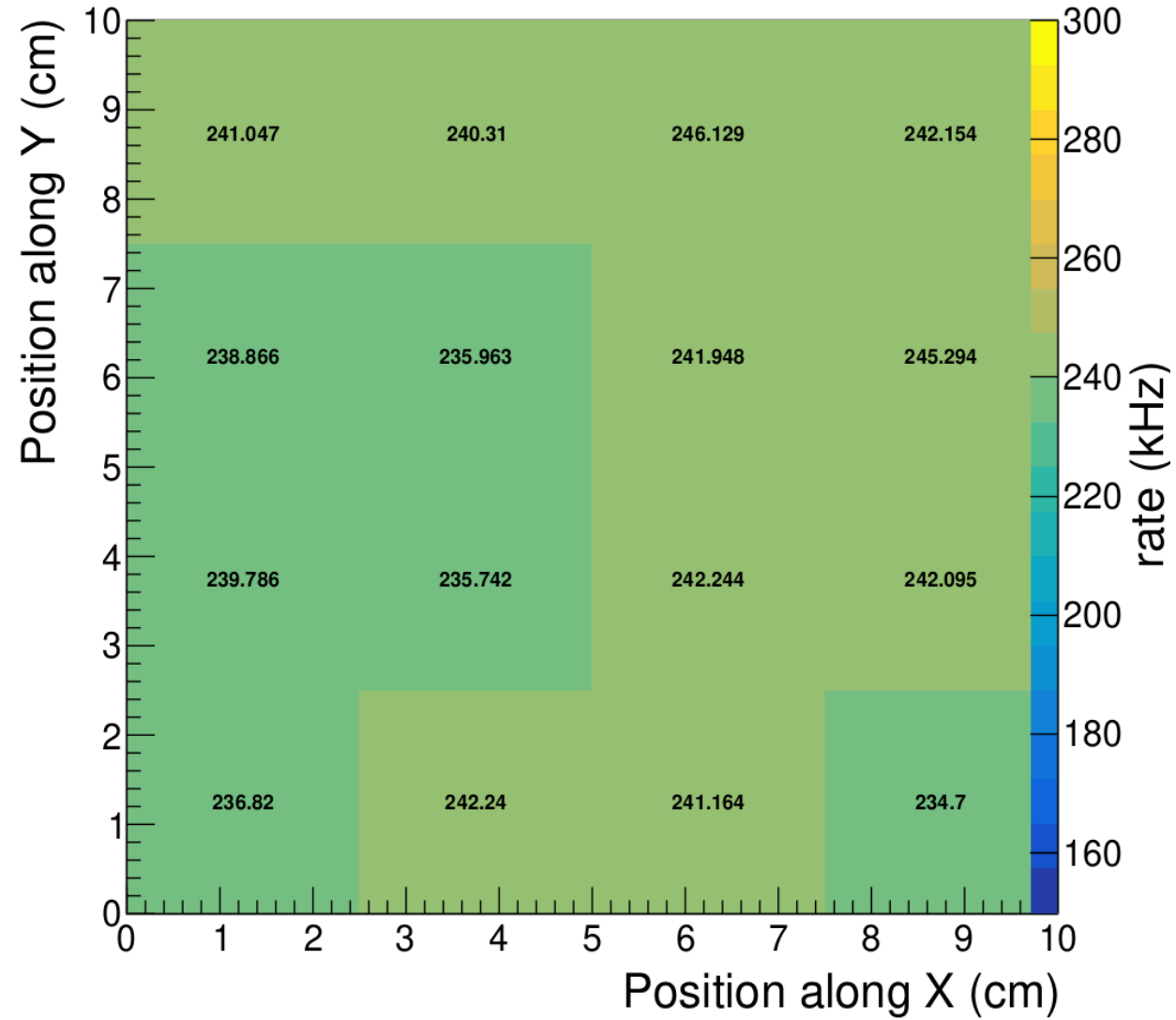


SM GEM; $\Delta V \sim 403$ V; Ar/CO₂ : 70/30
Fluctuation < 10%

Uniformity in count rate of a triple GEM chamber



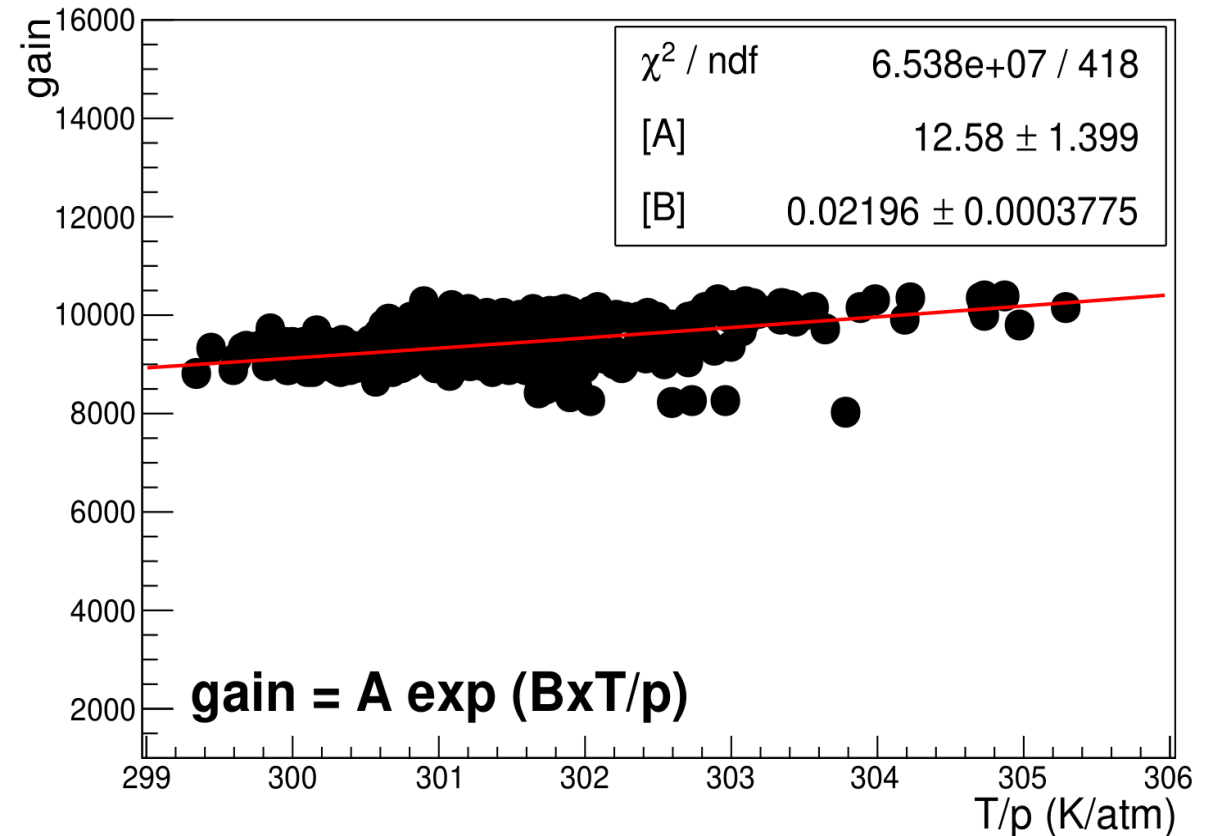
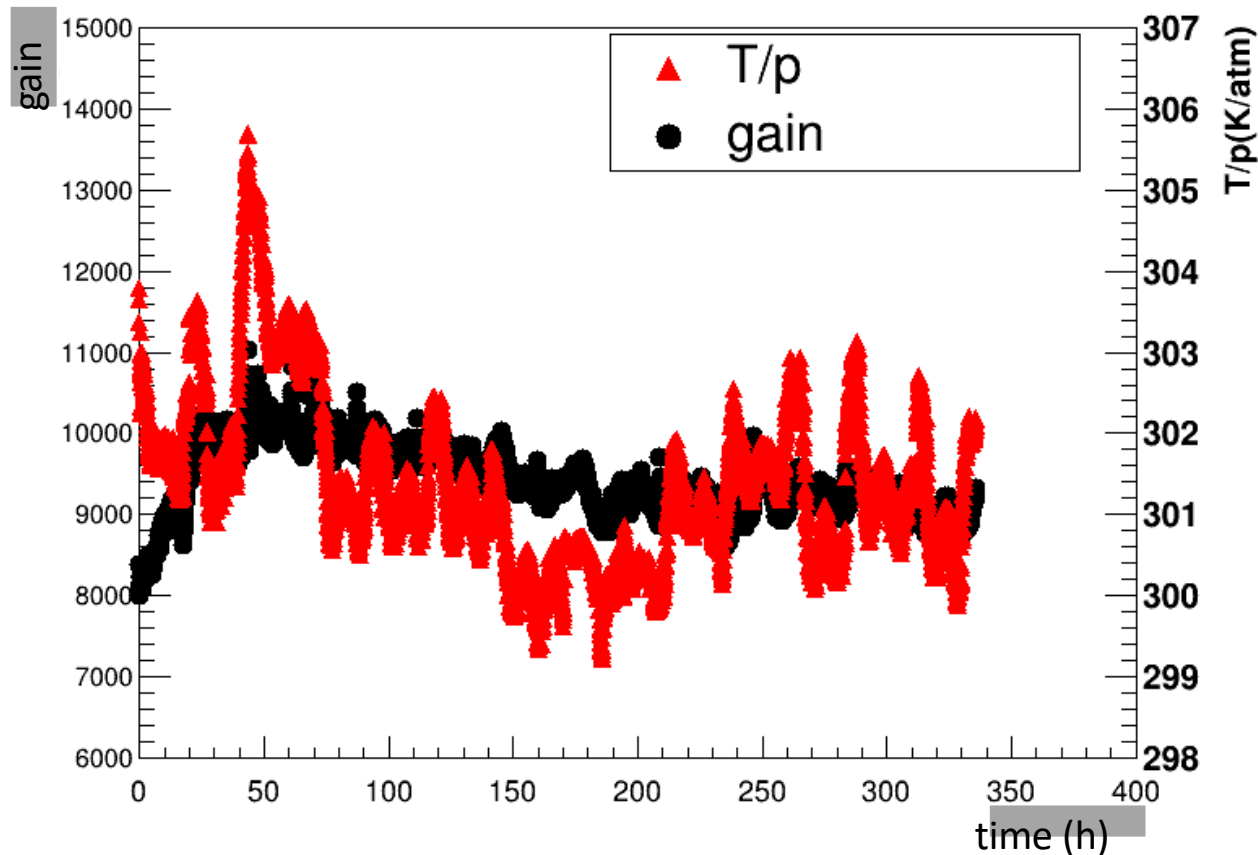
DM GEM; $\Delta V \sim 386$ V; Ar/CO₂ : 70/30
Fluctuation < 20%



SM GEM; $\Delta V \sim 403$ V; Ar/CO₂ : 70/30
Fluctuation < 5%

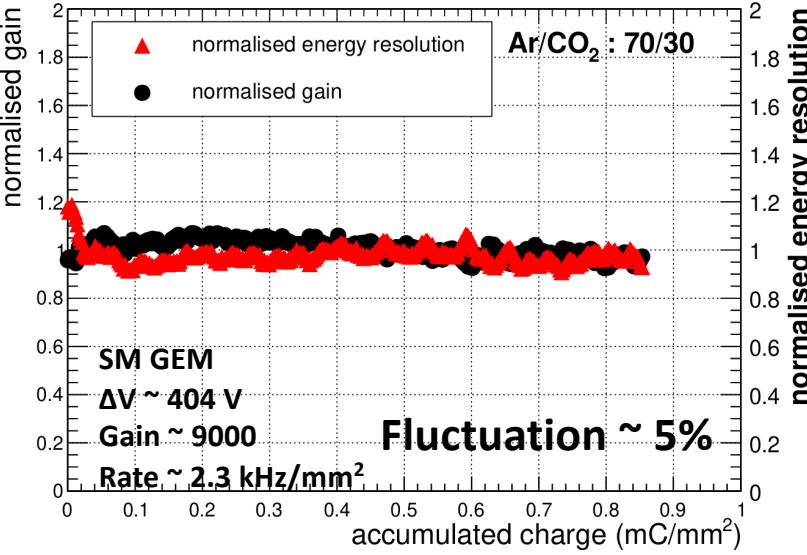
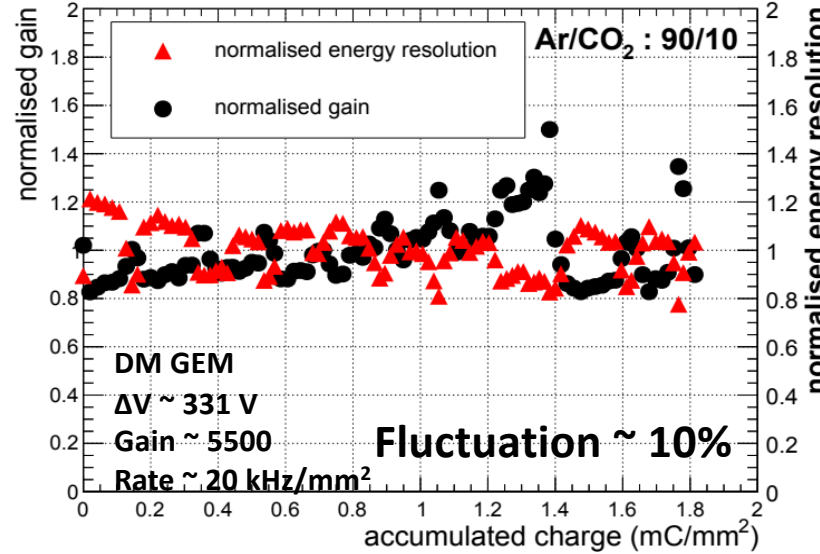
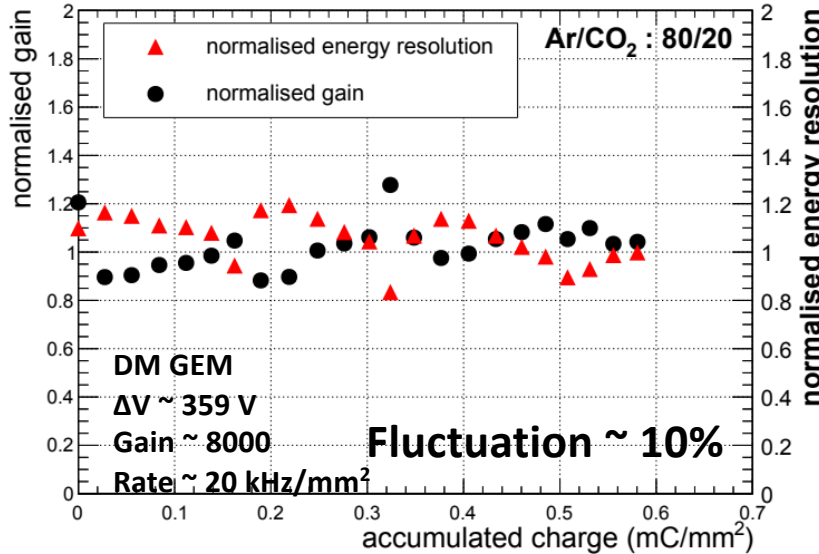
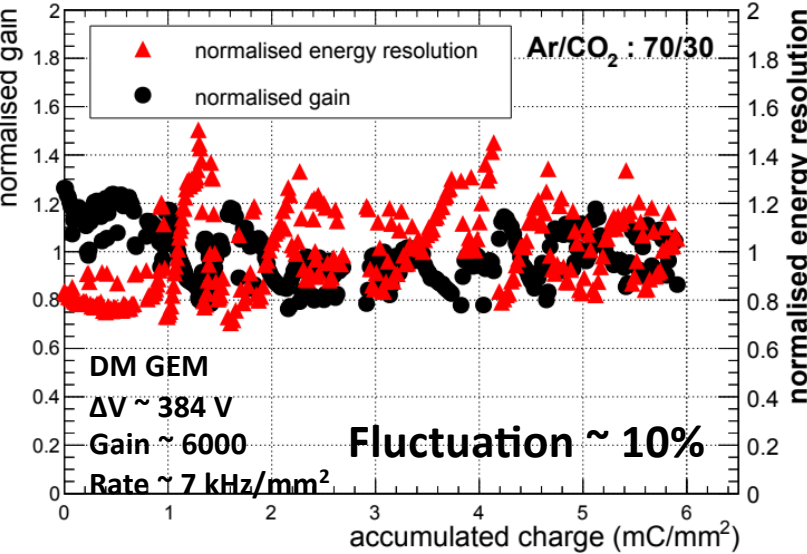
Long-term stability study of triple GEM prototypes

Variation of gain with T/p



- Gain of the chamber can be expressed as e^α , where α is the first Townsend coefficient
- Townsend coefficient $\alpha \propto 1/\rho \propto T/p$; ρ = mass density, T = temperature, p = pressure
- Gain of the chamber depends on the variation of T/p
- Gain is normalised using a parameterisation of the form $Ae^{(BT/p)}$

Normalised gain & energy resolution vs accumulated charge



$$\frac{dq}{dA} = \frac{r \times n \times e \times G \times dt}{dA}$$

r = rate, n = no of primary electrons, dt = time
 e = electronic charge, G = gain, dA = irradiated are

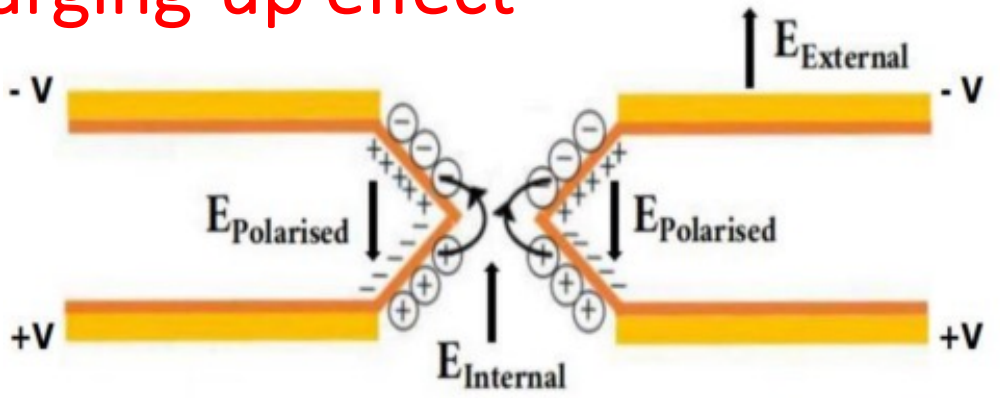
Gain and energy resolution is normalised by T/p ratio to nullify the effects of temperature and pressure variations

No significant degradation in normalised gain and energy resolution is observed

Typical accumulated charge for 10 CBM years is $\sim 0.8 \text{ mC/mm}^2$ at the gain of 10^3

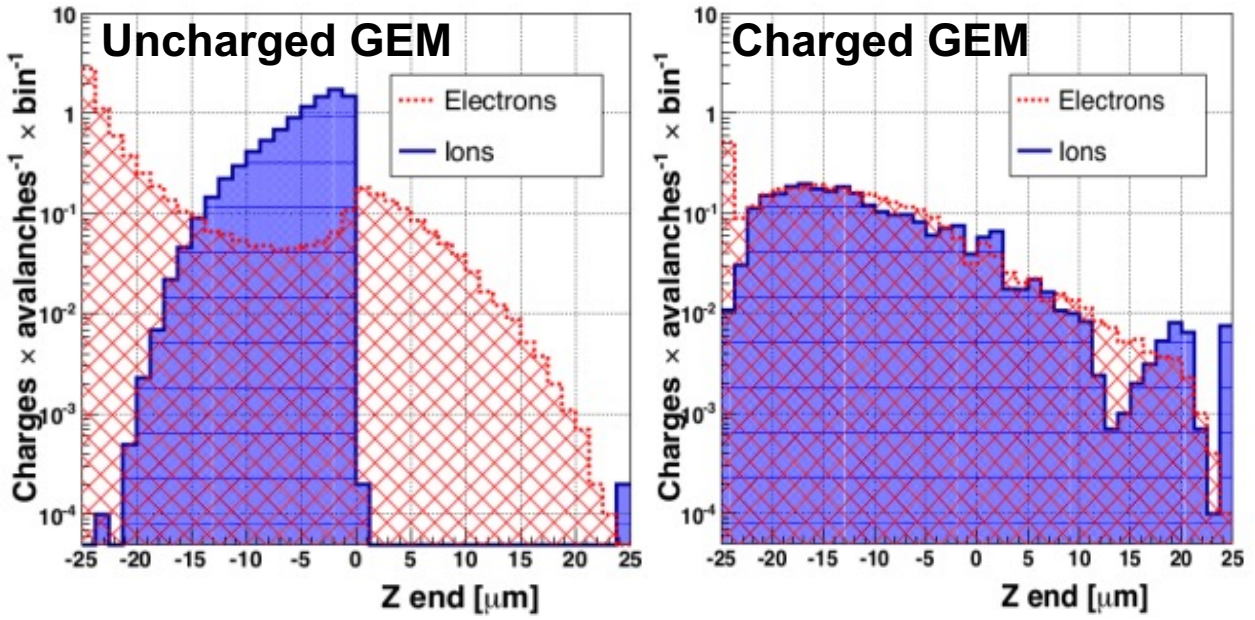
Charging-up effect in triple GEM chamber prototypes

Charging-up effect



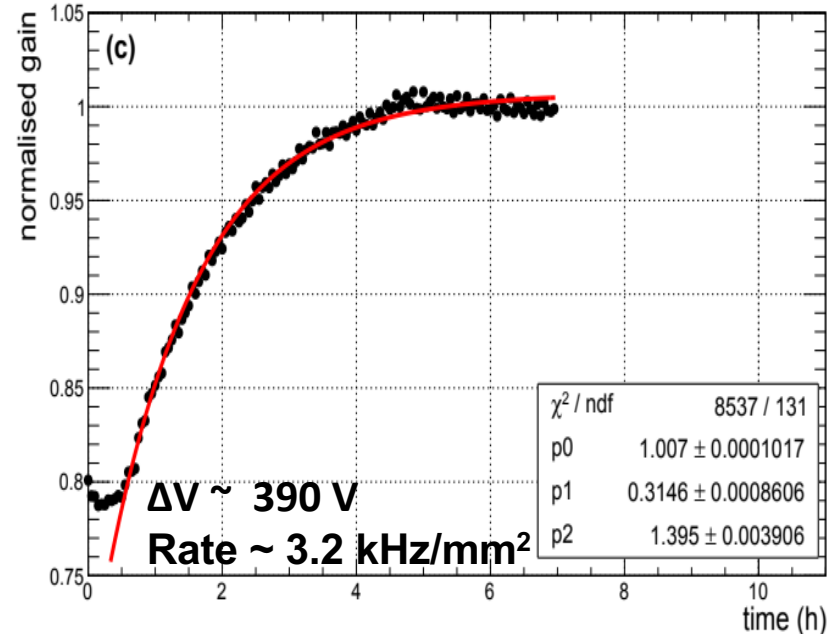
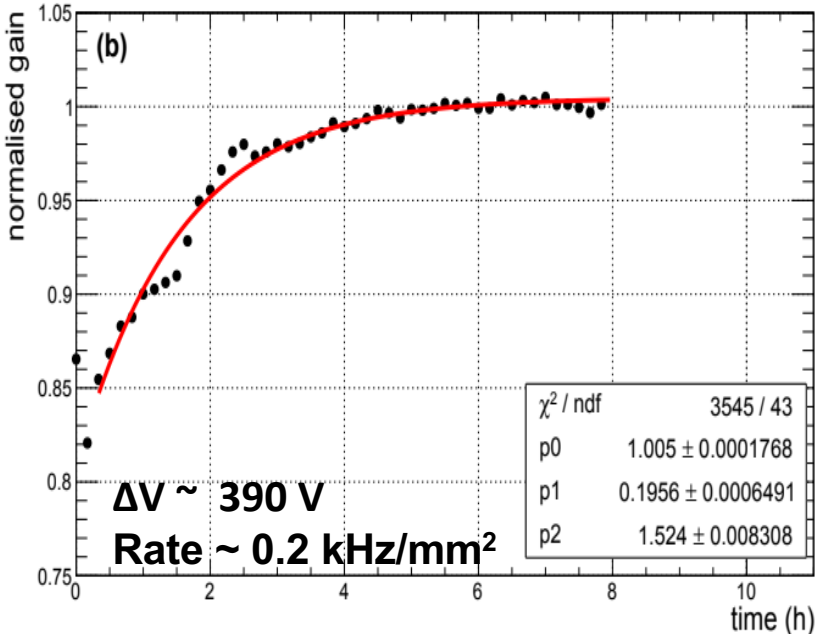
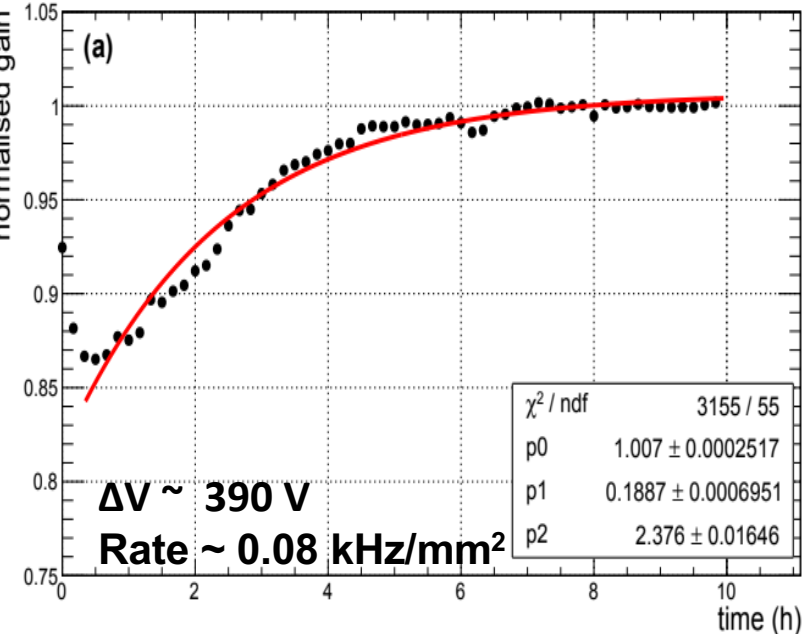
Schematic representation of the charging-up effect inside the GEM hole

- During the multiplication process inside the GEM hole, electrons and ions diffuse to the polyimide part of the GEM and adsorbed there.
- These new charges accumulate over time and dynamically change the electric field inside the hole. This is known as the charging-up effect.
- Those accumulated charges create a lensing effect and as a result, the gain increases for the first few hours of operation.
- After some time when the dynamical equilibrium is reached, the gain reaches asymptotically a constant value.



Simulated spatial distribution of deposited on the insulator surface of the uncharged and charged GEM foil

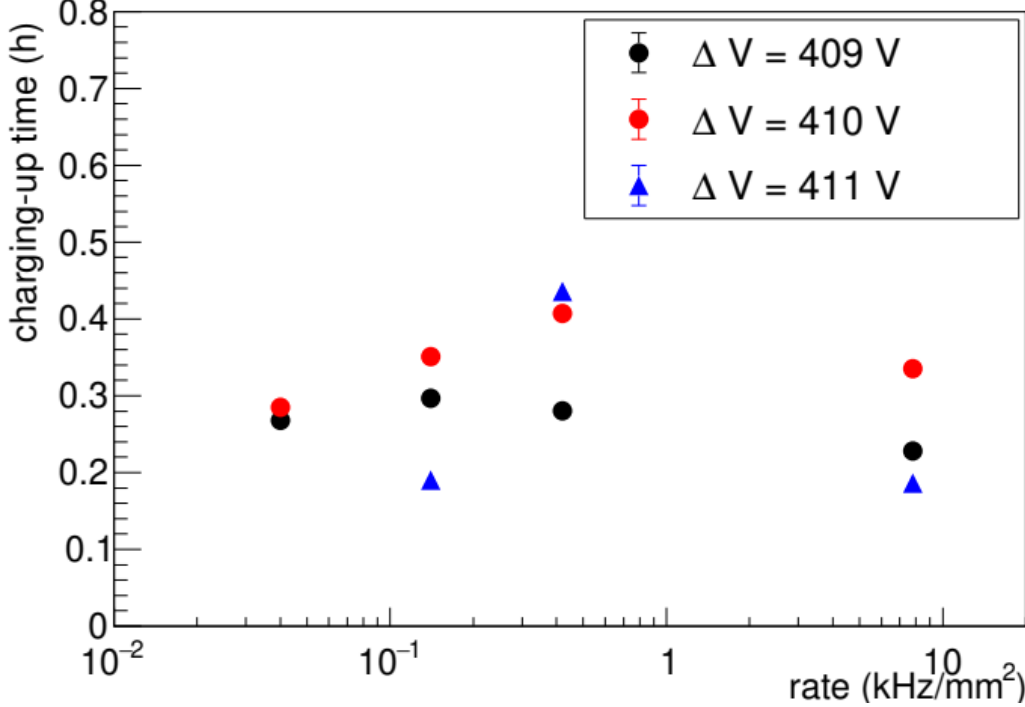
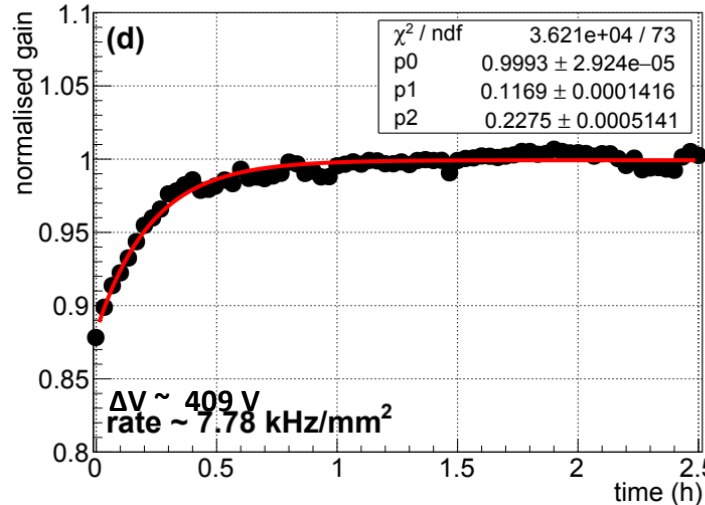
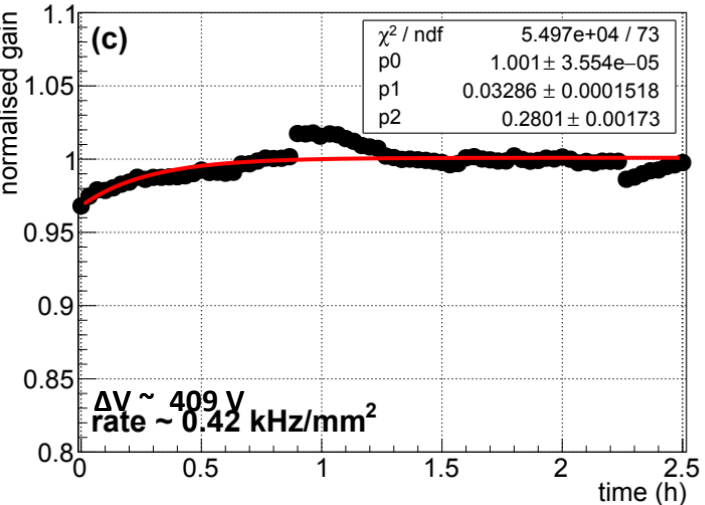
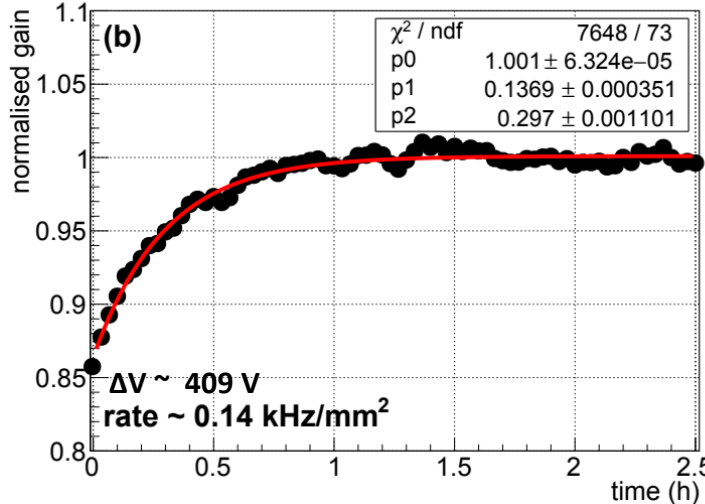
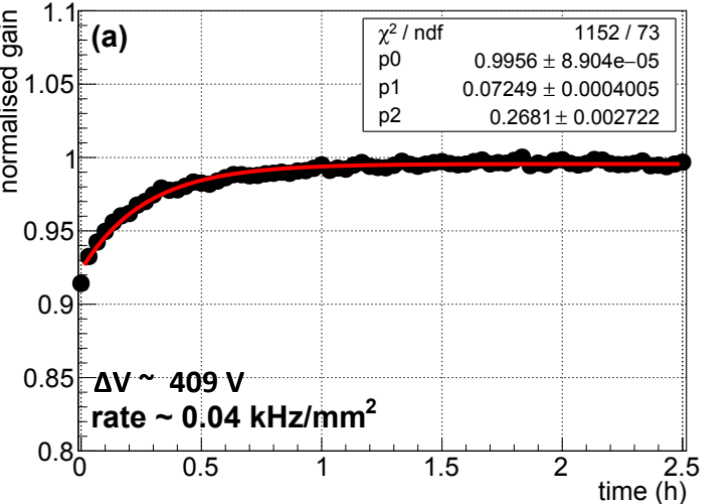
Charging-up effect in DM GEM



ΔV (V)	Rate (kHz/mm ²)	Charging-up time (hour)	Saturated gain
~ 390	~0.08	2.376(+0.0165)	~4900
	~0.2	1.524(+0.0083)	~5100
	~3.2	1.395(+0.0039)	~5500

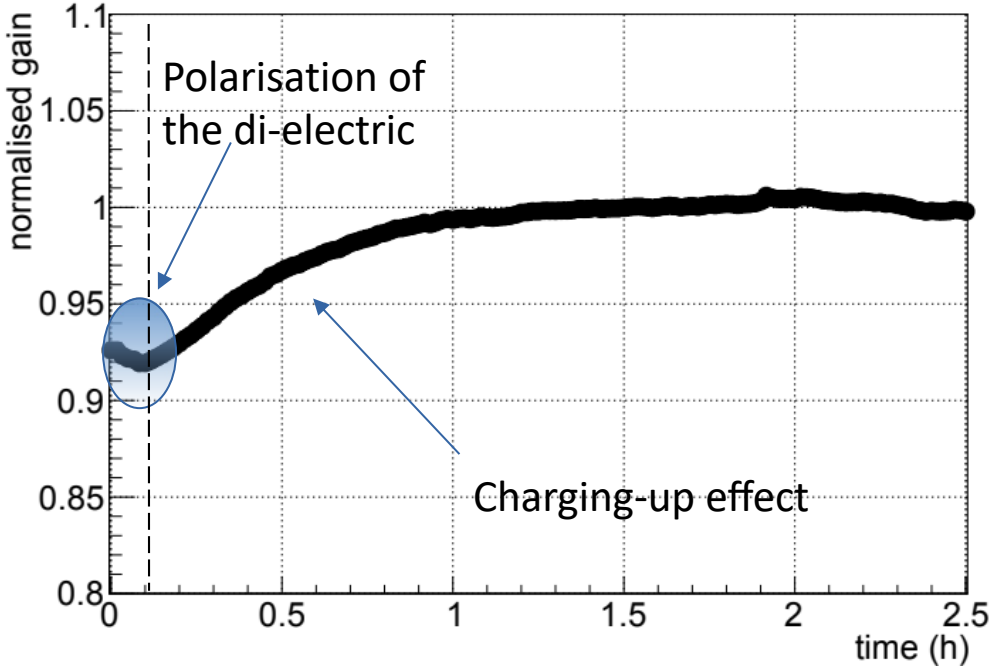
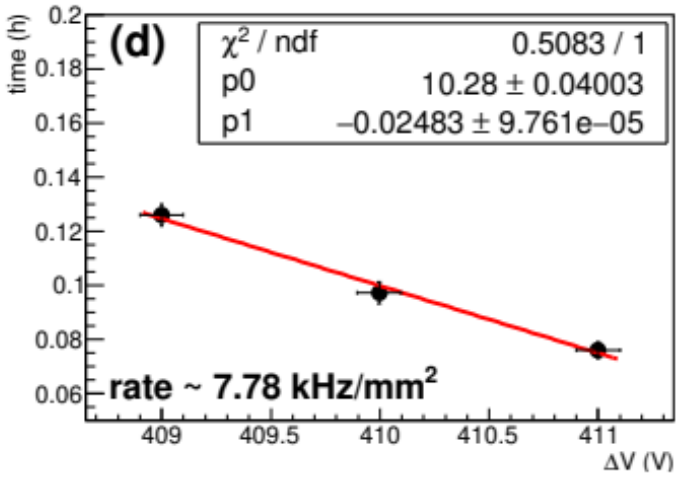
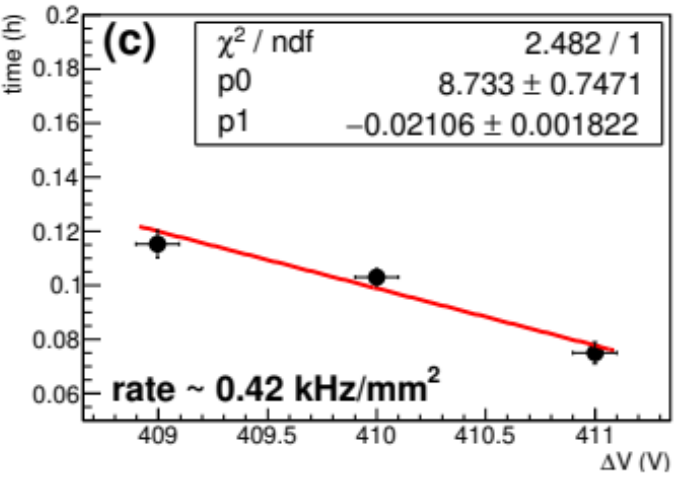
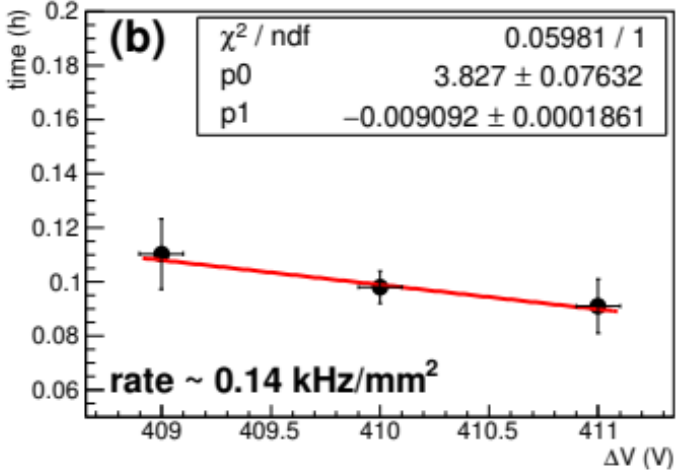
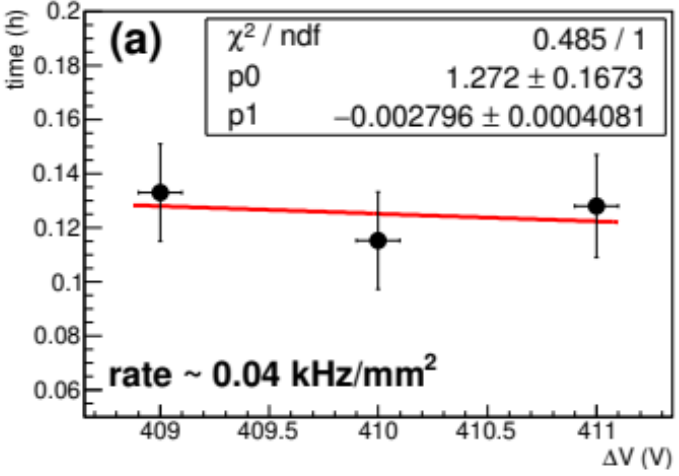
- Gain is normalised to eliminate the effects of temperature and pressure
- Normalised gain is fitted with $p_0 (1 - p_1 e^{-t/p_2})$, taking analogy from the charging-up of RC network

Charging-up effect in SM GEM



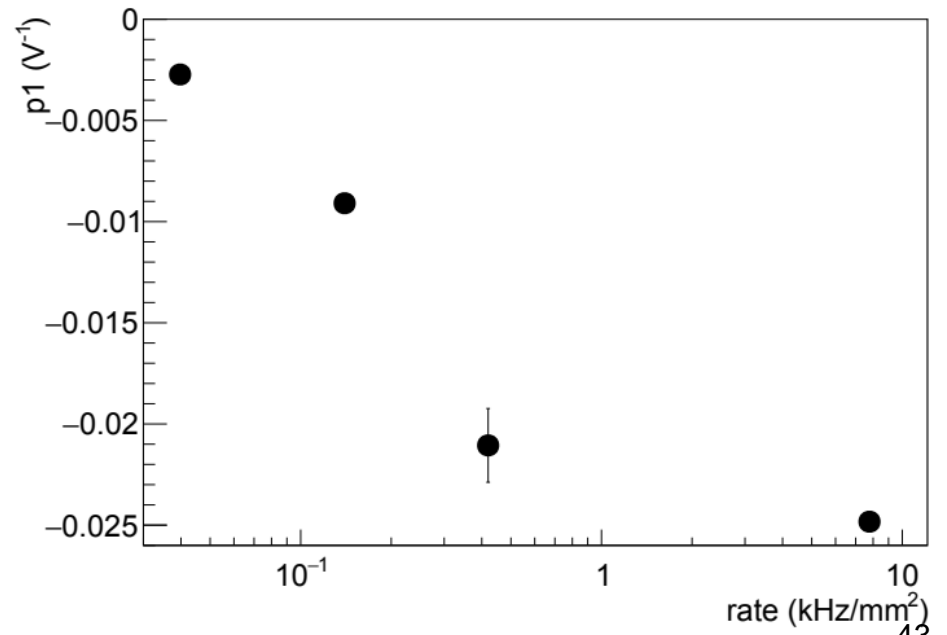
- Charging-up time is found to be between 0.2 – 0.4 hours for the saturation gain $\sim 10^4$

Effect of di-electric polarisation



- The time up to which the gain decreases initially due to the polarisation effect is anti-correlated with the voltage across the GEM foil.

- The rate of decrease of time with ΔV increases with the increasing rate of irradiation



Measurement of spark probability

Spark probability measurement

Objective

Study of the spark probability for a SM triple Gas Electron Multiplier (GEM) detector with pion beam and shower.

Summary of the test beam

Detector:

-> Single mask triple GEM detector

Measurement with:

-> Pion beam

-> Pion beam with absorber:
Shower

Measured parameters:

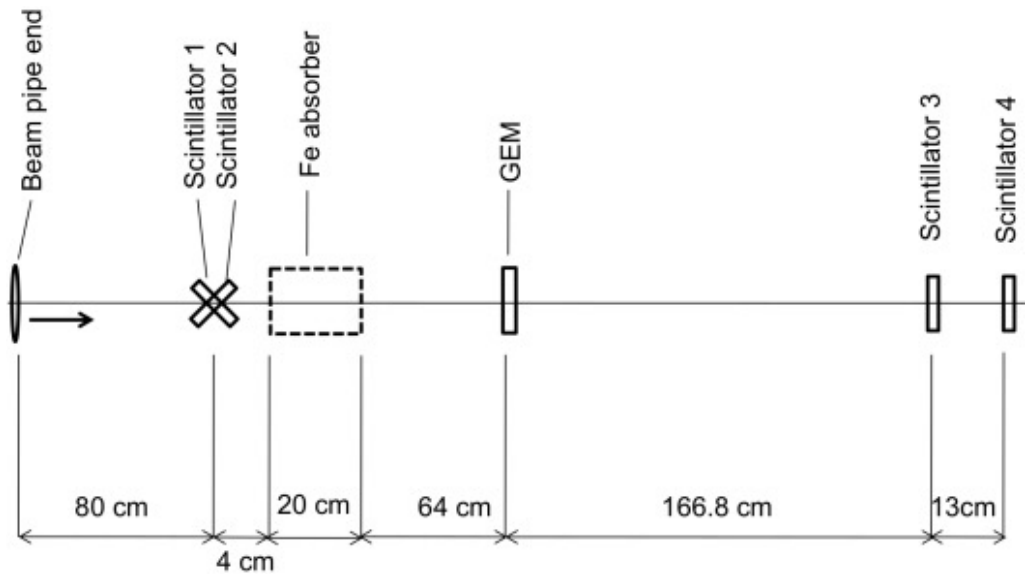
-> Current

-> Voltage

-> Trigger and GEM counts

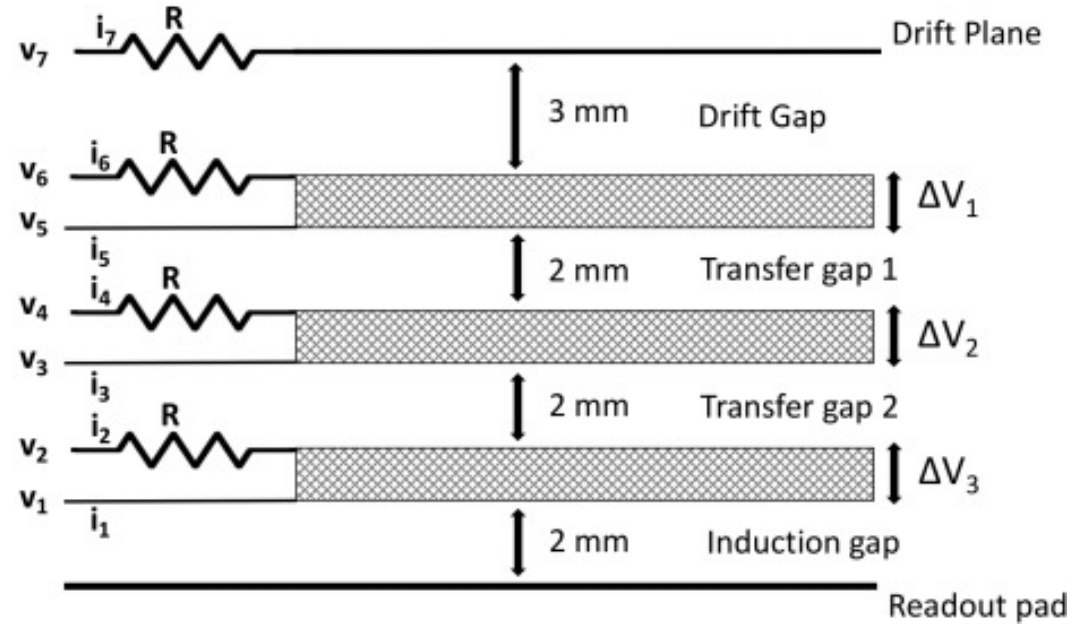
-> GEM signal

Experimental setup

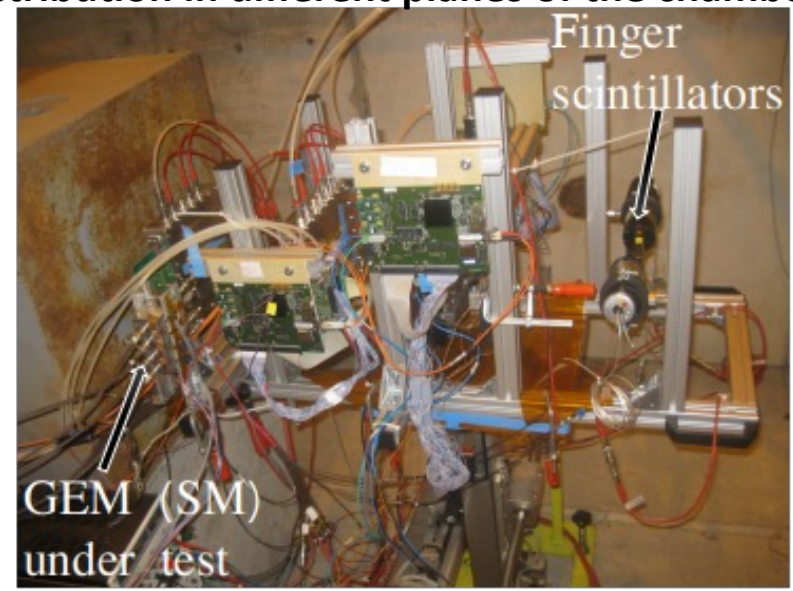


A sketch of the experimental setup

- Gas mixture: Ar/CO₂: 70/30
- 7 channel HVG210 power supply
- Readout plane consists of 512 pads of dimension 4x4 cm²
- 4 sum-up boards of 128 pins each are used for signal collection
- PXI LabView based DAQ is used
- 10 MΩ protection resistance is used on the top of each GEM layer

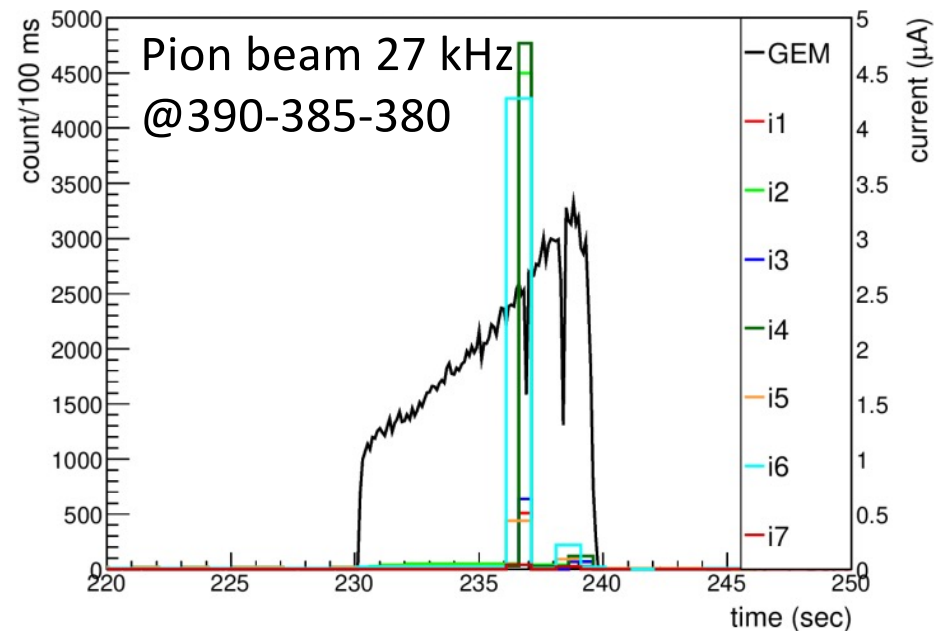
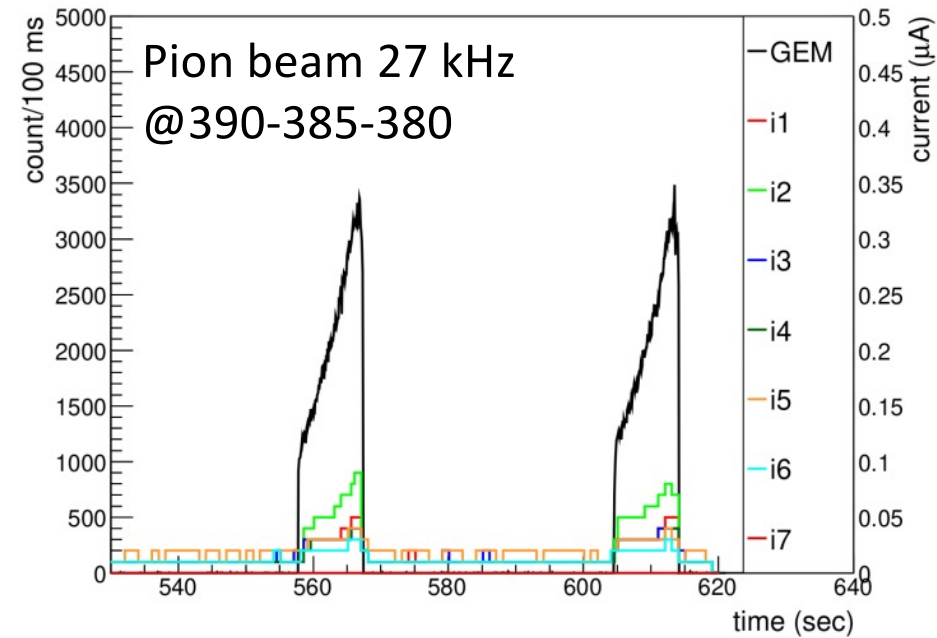


Arrangement of GEM foils, voltage and current distribution in different planes of the chamber



Setup for pion beam

Spill structure



Identify a spark

Absence of signal

-> Drop in the counting rate of GEM signals

Detection of high current

-> Sudden jump in the Current

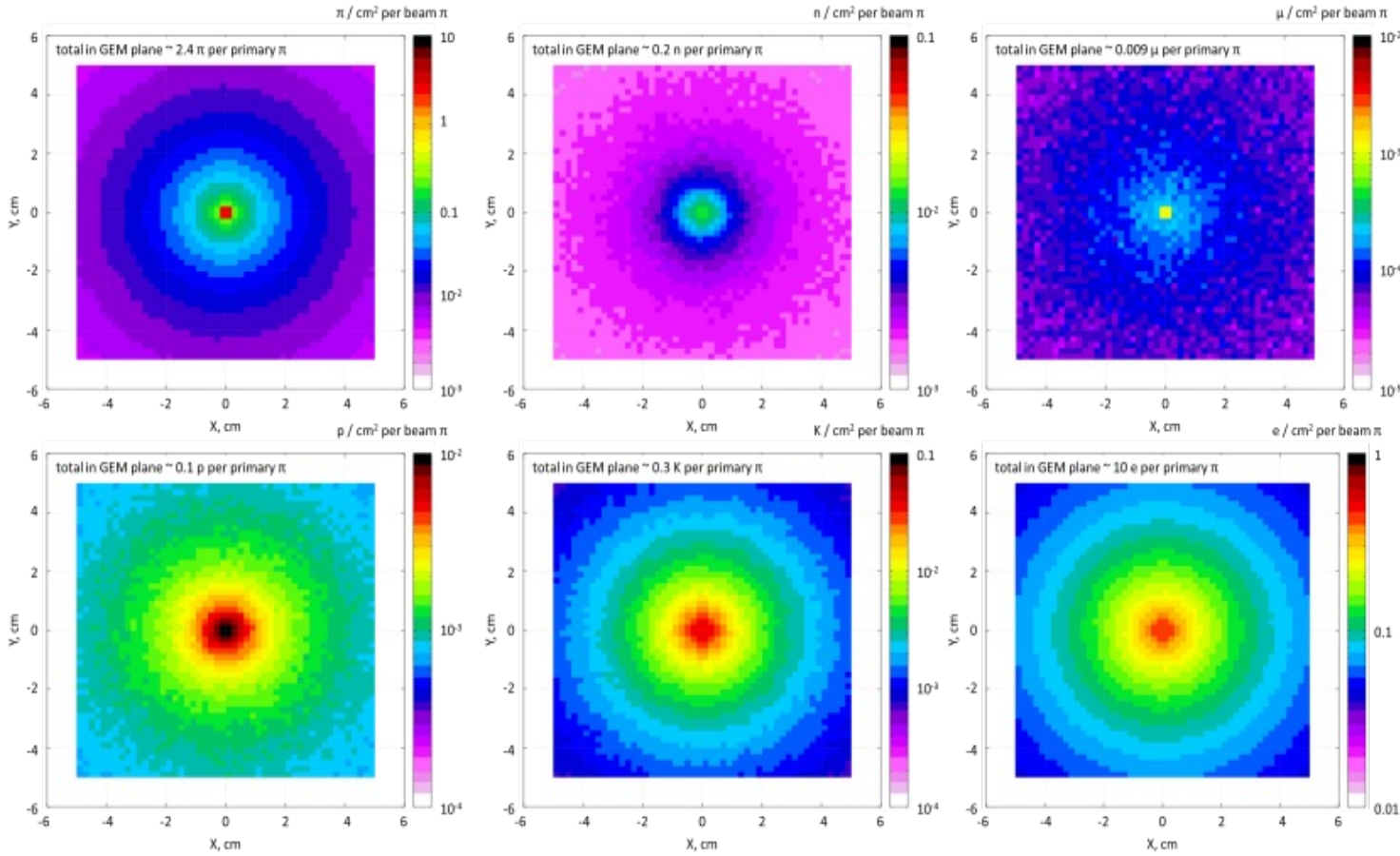
Pion beam rate	Particle rate on GEM
8 kHz	0.8 kHz/mm ²
27 kHz	2.7 kHz/mm ²
43 kHz	4.3 kHz/mm ²
48 kHz	4.8 kHz/mm ²
150 kHz	15 kHz/mm ²
170 kHz	17 kHz/mm ²

150 GeV/c pion beam

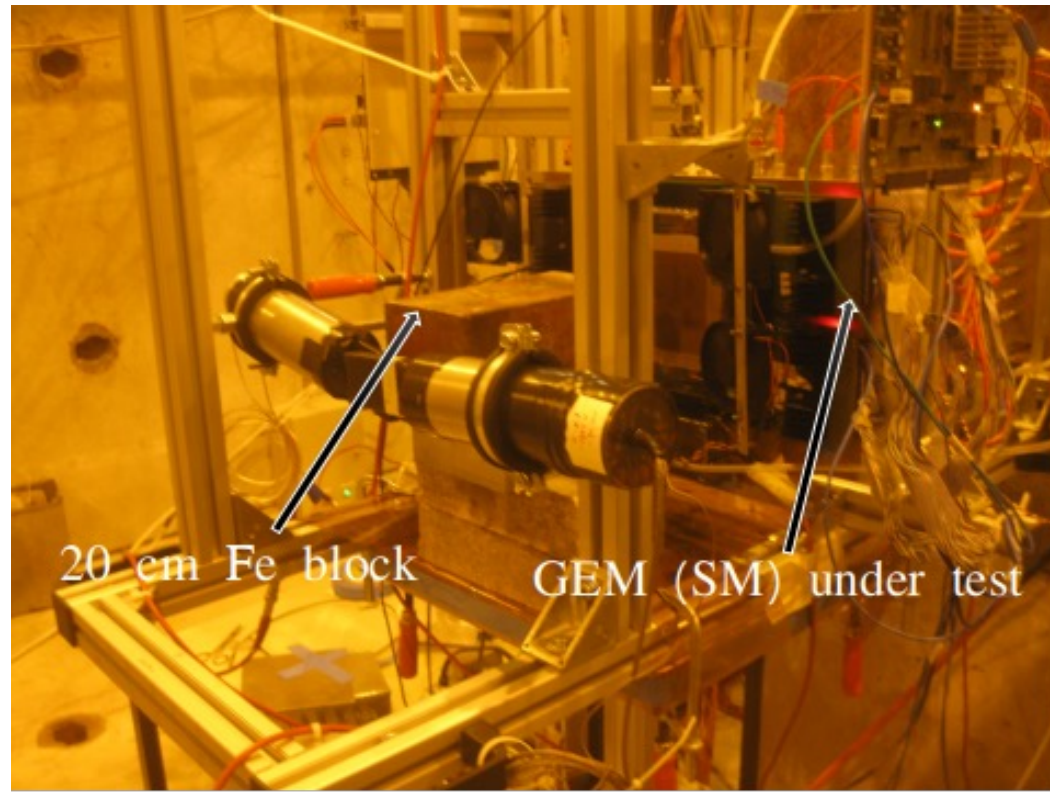
From simulation, it is found that the particle rate in the first two stations of MuCh will be $\sim 8 \text{ kHz/mm}^2$ and 1 kHz/mm^2 for central Au-Au collision at 8 AGeV/c respectively

Particle production during shower

Pion beam rate	Particle rate on GEM
6 kHz	0.008 kHz/mm ²
50 kHz	0.065 kHz/mm ²
120 kHz	0.16 kHz/mm ²



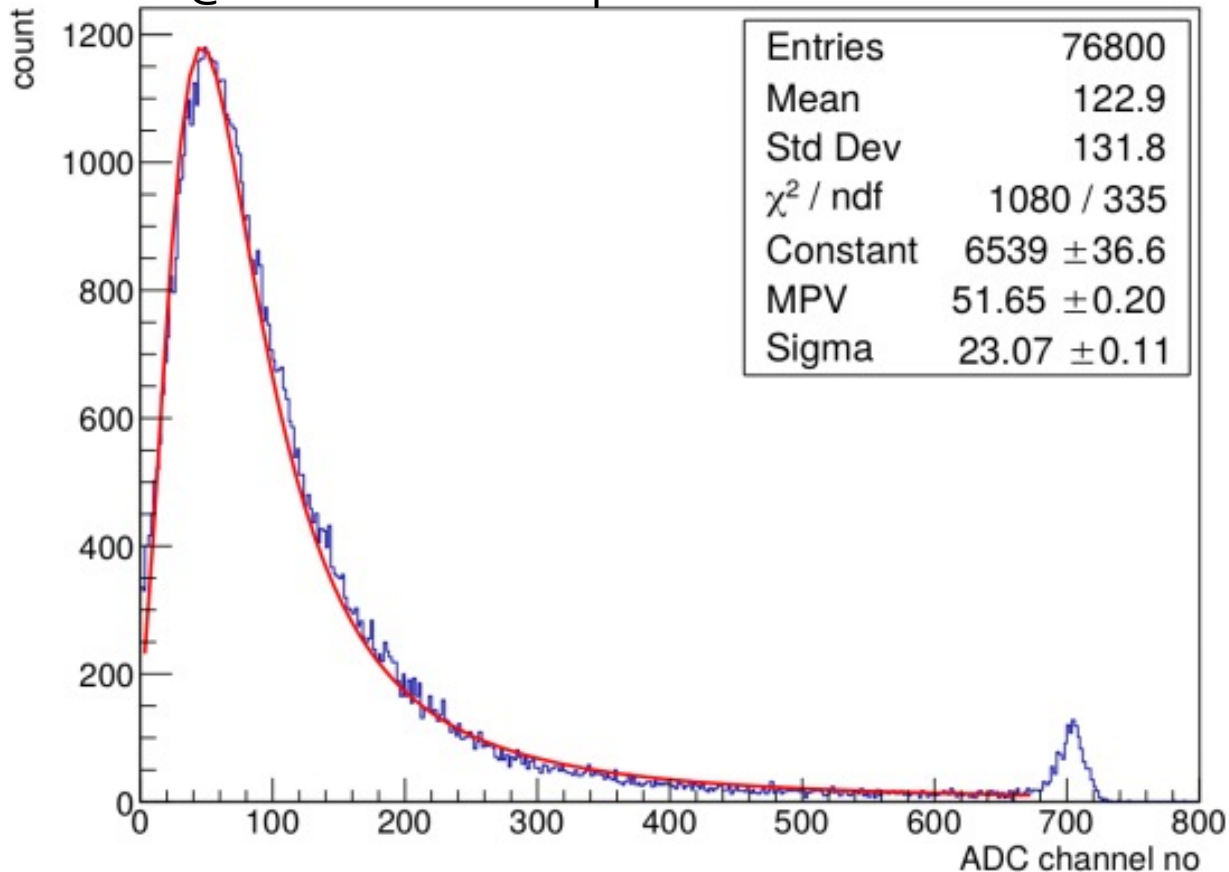
Particle production using shower from FLUKA simulation (Courtesy: Anna Senger)



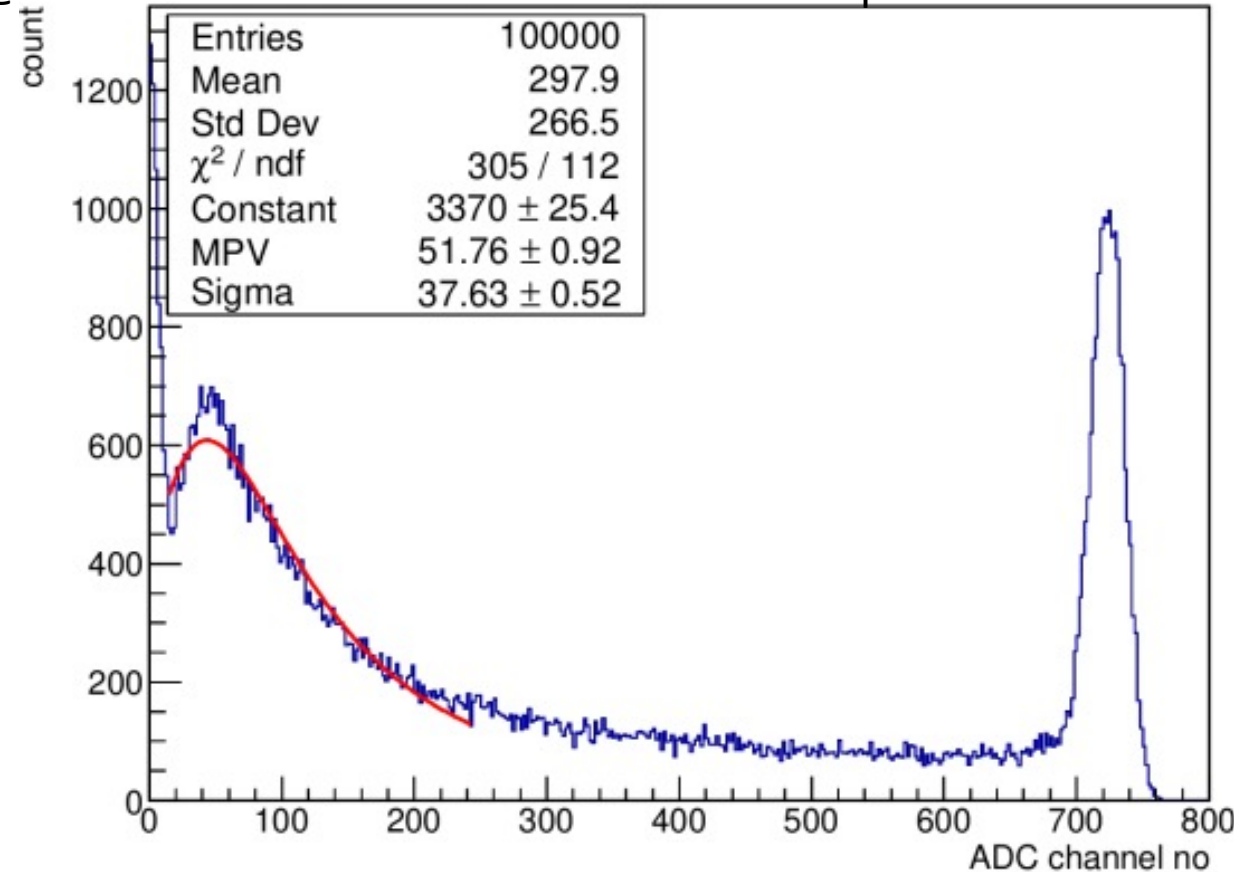
Setup for shower measurement

ADC distribution

@390-385-380 with pion beam: Rate 27 kHz

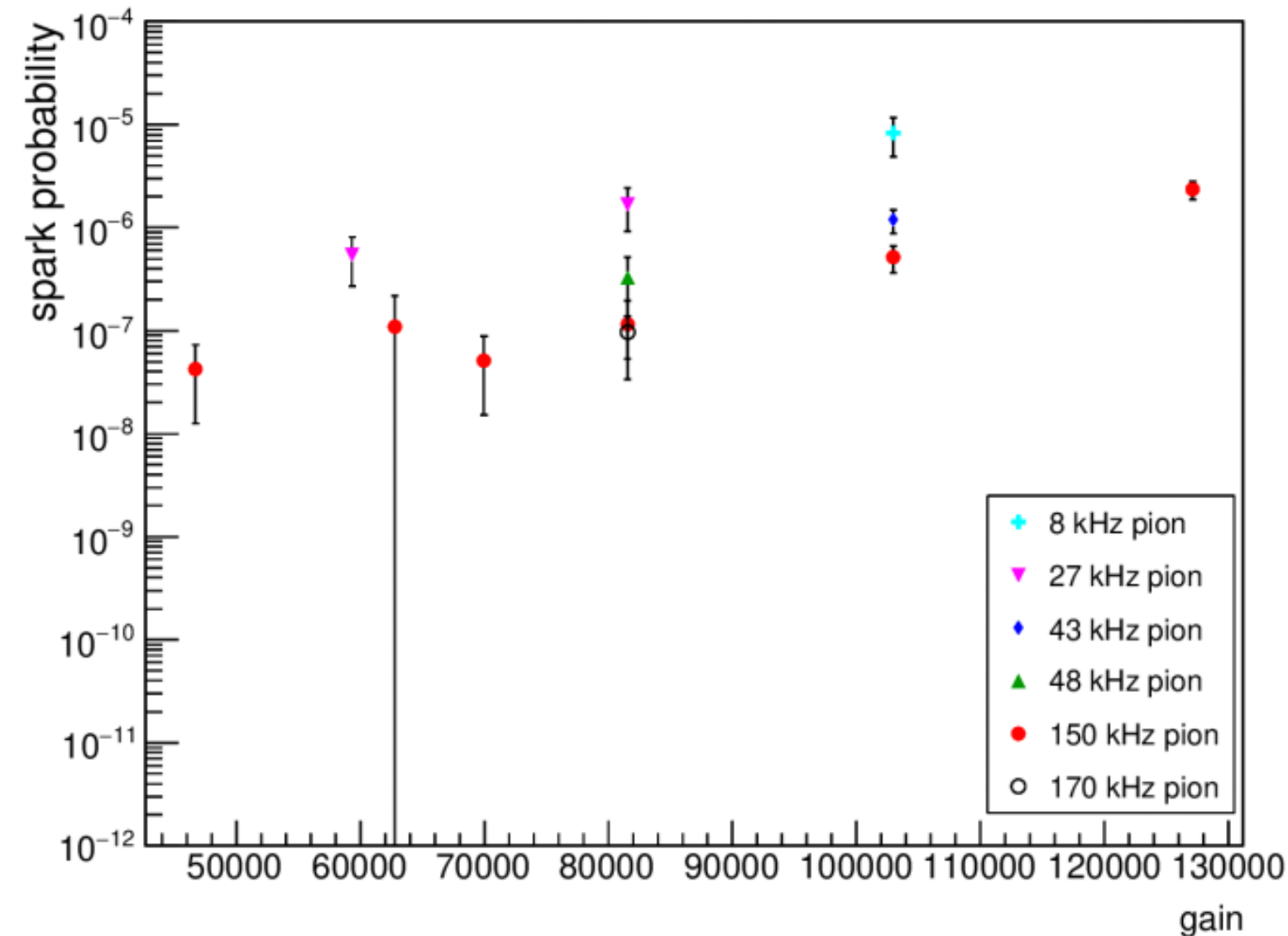


@390-385-380 with shower: Rate 1.5 kHz of pion on 20 cm Fe



- MPV is found to be same for pion beam and shower but a large saturation peak is observed for shower.
- Mean of the distribution is ~ 2.5 higher in shower as compared to pion beam.

Spark probability as a function of gain for pion



Summary

Drift gap : 3mm

Protection resistance : 10 M Ω (On drift and top layers of the GEM foil)

Spark probability was measured for pion beam and shower induced by pion beam on a 20 cm thick Fe

Operational gain : 40,000 - 1,30,000

Spark probability $\sim 10^{-7}$ for 150 GeV/c pion beam at gain between 40,000 - 80,000

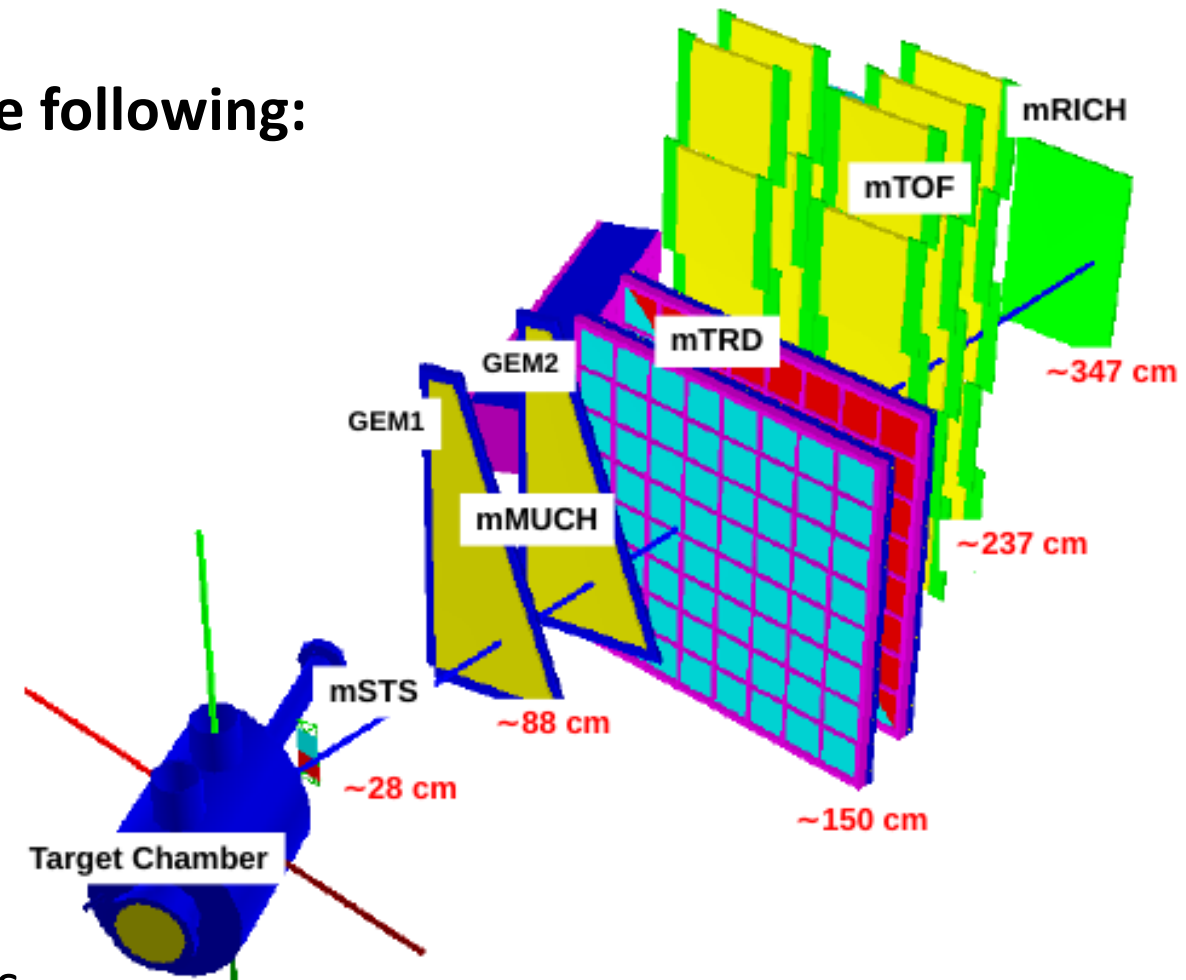
Discharge probability: No. of Discharge/ No. of incident particle

GEM chambers @mCBM

mCBM @GSI (SIS-18)

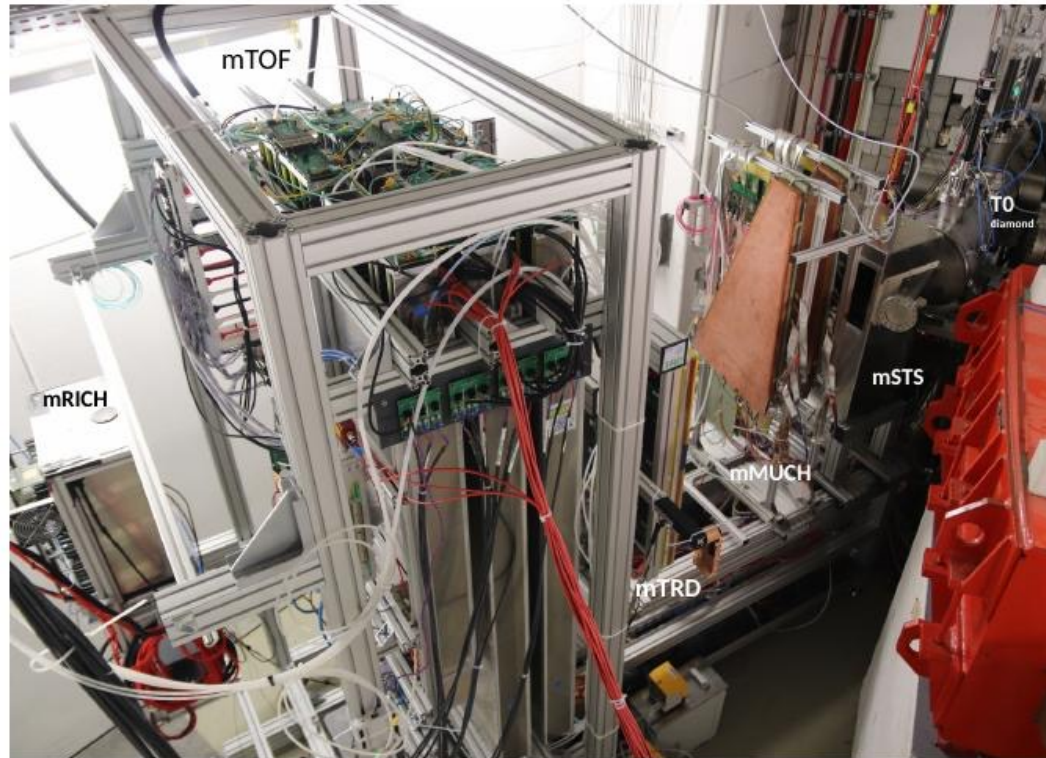
The proposed aims of the mCBM campaign are the following:

- Understanding of the detector sub-systems performance in high rate nucleus-nucleus collision environment
- Free-streaming data acquisition including the data transfer and handling
- Implementation and tuning of the online track and event reconstruction as well as the event selection algorithms
- Understanding of the detector control systems



Schematic of the mCBM experimental setup

mCBM @ GSI (SIS-18)



Detector setup at mCBM cave



GEM modules of mMUCH at
mCBM cave



GEM modules of mMUCH

Summary

- **Characteristics studies of triple GEM chambers**
 - > Long term stability study doesn't show any significant degradation in the performance in terms of gain and energy resolution of the chamber
- **Spark probability measurement of a triple GEM chamber prototype**
 - > The spark probability is found to be $\sim 10^{-7}$ for the pion beam of momentum ~ 150 GeV/c for a gain of $\sim 10^4$
- **Real size triple GEM chambers are tested at mCBM@SIS18**

From all the results of the detailed R&D on GEM, it can be concluded that GEM is one of the best options for a tracking device in the high rate CBM experiment

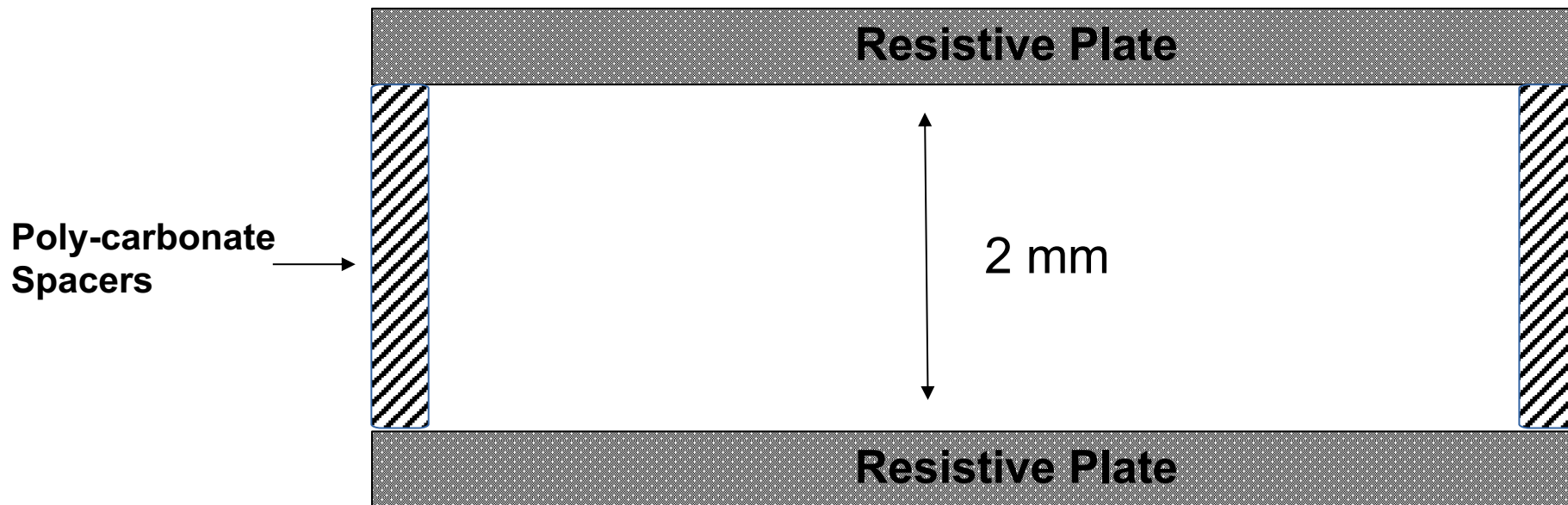
General structure of RPC

General structure of RPC

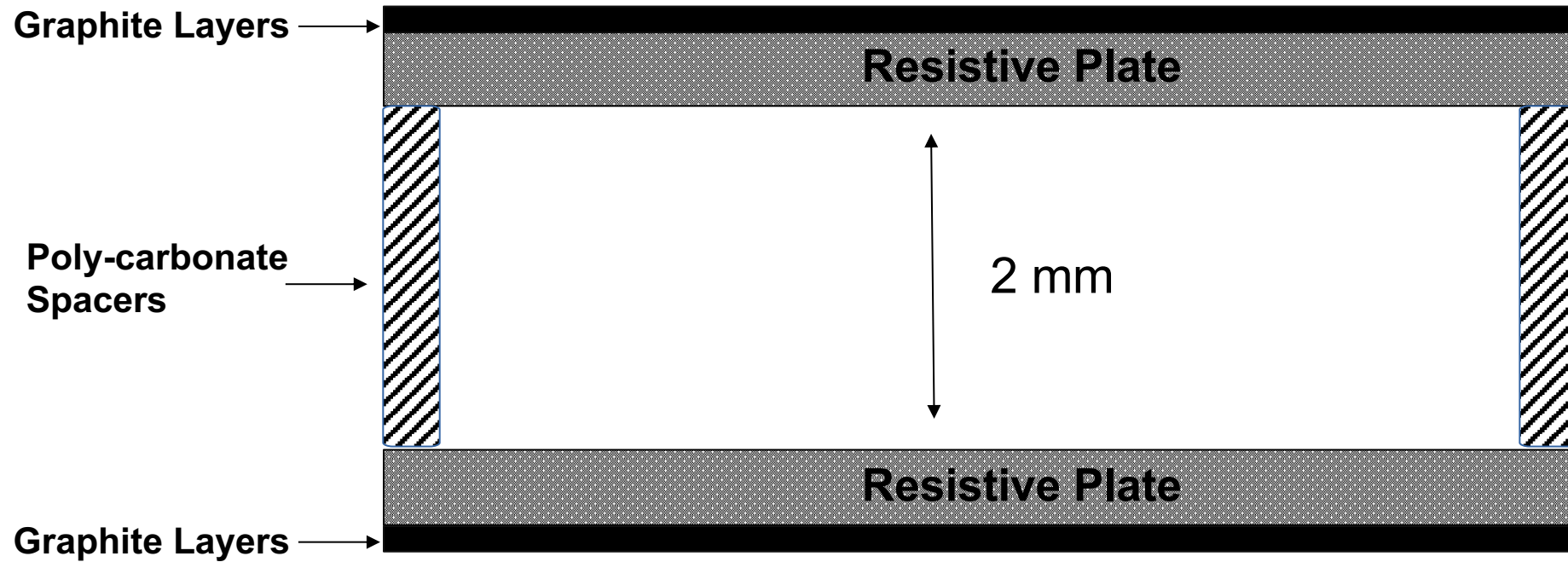
Resistive Plate

Resistive Plate

General structure of RPC



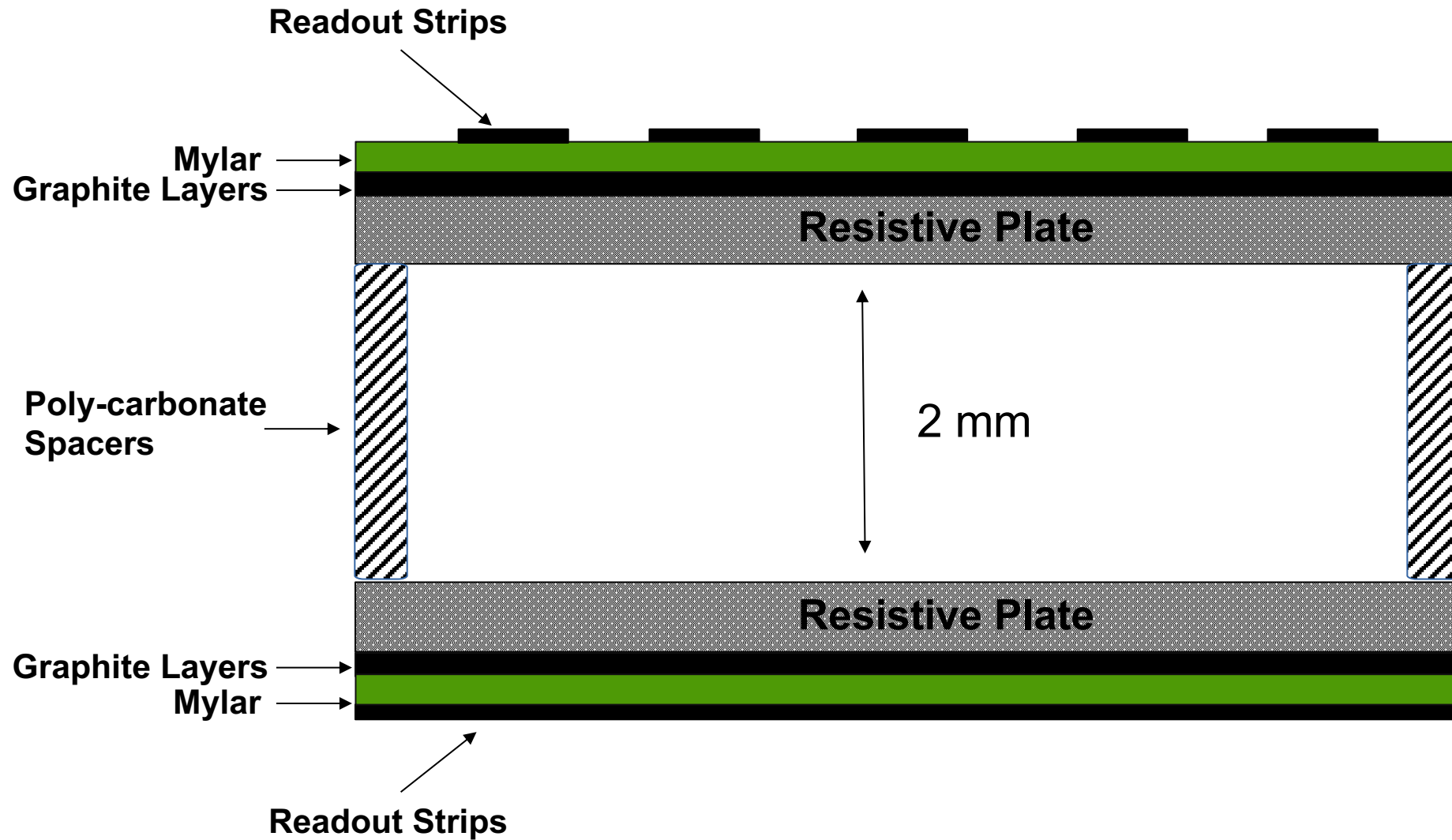
General structure of RPC



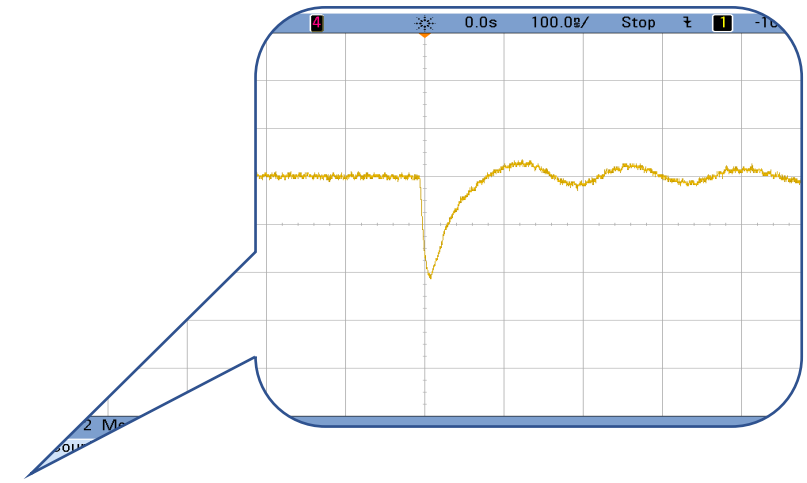
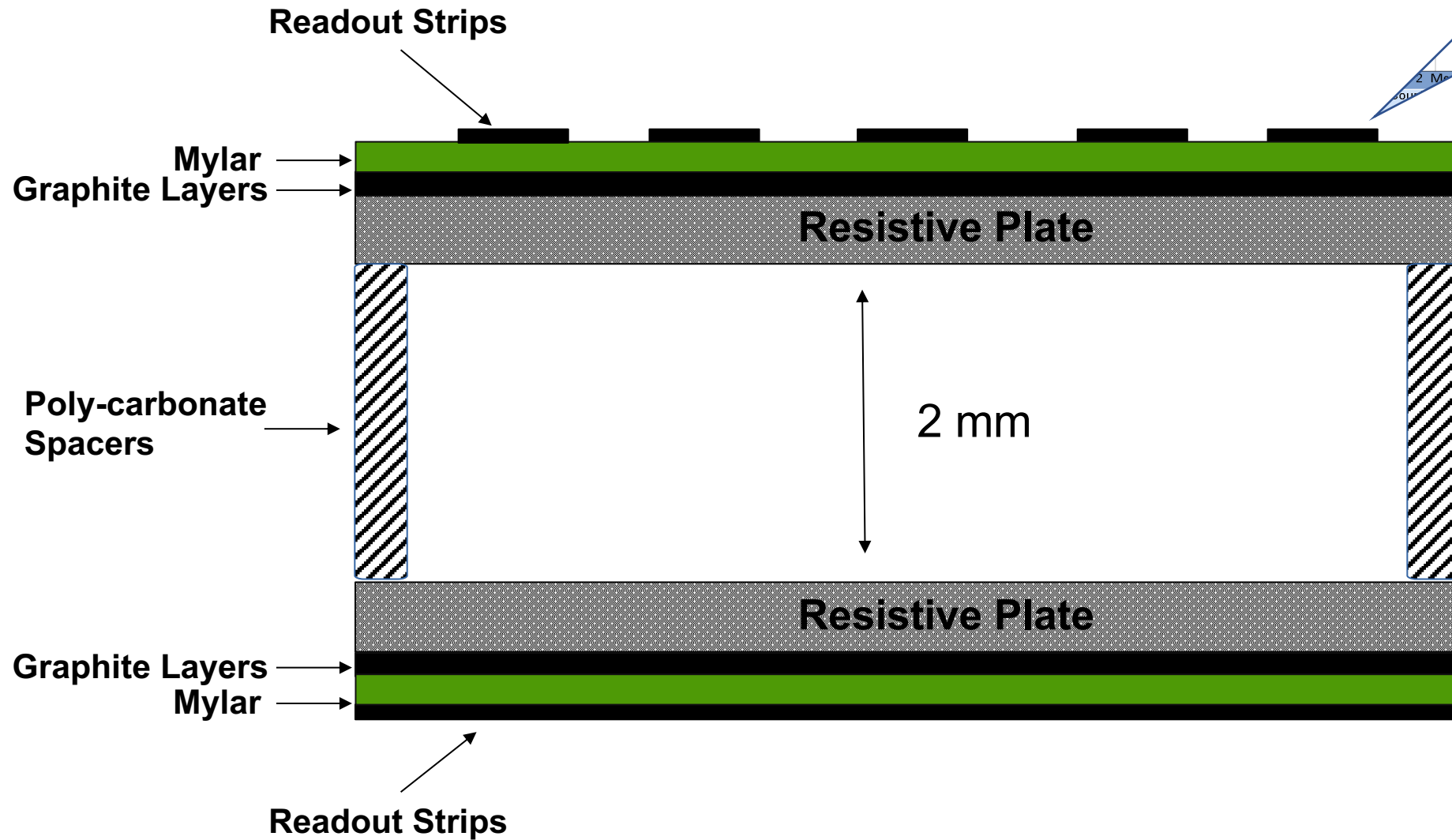
General structure of RPC



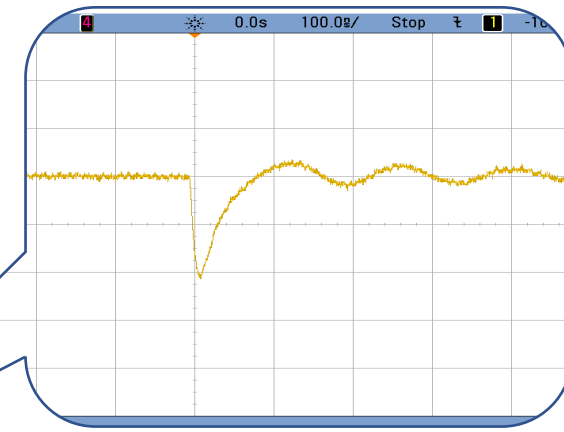
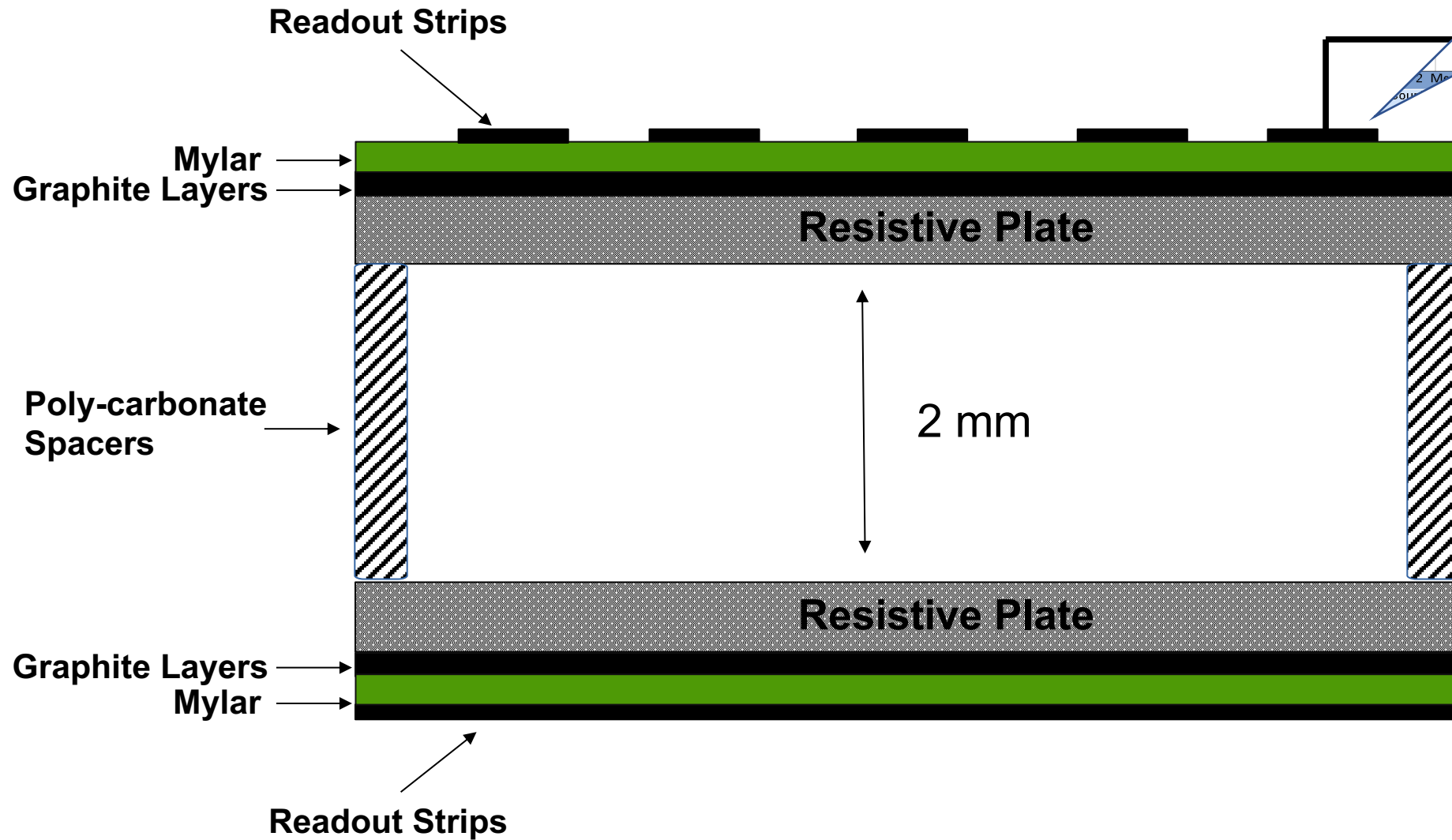
General structure of RPC



General structure of RPC

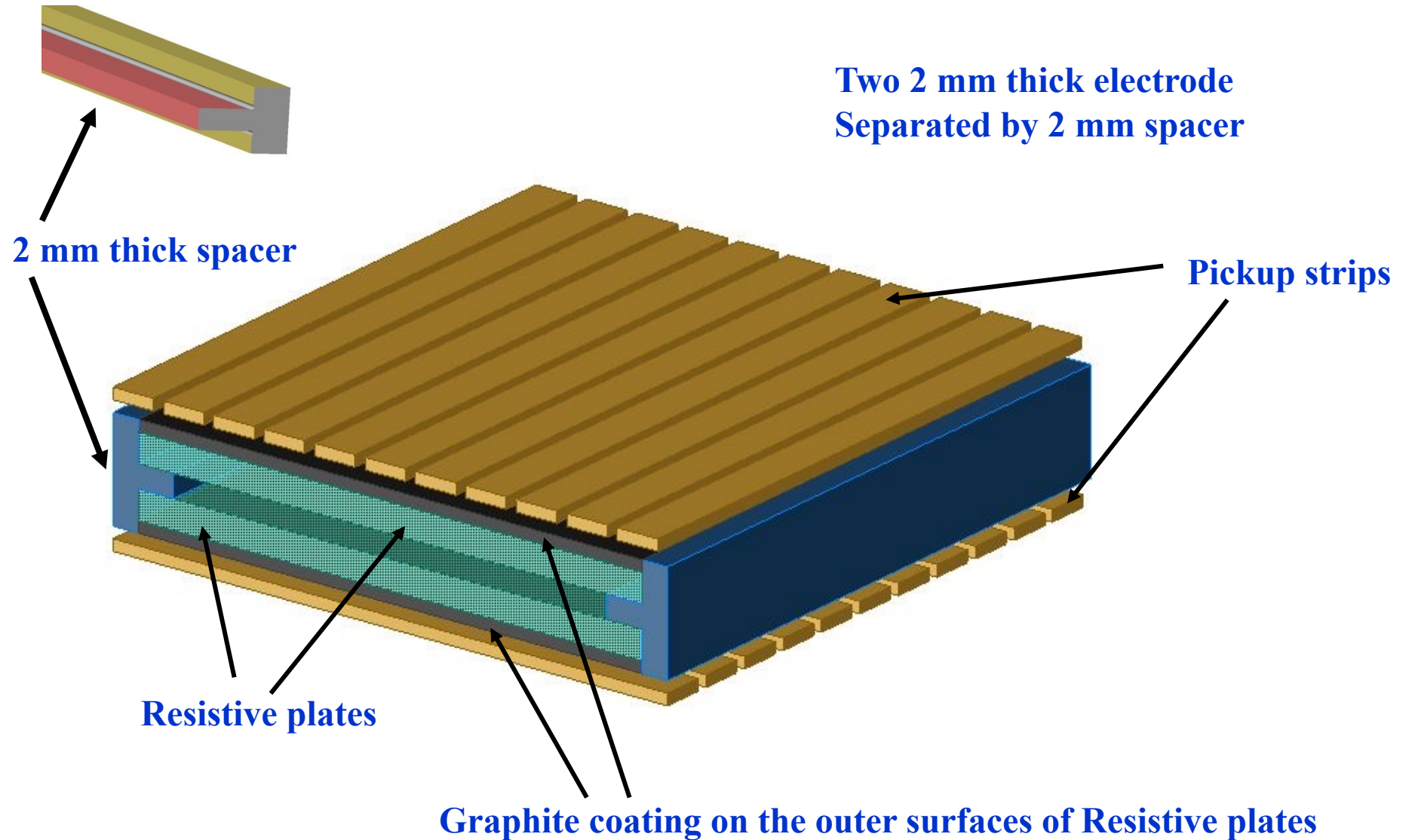


General structure of RPC



**Electronics
&
Data Acquisition**

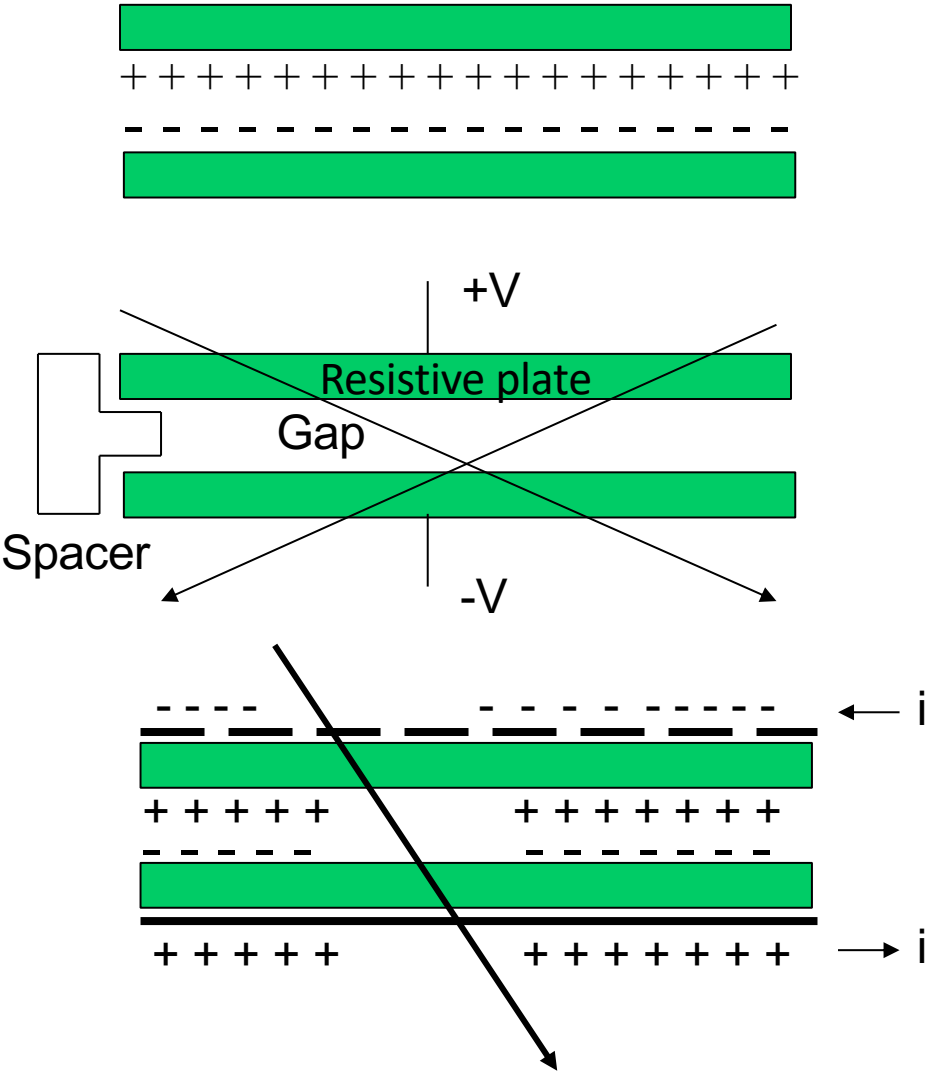
RPC in artistic impression



Features of RPC

- Built from simple and common materials
- Low fabrication cost per unit area
- Easy to construct and operate
- Simple signal pick up and readout system
- Large detector area coverage
- High efficiency (>90%) and good time resolution ($\sim 2\text{ns}$)
- Particle tracking capability and good position resolution ($\sim \text{cm}$)
- Two-dimensional (x and y) readout from the same chamber
- Long term stability

Basic principle of RPC



Surface of resistive electrodes are charged from power supply. Charge-up process is slow due to high resistivity of the material.

A passing charged particle induces an avalanche, which develops into a spark. The discharge stops when local charge is used up. This region is dead until recharged through the bulk resistivity of the plates ($10^{11} \Omega \text{ cm.}$)

When readout strips are placed, induced charge is either drawn in or drawn out from the readout board, generating voltage signals of opposite polarities.

Charge up time after each discharge

$$\begin{aligned}\tau &= R_{bakelite}C \simeq \left(\frac{\rho_{bakelite}d_{bakelite}}{A} \right) \left(\frac{\kappa_{gas}\epsilon_0 A}{d_{gas}} \right) \\ &= \rho_{bakelite}\kappa_{gas}\epsilon_0 \\ &\simeq (5 \times 10^{10}\Omega m)(\sim 4)(8.85 \times 10^{-12}F/m) \simeq 2sec\end{aligned}$$

$R_{bakelite}$ - Resistance of the electrode plate

C - Chamber capacitance

$\rho_{bakelite}$ - Bulk resistivity of the material of the plate

$d_{bakelite}$ - Thickness of the plate

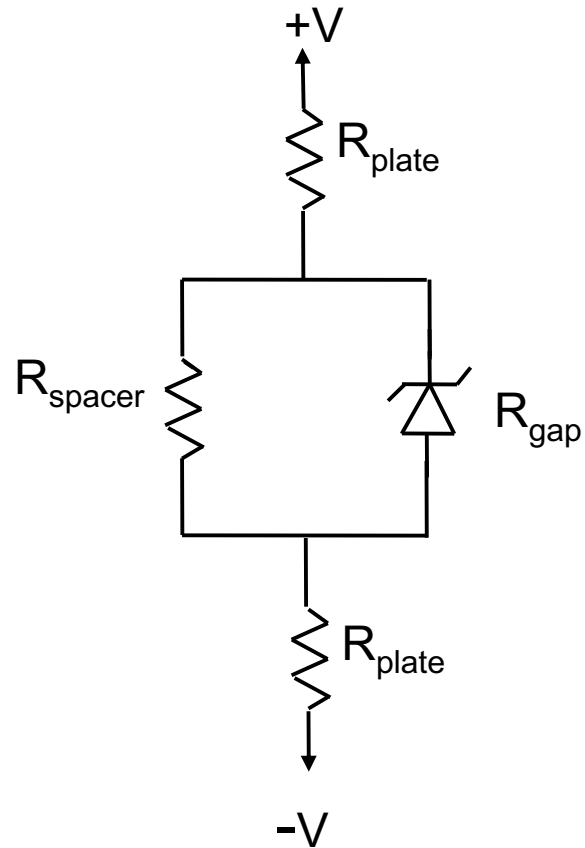
A - Area of the chamber

κ_{gas} - Dielectric constant of the gas

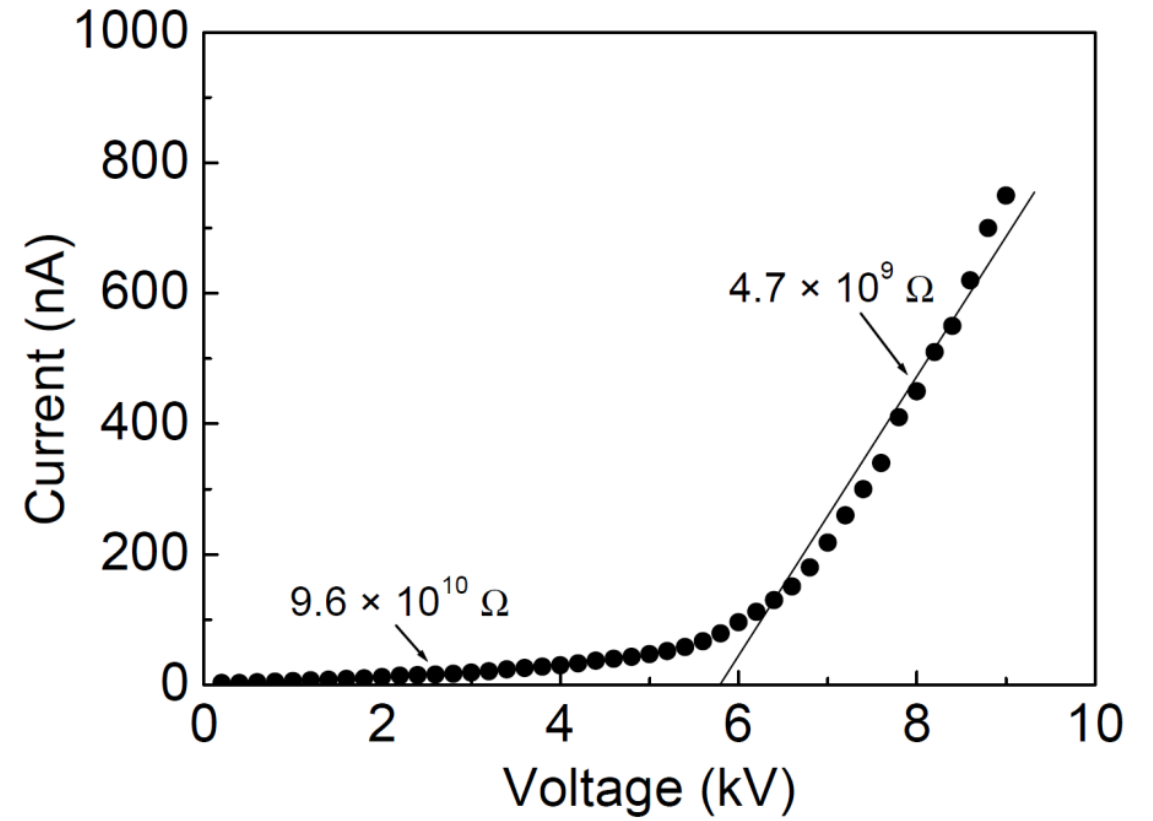
ϵ_0 - Permittivity of the free space

Each discharge is localized to $\sim 0.1 \text{ cm}^2$ (in streamer mode). Therefore, RPC with 0.2 Hz/cm^2 count rate suffers dead time fraction of $0.2 \times 0.1 \times 2 = 0.04$. So one should aim to build and operate RPC with less than 0.2 Hz/cm^2 in order to keep the dead time fraction below 5%.

Equivalent circuit representation of RPC



- Low voltage
 $R_{\text{gap}} \approx \infty$
 $\frac{dV}{dI} = R_{\text{spacer}}$
- High voltage
 $R_{\text{gap}} \approx 0$
 $\frac{dV}{dI} = R_{\text{plate}}$



RPC mode of operations

Let, n_0 = No. of electrons in a cluster

α = Townsend coefficient (No. of ionisations per unit length)

β = Attachment coefficient (No. of electrons captured by the gas per unit length)

Then the no. of electrons reaching the anode,

$$n = n_0 e^{(\alpha - \beta)x}$$

Where x = Distance between anode and the point where the cluster is produced

- ★ Gain of the detector, $M = n/n_0$
- ★ M decides the mode of RPC operation.
- ★ $M > 10^8 \rightarrow$ Streamer mode ;
- ★ $M \ll 10^8 \rightarrow$ Avalanche (Proportional mode)

RPC mode of operations (contd.)

- ★ A planar detector with resistive electrodes
≈ Set of independent discharge cells
- ★ From the expression for the capacitance of a planar condenser
Area of such cells is proportional to the total average charge,
Q that is produced in the gas gap

$$A = \frac{Qd}{\epsilon_0 V}$$

Where, d = gap thickness

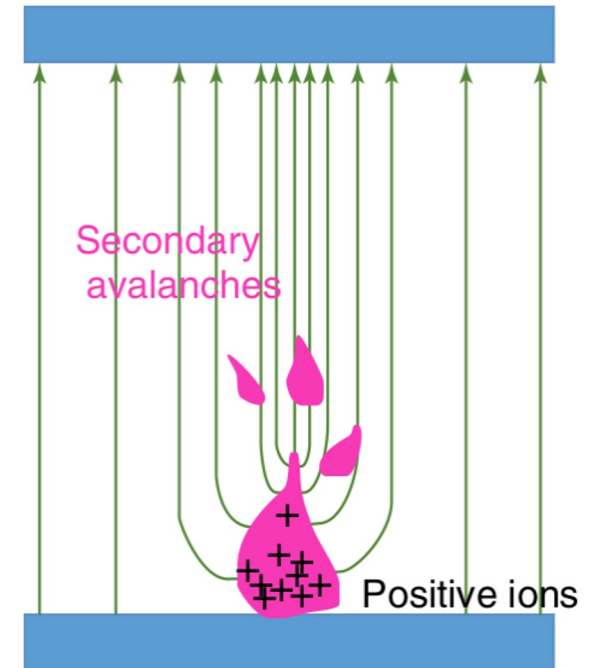
V = voltage applied to the electrodes

ϵ_0 = dielectric constant of the gas

Lower the Q, Lower the area of the cell (that is 'dead' during a hit) and hence higher the rate handling capability of RPC

Q ~ 100 pC = Streamer mode

Q ~ 1 pC = Avalanche (Proportional mode)



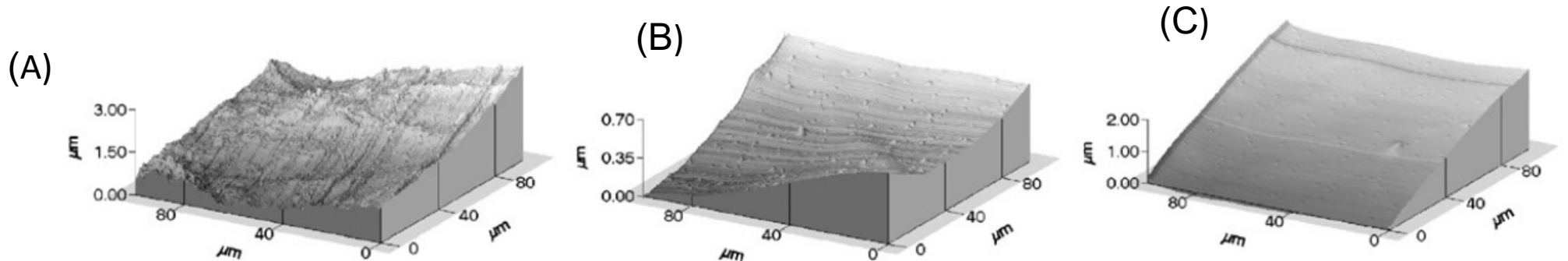
RPC used so far

Experiment	Application	Area (m^2)	Electrode material	Volume resistivity (Ω cm)	No. of gaps	Gap (mm)	Mode of operation
BaBar	Trigger	2000	Bakelite	$10^{11} - 10^{12}$	1	2	Streamer
Belle	Trigger	2000	Glass	$> 10^{12}$	2	2	Streamer
ALICE-Muon	Trigger	140	Bakelite	3×10^9	1	2	Streamer
ALICE-TOF	Timing	150	Glass	10^{13}	10	0.25	Avalanche
ATLAS	Trigger	6550	Bakelite	$(1-4) \times 10^{10}$	1	2	Avalanche
CMS	Trigger	4000	Bakelite	$\sim 10^{10}$	2	2	Avalanche
STAR	Timing	60	Glass	$10^{12} - 10^{13}$	6	0.22	Avalanche
PHENIX	Trigger	-	Bakelite	10^{10}	2	2	Avalanche
OPERA	Trigger	3200	Bakelite	$> 5 \times 10^{11}$	1	2	Streamer
BESIII	Trigger	1200	Bakelite	$10^9 - 10^{13}$	1	2	Streamer
YBJ-ARGO	Trigger	5600	Bakelite	$(0.5-1) \times 10^{12}$	1	2	Streamer
HARP	Timing	10	Glass	10×10^{12}	4	0.3	Avalanche
HADES	Timing	8	Glass	5×10^{12}	4	0.3	Avalanche
FOPI	Timing	5	Glass	10^{12}	6	0.3	Avalanche
CBM-TOF	Timing	120	Glass	$(3-4) \times 10^{10}$	6	0.22	Avalanche
NeuLAND	Timing	4	Glass	-	3	0.3	Avalanche

Problems with bakelite electrode surfaces

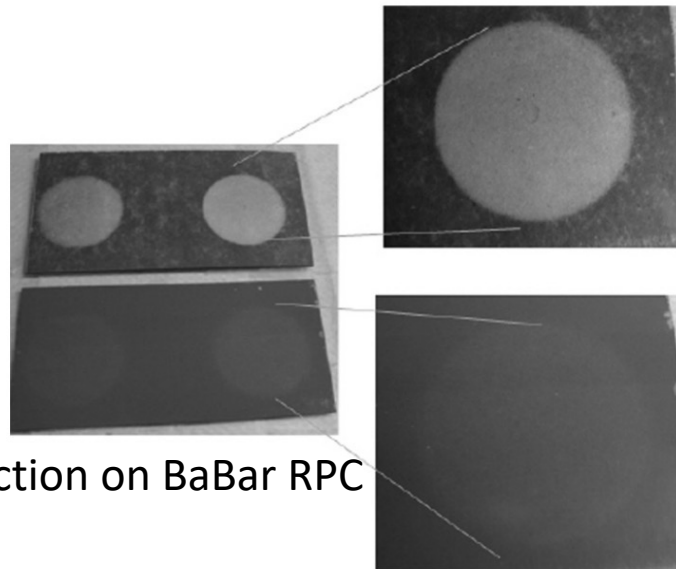
C. Lu, Nucl. Instr. and Meth. A 602 (2009) 761

1. Surface non-uniformity

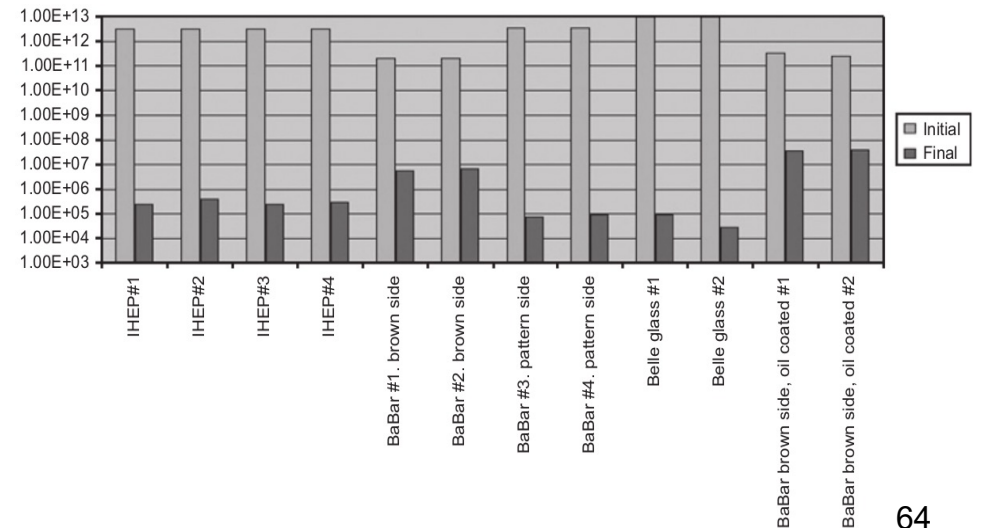


(A) bare surface (B) coated with 30/70 of Linseed oil/2-propanol (C) coated with 70/30 of Linseed oil/2-propanol

2. HF vapor attack



HF vapor corrosive action on BaBar RPC Bakelite surface



Advantages of linseed oil coating

- The linseed oil coating reduces the spurious micro discharge on the inner surfaces. If the micro discharge probability is reduced, we can have a better performance compared to the RPC without oil coating.
- To reduce the after-pulse / noise rate, low UV sensitive material for the electrode is desirable.
- Linseed oil coating on the bakelite surface can effectively protect it from the HF vapor attack.
- Uncured linseed oil can form short path and therefore, spurious discharges can take place reducing efficiency.

Conventional technique of linseed oil coating

- Usually, linseed oil treatment the inner surfaces of the RPC is done after making the gas gap.
- Gap is filled with low viscous linseed oil and thinner solution and the liquid is drained out slowly.
- Dry air is flown through the gas gap to cure the thin linseed oil layer left on all the inner surfaces of the plates as well as those of the spacers.

New technique of linseed oil coating

- In the present work the linseed oil coating is done on bakelite plate before making the gas gap.
- We take about 2g of linseed oil is applied over the 27 cm × 27 cm area of each plate.
- The linseed oil is distributed over the surfaces and both the plates are left for 15 days in a sealed box for curing.
- The advantage of this procedure is that after linseed oil coating it can be checked visually whether the curing is properly done or any uncured droplet of linseed oil is present.

Fabrication steps

Fabrication steps

Resistivity= $3 \times 10^{10} \Omega \text{ cm}$



Application of linseed oil on the bakelite surface

Fabrication steps

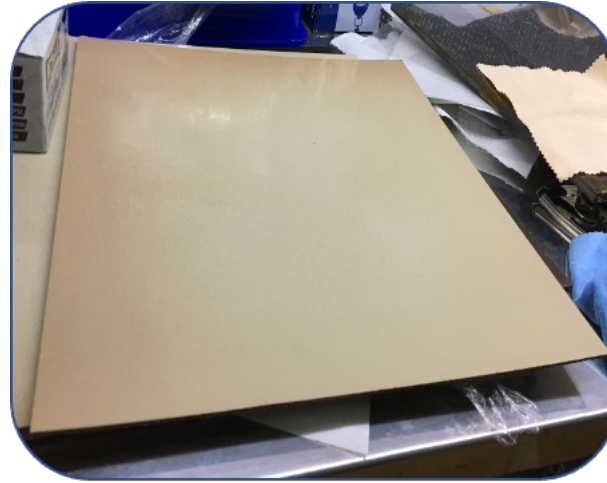
Resistivity= $3 \times 10^{10} \Omega \text{ cm}$



Application of linseed oil on the bakelite surface

Fabrication steps

Resistivity= $3 \times 10^{10} \Omega \text{ cm}$

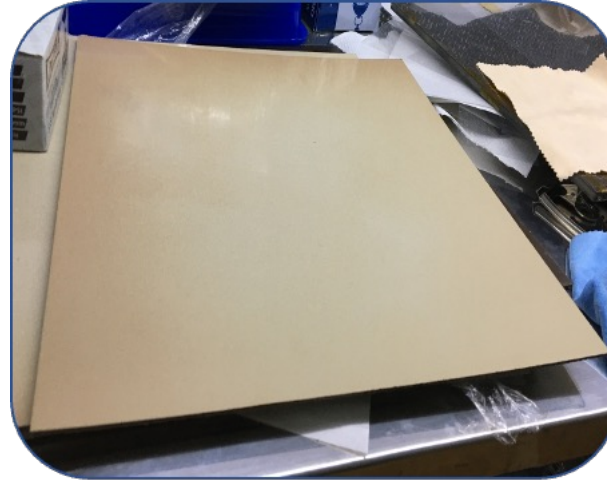


Application of linseed oil on the bakelite surface

Cured linseed oil coated bakelite surface

Fabrication steps

Resistivity= $3 \times 10^{10} \Omega \text{ cm}$



Application of linseed oil on the bakelite surface

Cured linseed oil coated bakelite surface

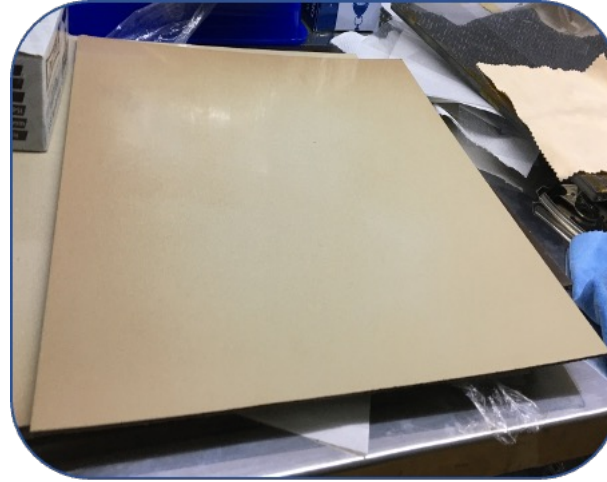
Gas nozzles and spacers

Fabrication steps

Resistivity= $3 \times 10^{10} \Omega \text{ cm}$



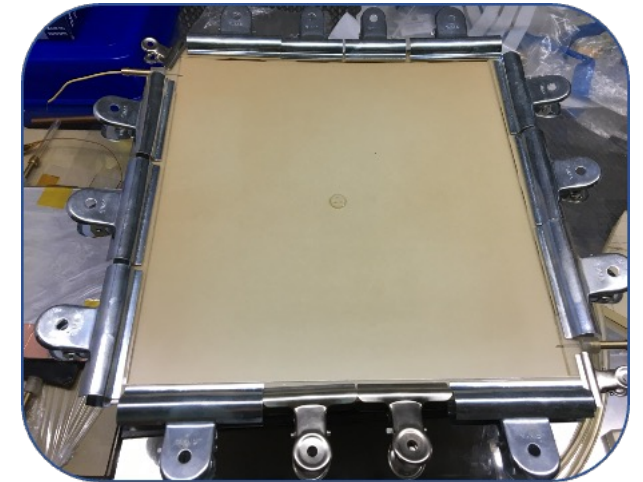
Application of linseed oil on the bakelite surface



Cured linseed oil coated bakelite surface



Gas nozzles and spacers



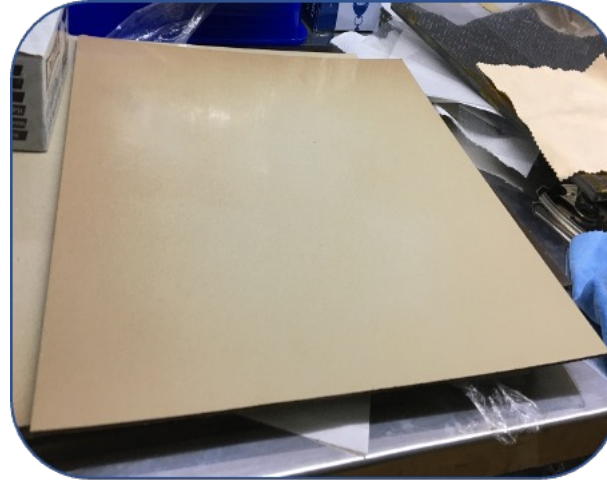
Gluing of spacers and nozzles

Fabrication steps

Resistivity= $3 \times 10^{10} \Omega \text{ cm}$



Application of linseed oil on the bakelite surface



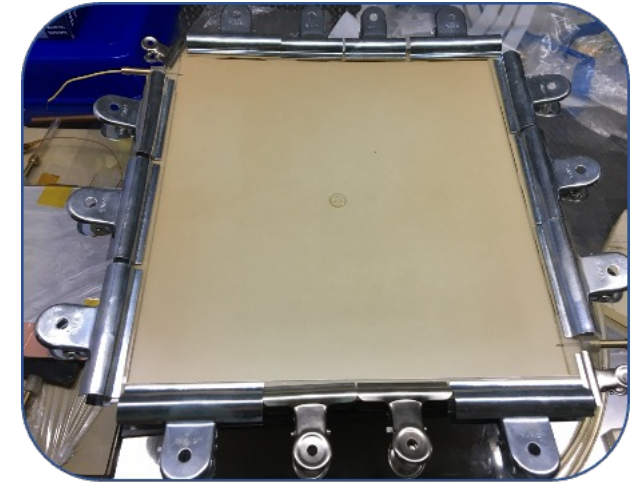
Cured linseed oil coated bakelite surface



Gas nozzles and spacers



Making of gas gap



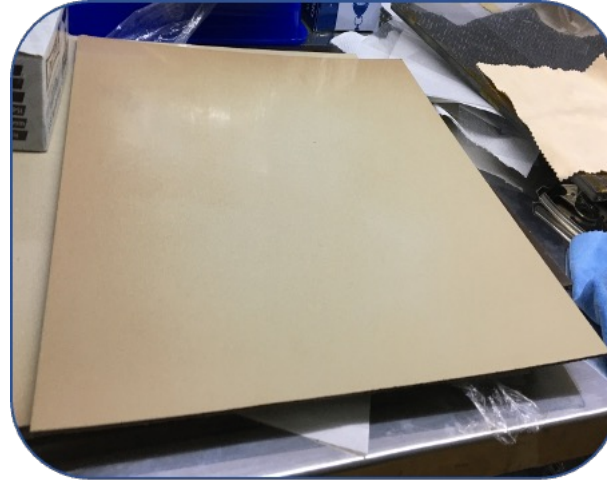
Gluing of spacers and nozzles

Fabrication steps

Resistivity= $3 \times 10^{10} \Omega \text{ cm}$



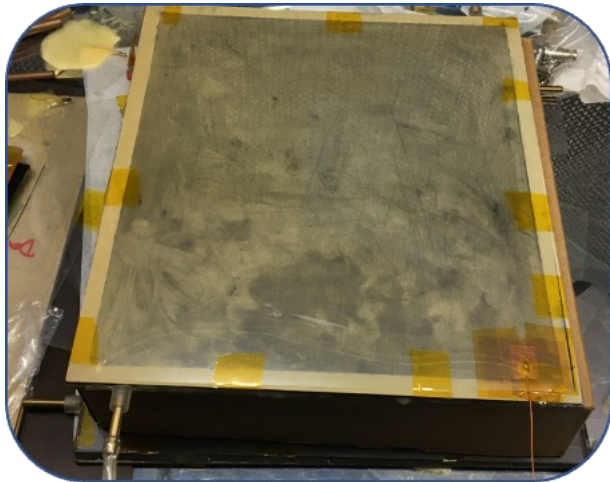
Application of linseed oil on the bakelite surface



Cured linseed oil coated bakelite surface



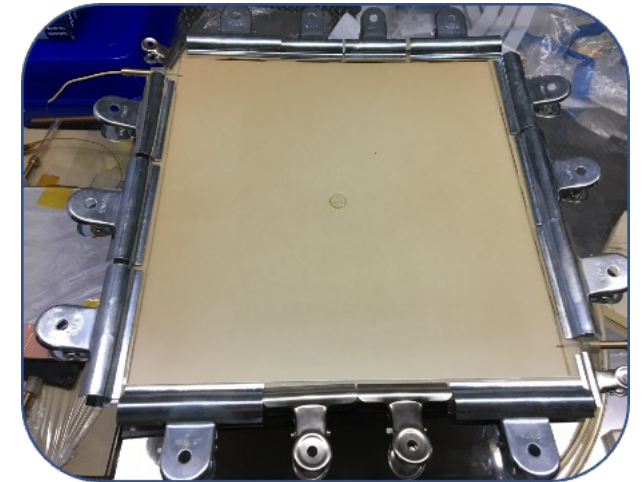
Gas nozzles and spacers



Complete RPC module after graphite coating

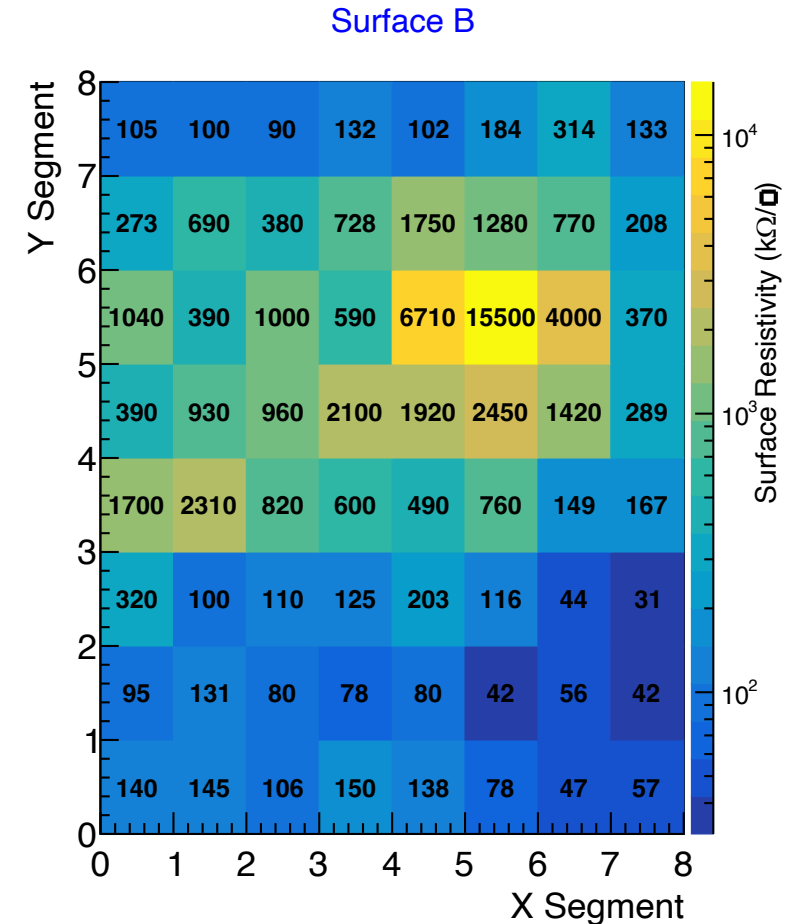
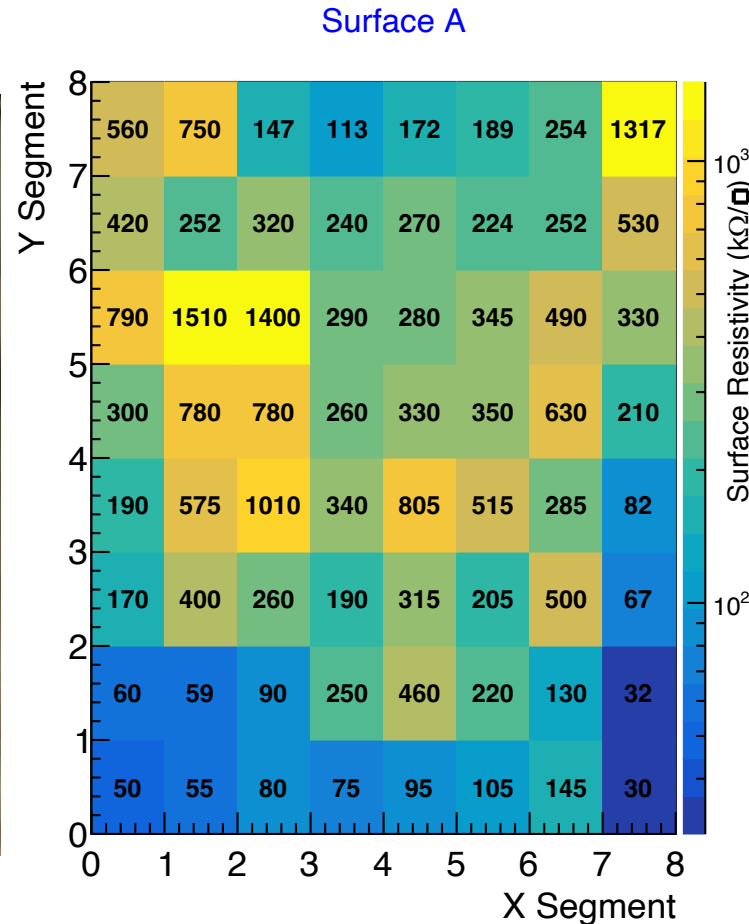


Making of gas gap



Gluing of spacers and nozzles

Measurement of surface resistivity

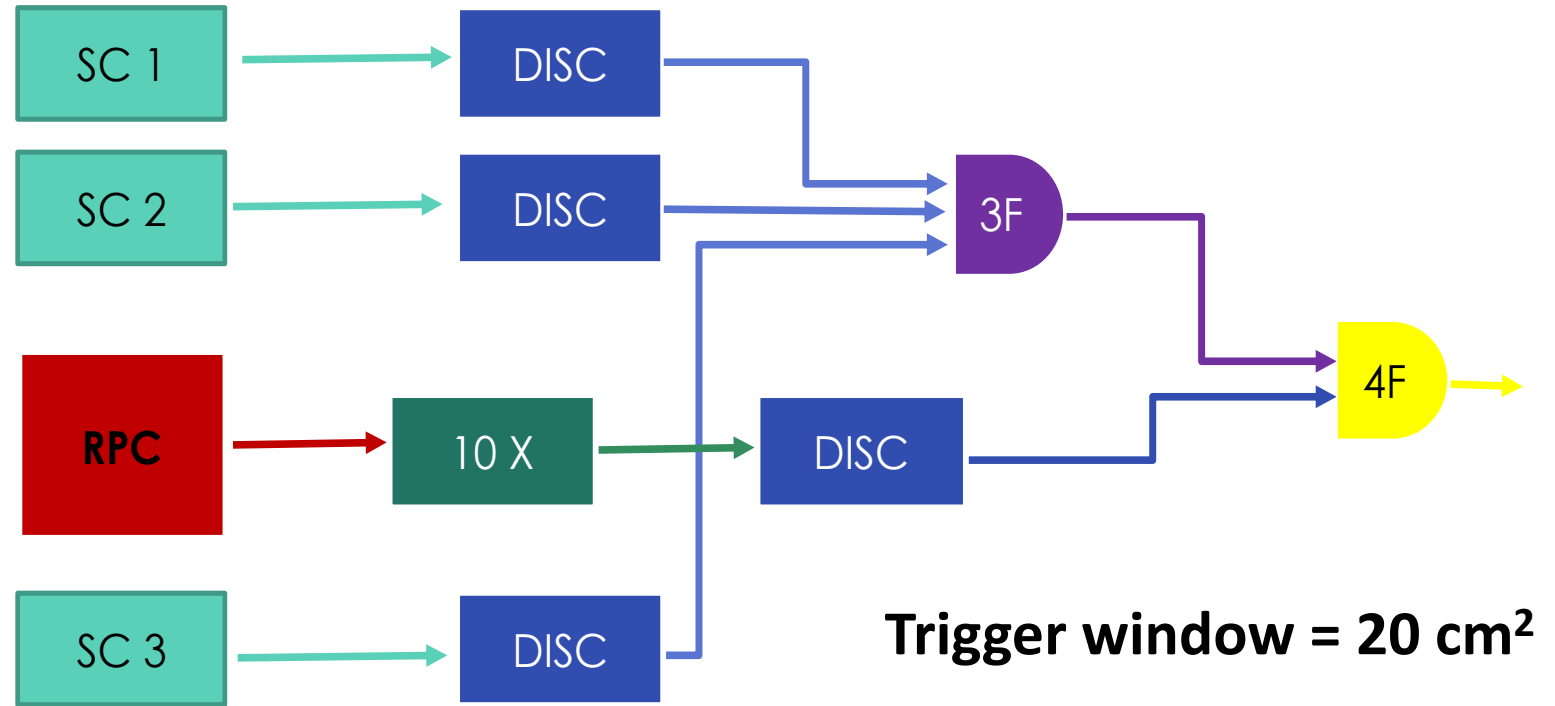


Average surface resistivity of **Surface A** = **358 $k\Omega/\square$** and **Surface B** = **409 $k\Omega/\square$**

Efficiency measurement



A. Sen et al., 2020 JINST 15 C06055



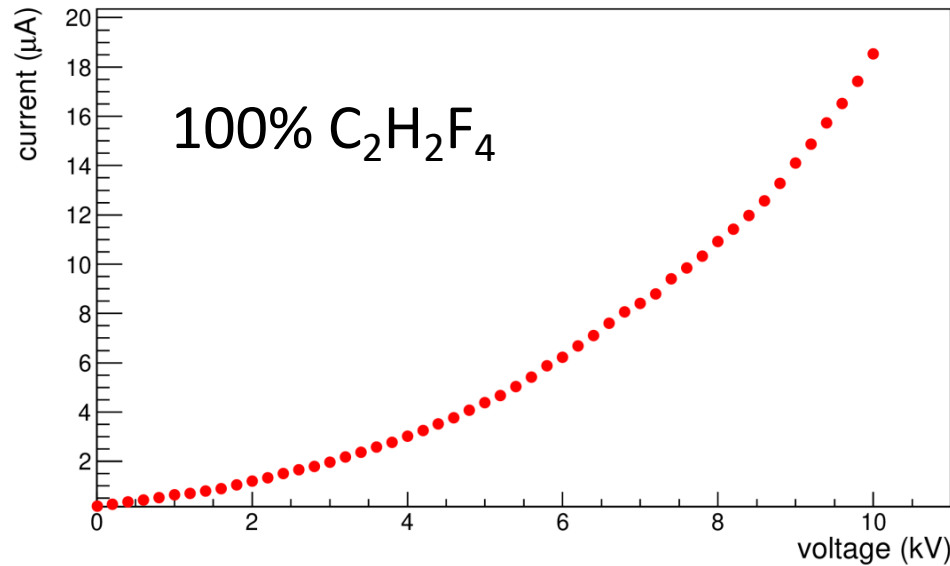
Trigger = SC1 .AND. SC2 .AND. SC3

Efficiency = $\frac{\text{RPC signal in coincidence with trigger (4F)}}{\text{Trigger (3F)}}$

- Threshold to the Sc: - 15 mV
- Threshold to RPC: - 15 mV

Results

A. Sen et al., NIM A 1024 (2022) 166095



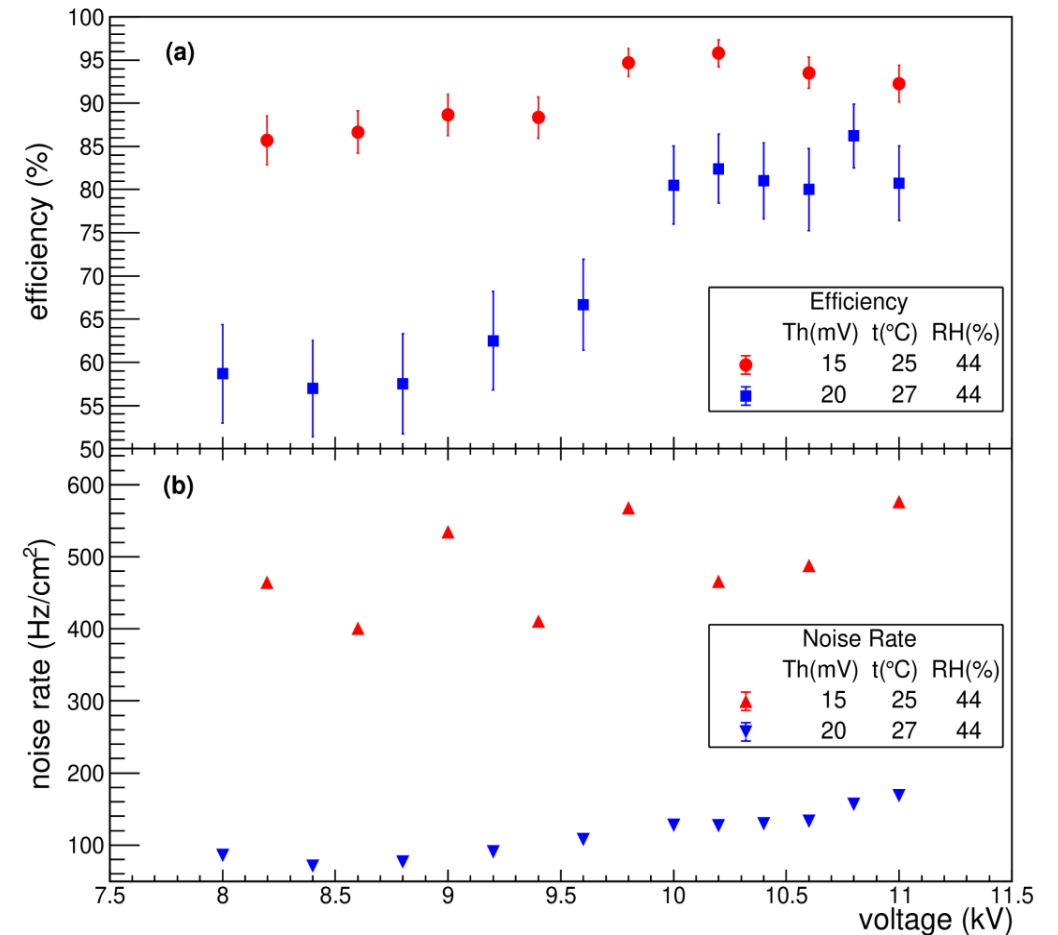
Leakage current as a function of the applied voltage

@ -15 mV threshold

- Efficiency: ~ 95±1% from 9.4 kV onwards
- Noise rate ~ 500 Hz/cm²

@-20 mV threshold

- Efficiency: ~ 85±5% from 10.1 kV onwards
- Noise rate ~ 200 Hz/cm²

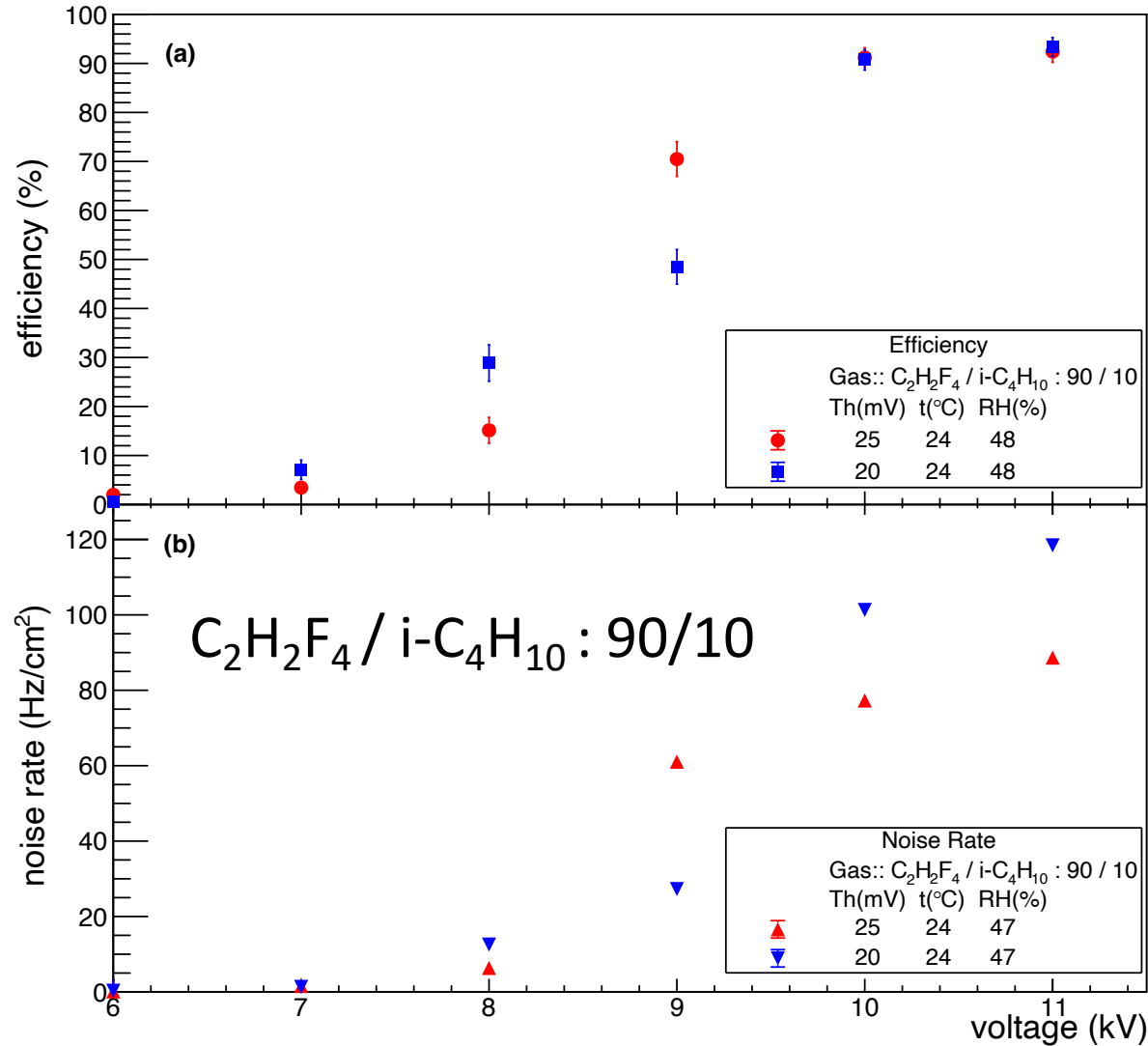


(a) The efficiency vs the applied voltage

(b) Noise rate as a function of the applied voltage

Results

A. Sen et al., arXiv: 2206.04259



@ -20 mV threshold

- Efficiency: ~ 95±2% from 10 kV onwards
- Noise rate ~ 120 Hz/cm²

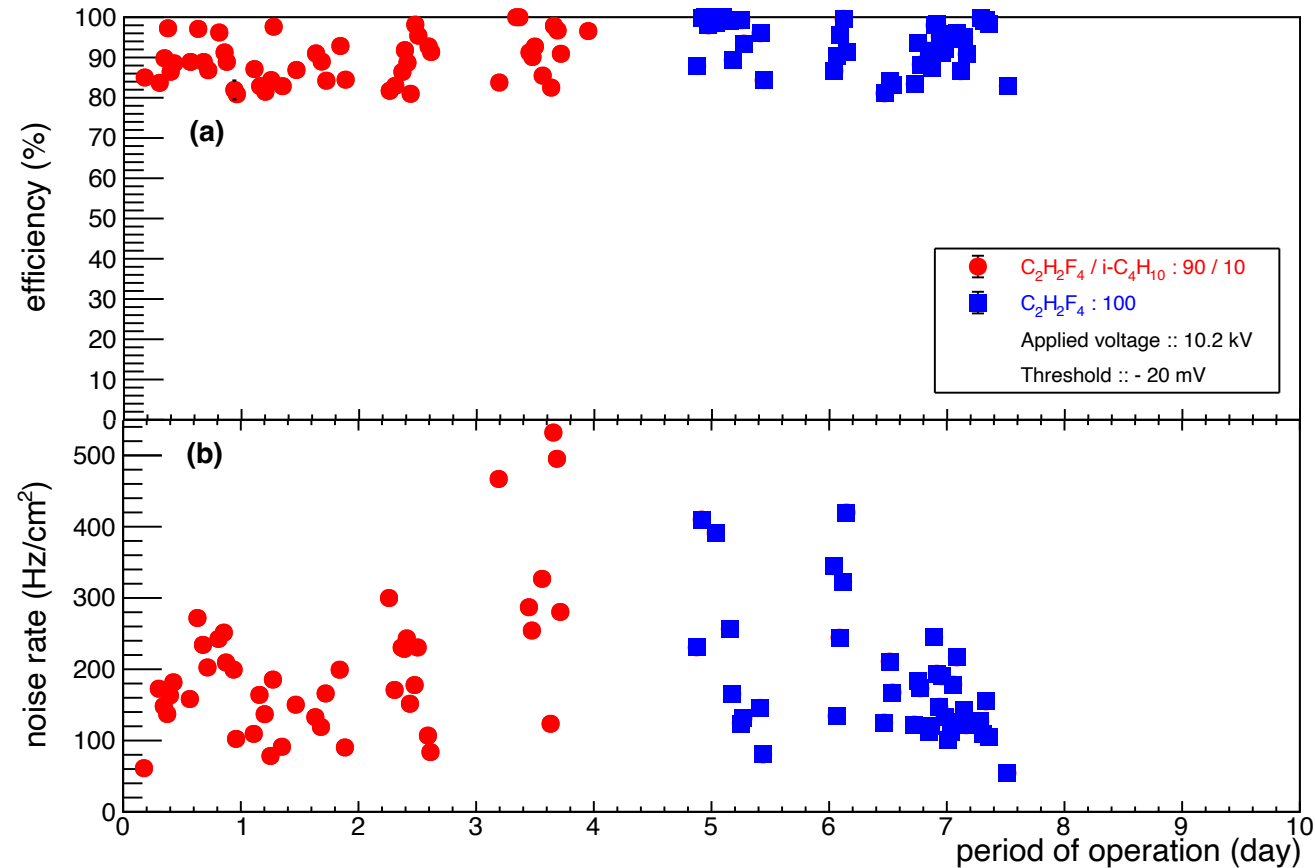
@ -25 mV threshold

- Efficiency: ~ 95±2% from 10 kV onwards
- Noise rate ~ 80 Hz/cm²

(a) The efficiency vs the applied voltage

(b) Noise rate as a function of the applied voltage

Stability test results (preliminary)

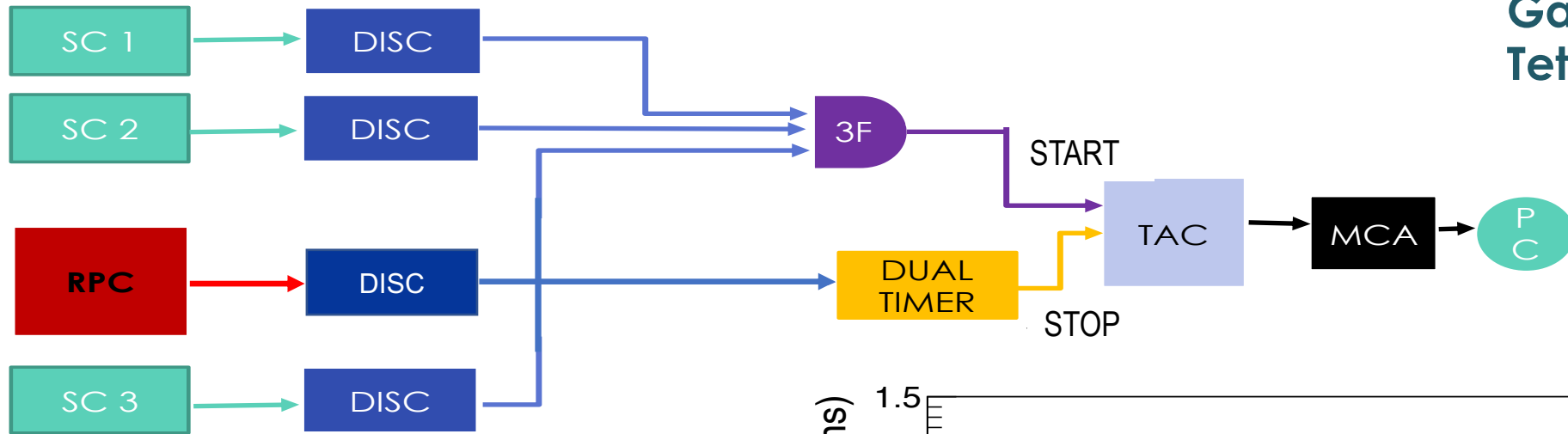


@ 10.2 kV applied voltage and -20 mV threshold

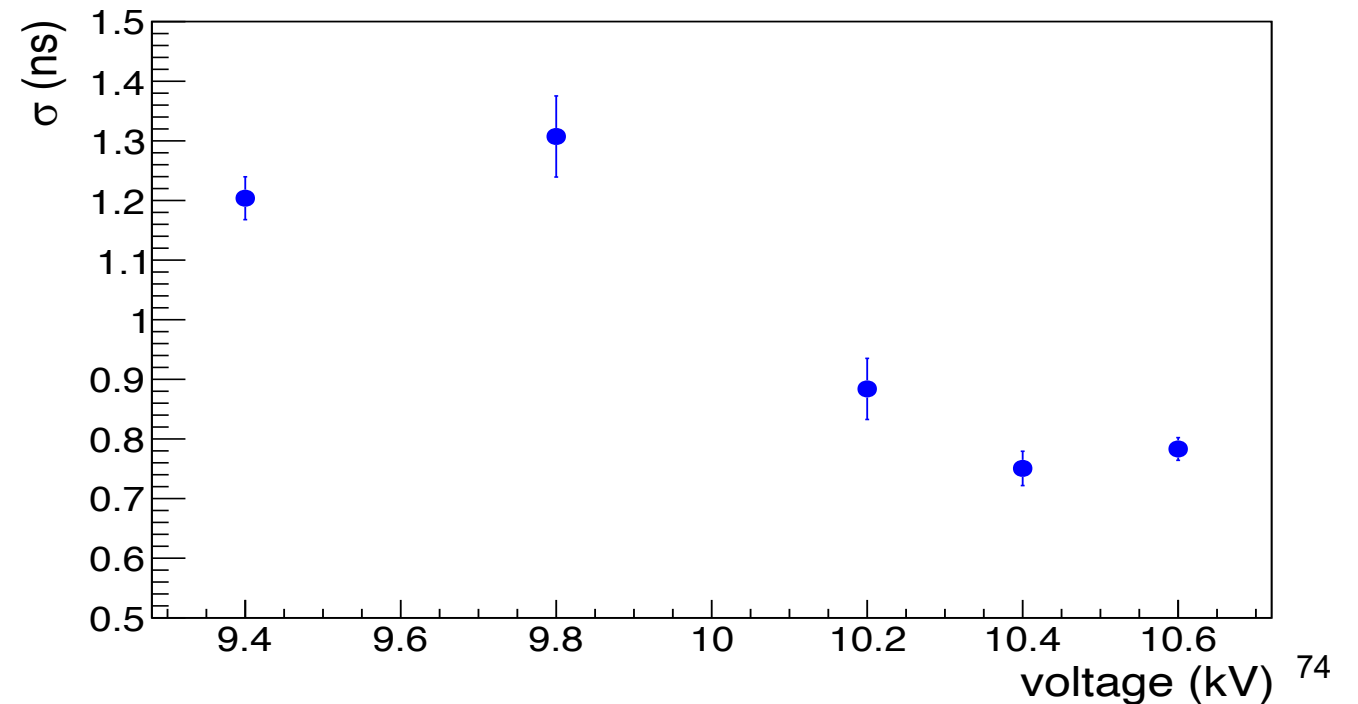
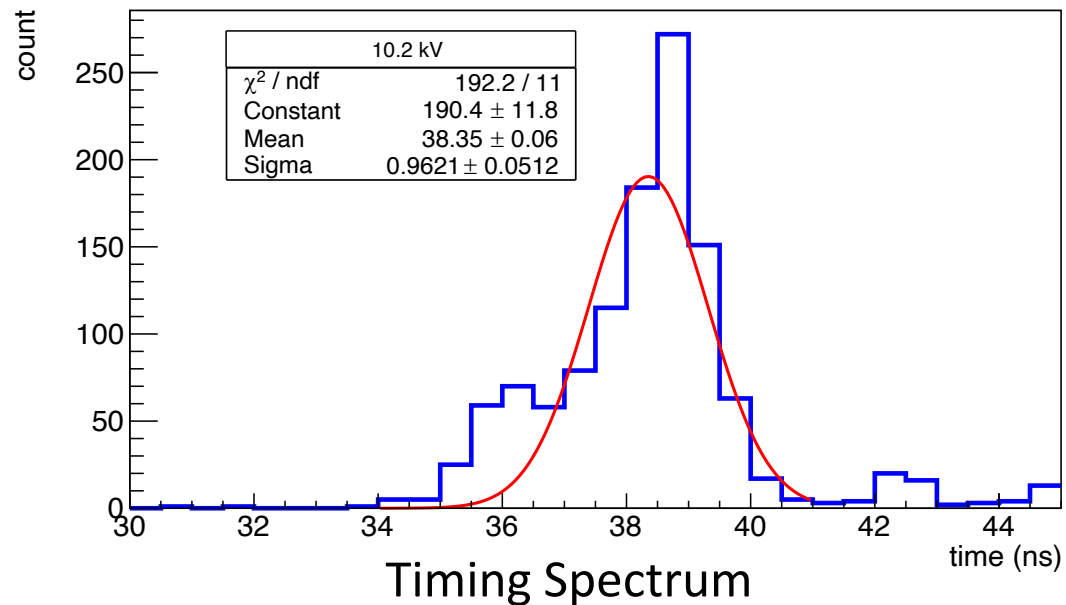
- **Efficiency: 89% from Noise rate ~ 181 Hz/cm² for C₂H₂F₄ / i-C₄H₁₀ : 90/10**
- **Efficiency: 93% from Noise rate ~ 155 Hz/cm² for C₂H₂F₄ : 100%**

Time resolution measurement

Gas: 100 %
Tetrafluoroethane



Time resolution
 $\sim 0.8 \pm 0.06$ ns (σ)



Summary

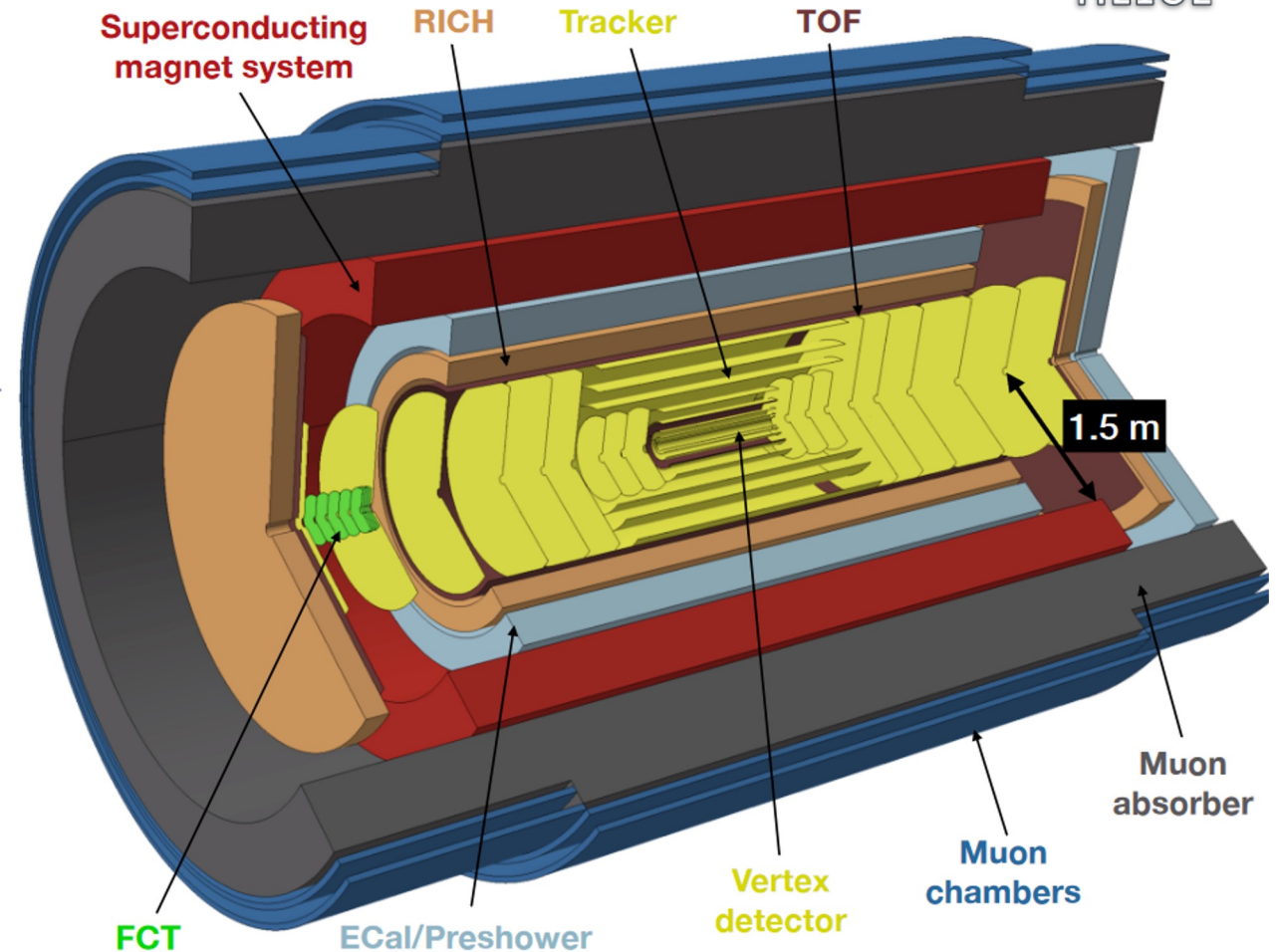
- Several RPC modules are build with locally available bakelite material
- Resistivity measurement set-up and cosmic ray test set-up is currently operational
- **A new technique is introduced for linseed oil coating in bakelite RPC**
- With linseed oil coated electrode an efficiency $\sim 95\pm 1\%$ for -15 mV threshold
efficiency $\sim 85\pm 5\%$ for -20 mV threshold for 100% $C_2H_2F_4$ gas
- The time resolution of the chamber is found to be $\sim 0.8\pm 0.06$ ns (σ)
- For $C_2H_2F_4$ / i- C_4H_{10} : 90/10 gas composition an efficiency $\sim 95\%$ for both -20 mV and -25 mV threshold

ALICE3- Possible contribution from India

ALICE3



- ❖ Mostly silicon based detector
- ❖ Heavy-flavour hadrons ($p_T \rightarrow 0$, $|\eta| < 4$)
 - vertexing (decay chain), tracking (inv. mass resolution) and hadron ID (background suppression)
- ❖ Dielectrons (p_T 0.1 - 3 GeV/c, M_{ee} 0.1 - 4 GeV/c²)
 - vertexing (HF background suppression), tracking (inv. mass resolution) and electron ID
- ❖ Photons (100 MeV/c - 50 GeV/c, wide η range)
 - electromagnetic calorimetry
- ❖ **Quarkonia and Exotica ($p_T \rightarrow 0$)**
 - **muon ID**
- ❖ Ultrasoft photons ($p_T = 1 - 50$ MeV/c)
 - dedicated forward detector
- ❖ Nuclei
 - identification of $z > 1$ particles
- ❖ **key requirements:**
 - Tracking over large rapidity range
 - Excellent vertexing
 - Excellent particle identification
 - High rate capability



ALICE3 - Proposed detector technologies

- **Vertex:** ALICE ITS3 type Si pixel sensor (superALPIDE) - $\sigma_{\text{pos}} \sim 2.5 \mu\text{m}$
- **Tracking:** ALICE ITS2 type Si pixel sensor (ALPIDE) - $\sigma_{\text{pos}} \sim 10 \mu\text{m}$
- **Time of Flight:** CMOS/**LGAD/SPAD based** - $\sigma_t \sim 20 \text{ ps}$
- **RICH:** Aerogel + SiPM - $\sigma_\theta \sim 1.5 \text{ mrad}$
- **Muon system:** RPC or plastic scintillator + SiPM (required time resolution??)
- **EMCAL:** PbWO₄ crystal + **SiPM** - high energy resolution
- **Ultrasoft photon detection:** ALICE ITS2 type Si pixel sensor (ALPIDE)

Muon detection system

- ALICE3 solutions: Resistive Plate Chambers (RPC), Plastic scintillator coupled to SiPM
- The moderate charged particle rate of 3 Hz/cm²
- Granularity of ~ 5x5 cm² pad size
- Readout channels ~ 40k
- **Option – I (RPC)**
 - Well established and proven system - **good background in RPC in Indian group**
 - RPC operated in avalanche or streamer mode – scope for R&D on eco- friendly gas mixtures
 - RPC with 3 mm thick electrodes (glass, Bakelite or new material) – 10¹² ohm.cm bulk resistivity would suffice
- **Option – II (Plastic scintillator + SiPM)**
 - 5 cm wide scintillator strips placed orthogonally in 2 layers (20 cm gap between layers)
 - Indigenous SiPM based readout
 - Only caveat is that **the scintillators and WLS fibers** may have to be **commercially purchased**
 - Explore possibilities **to produce SiPMs in Indian Foundries (SCL, BEL, SITAR etc.)**

Major ongoing RPC development activities in Indian labs

India-based neutrino Observatory

- 51 kton muon detector
 - 1.9 m x 1.9 m x 2.4 cm single-gap chamber
 - 30,000 modules

 - R&D in several ALICE institutes
 - (VECC, SINP, NISER, BI)
 - 700psec time resolution (glass electrode)
 - 800 pico-sec (bakelite electrode)

 - Indigenous developments of
 - HV, LV, readout boards

 - Industries developed for mass production
1. Electrodes
 2. Skin printing
 3. pickup strip fabrication

High-rate RPC for CBM muon system

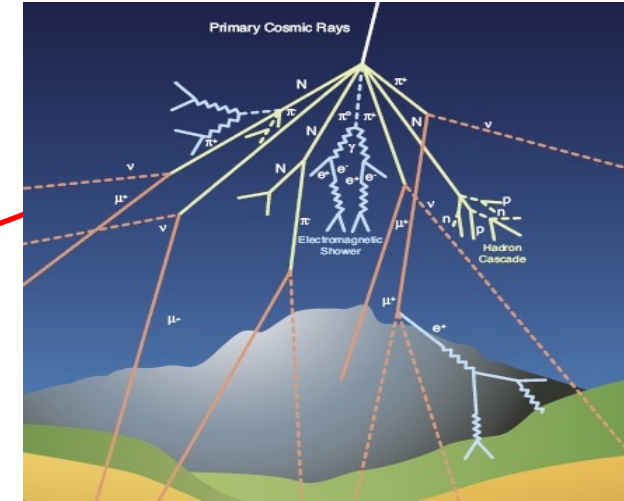
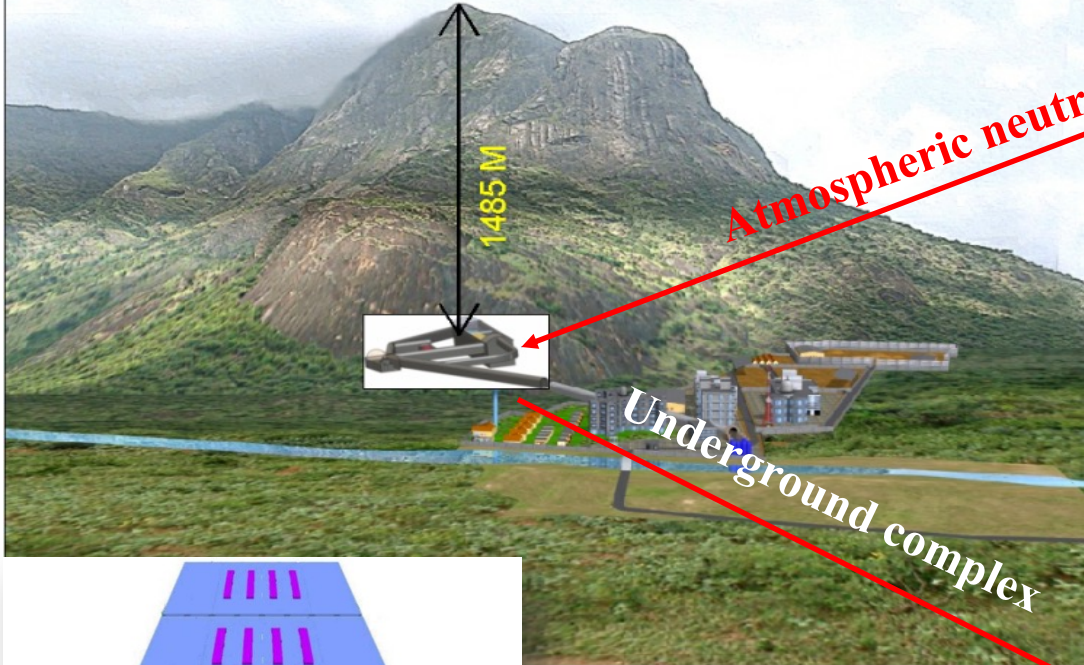
- Resistivity $\sim 10^{10}$ Ohm-cm
- Sector-shaped
- Projective Pad readout (pad size varies from 1cm to 5 cm)
- R&D on readout:
- NINO
- PADI
- STS/MUCH XYTER (CBM ASIC)

Tested at GIF++, SIS18 upto 10 kHz

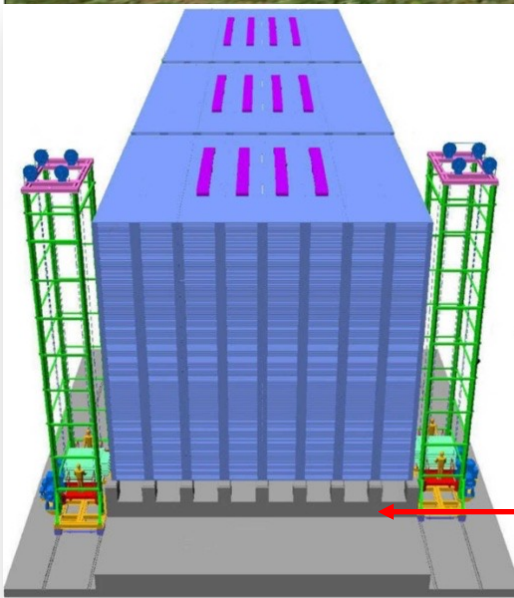
Several MRPC developed for different applications

India-based neutrino Observatory (INO)-ICAL Project

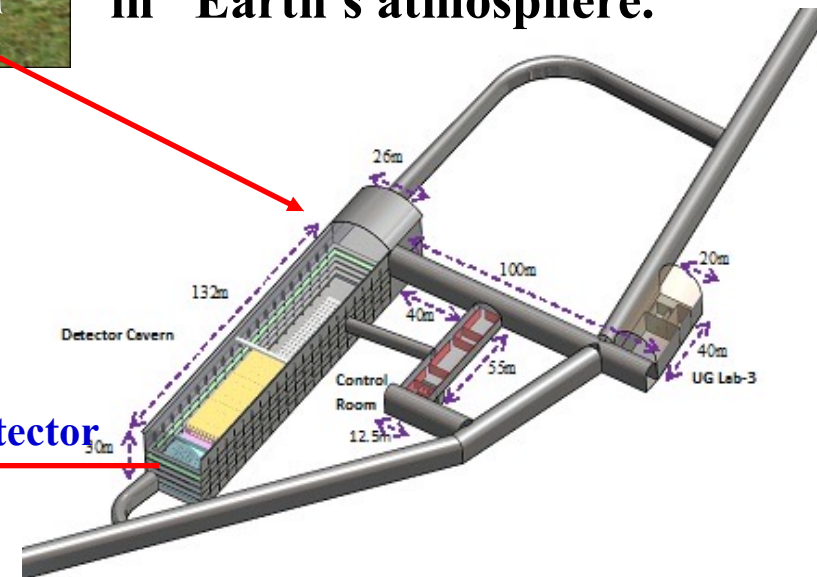
All major facilities are inside an underground cavern



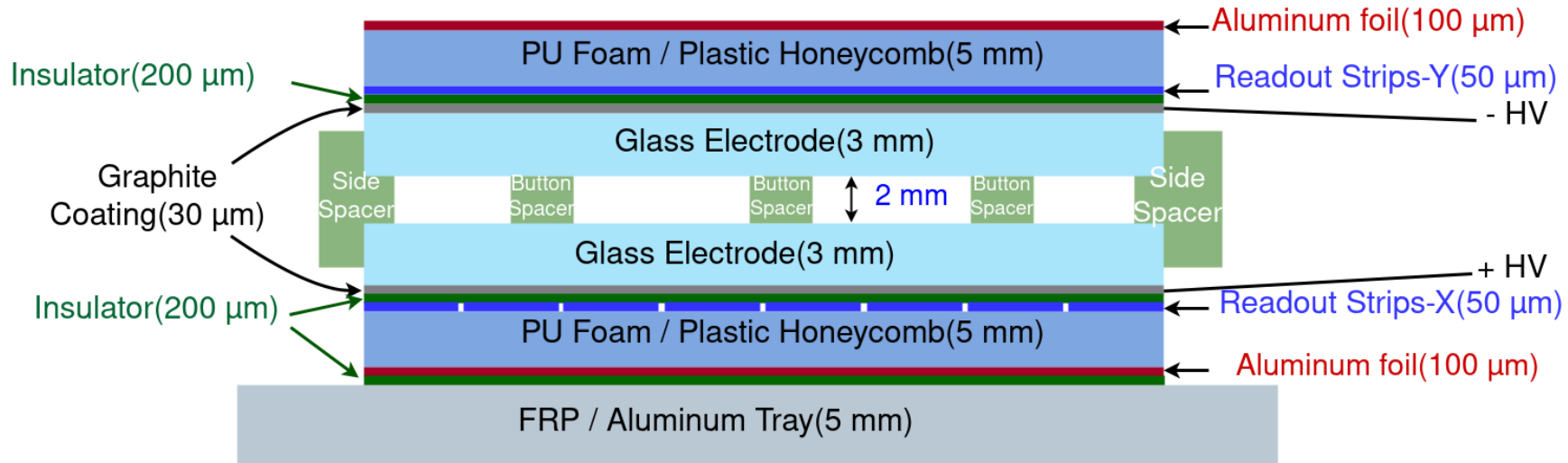
The magnetised ICAL detector will study neutrinos naturally produced in Earth's atmosphere.



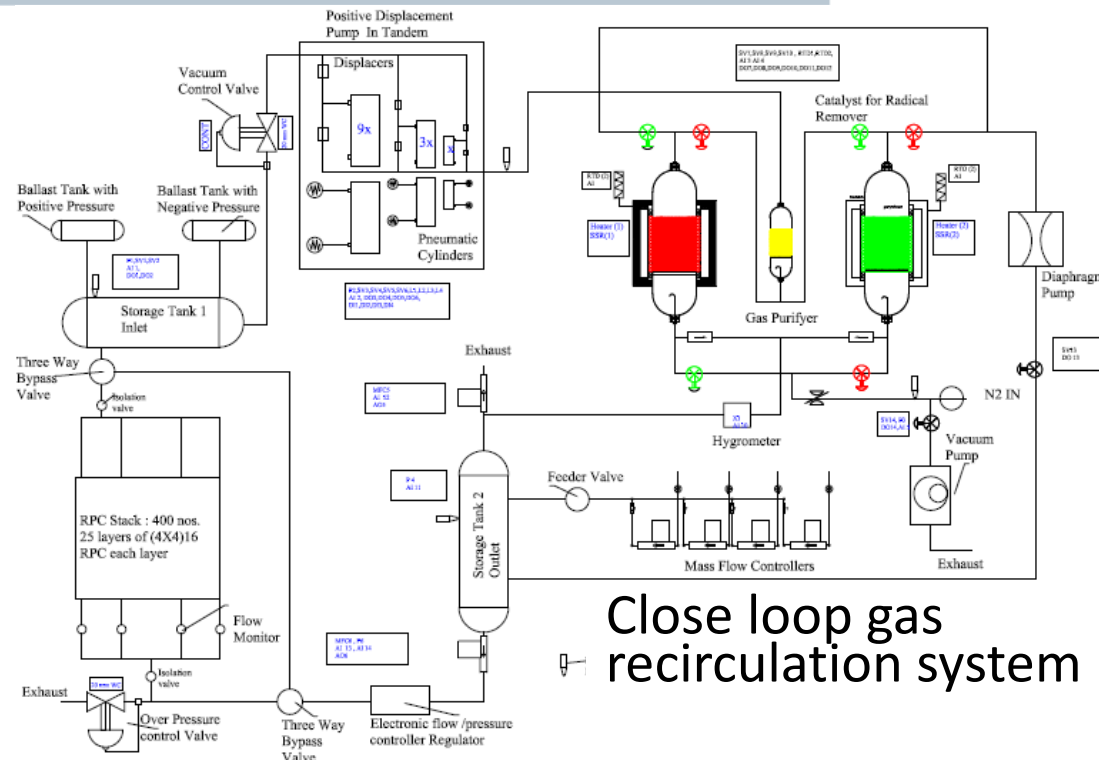
50Kton ICAL neutrino Detector



RPC R&D : The main detector component

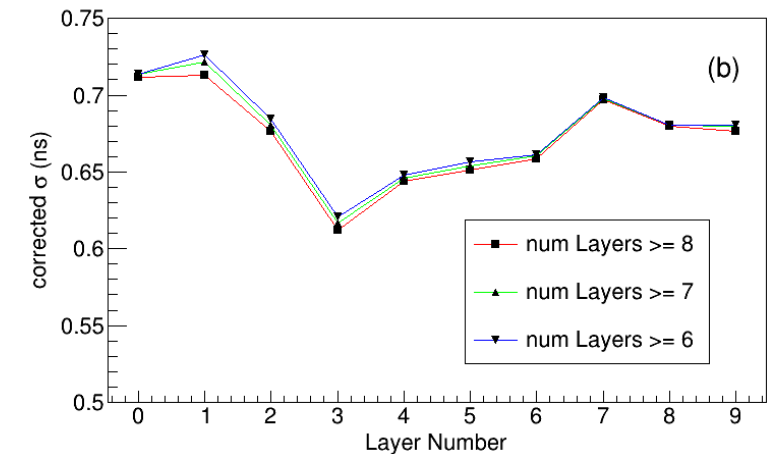
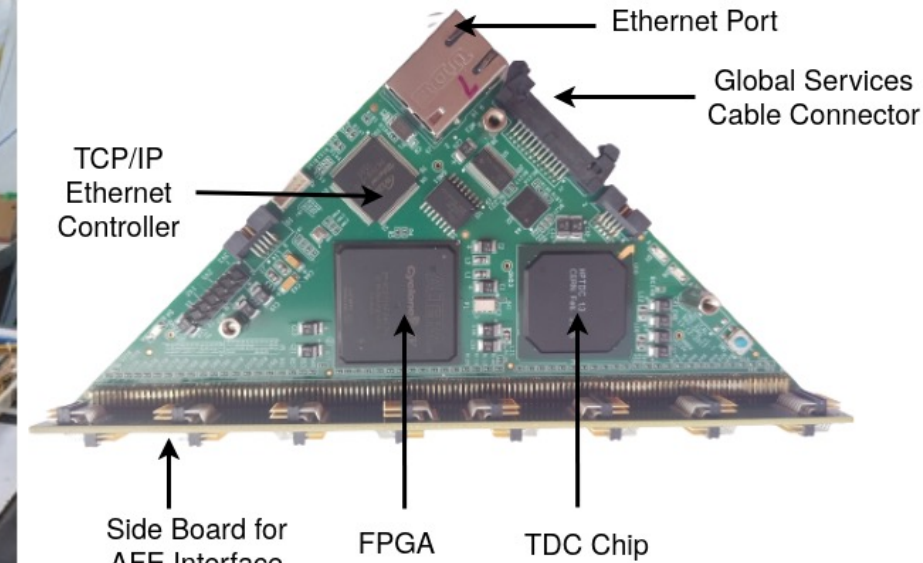
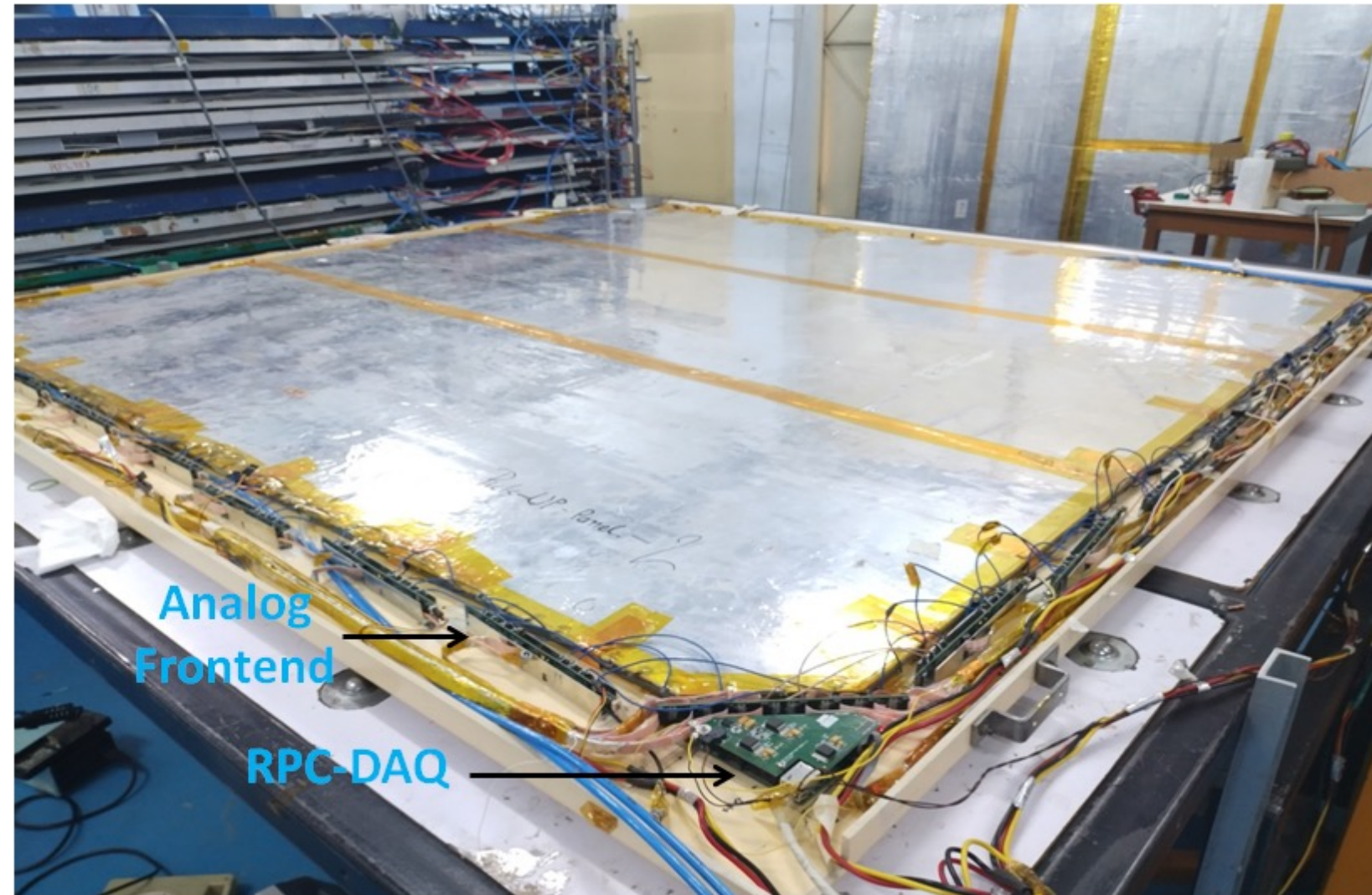


HV supply. Output voltage range is 0 to $\pm 6\text{KV}$ and upto $2\mu\text{A}$ current. Developed by BARC



Close loop gas recirculation system

Fully assembled glass-RPC module (2m x 2m) (TIFR)

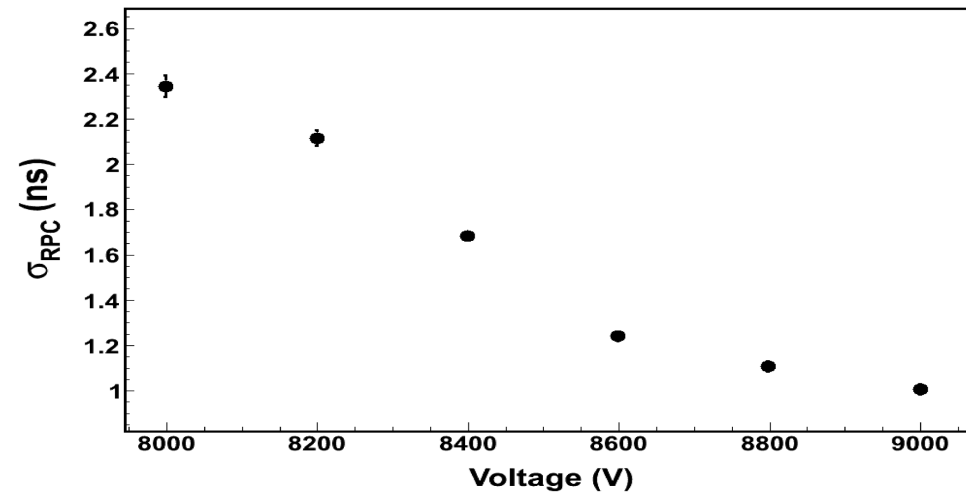
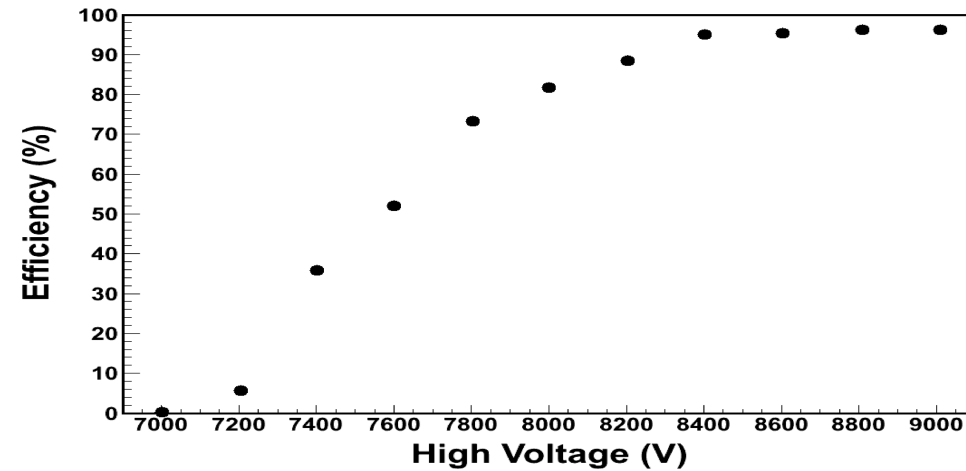


Oil-free large-size bakelite RPC (VECC)



Gas gap specifications:-

- Dimension – 245 cm X 125 cm X 0.2 cm.
- 4 gas inputs and 4 gas outputs



Real size bakelite-RPC for CBM-MuCh

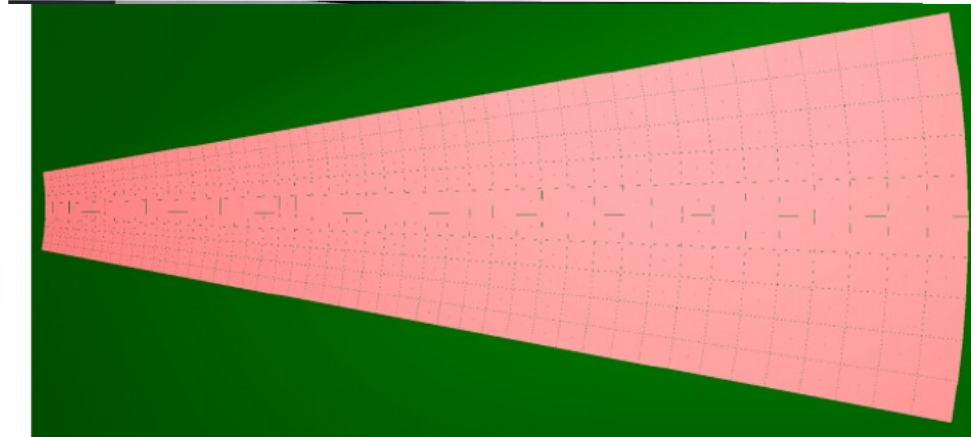


100.26 mm X 509.8 mm X 1179.21 mm

- Bulk resistivity of the electrodes of the RPC is $\sim(3 \times 10^9 - 1 \times 10^{10})\Omega \cdot \text{cm}$
- Each electrode thickness is **1.2 mm**
• (**down** by a factor of **1.7**).
- Gas gap is **2.0 mm** (for one chamber)
1.0 mm (for another chamber).

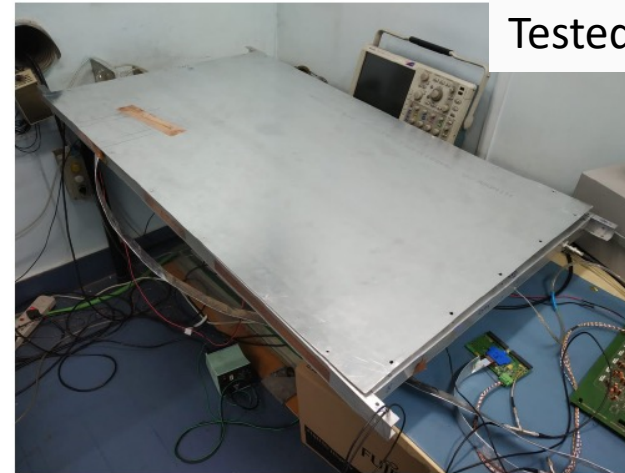
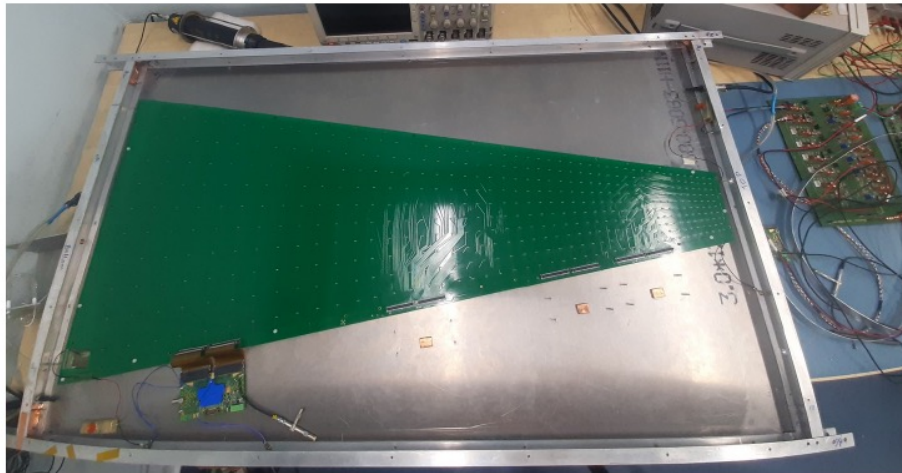
Test results of the Real size RPC with real size PCB

- Cosmic ray test has been done using the real Size PCB with gas mixture ratio,
R134a : iso-butane : SF₆ :: 95.2 : 4.5 : 0.3
- Progressive pads as pickup
Min Pad: 1.01 cm, Max. Pad: 5 cm
- Threshold : 6 fC



10.3 cm X 49.76 cm x 112 cm

Tested at GIF++ and at SIS18 using STS-MuCh XYTER board,
Tested upto 10 kHz/cm² at GIF++



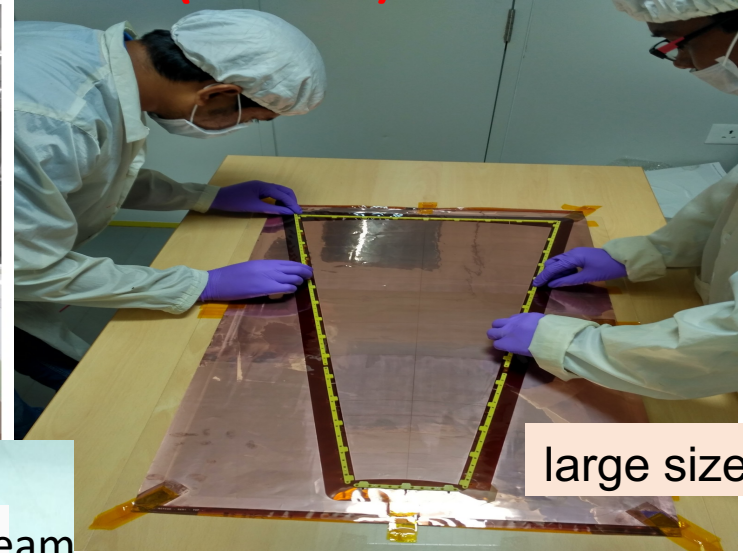
Real size detector with real size PCB inside the Al shielding box for testing at VECC

CBM-MuCh GEM Module Fabrication (VECC)

Dimension:
1 m length, 40 cm bigger width, 3-2-2-2
configuration

About 150 modules for two CBM-MuCh
station

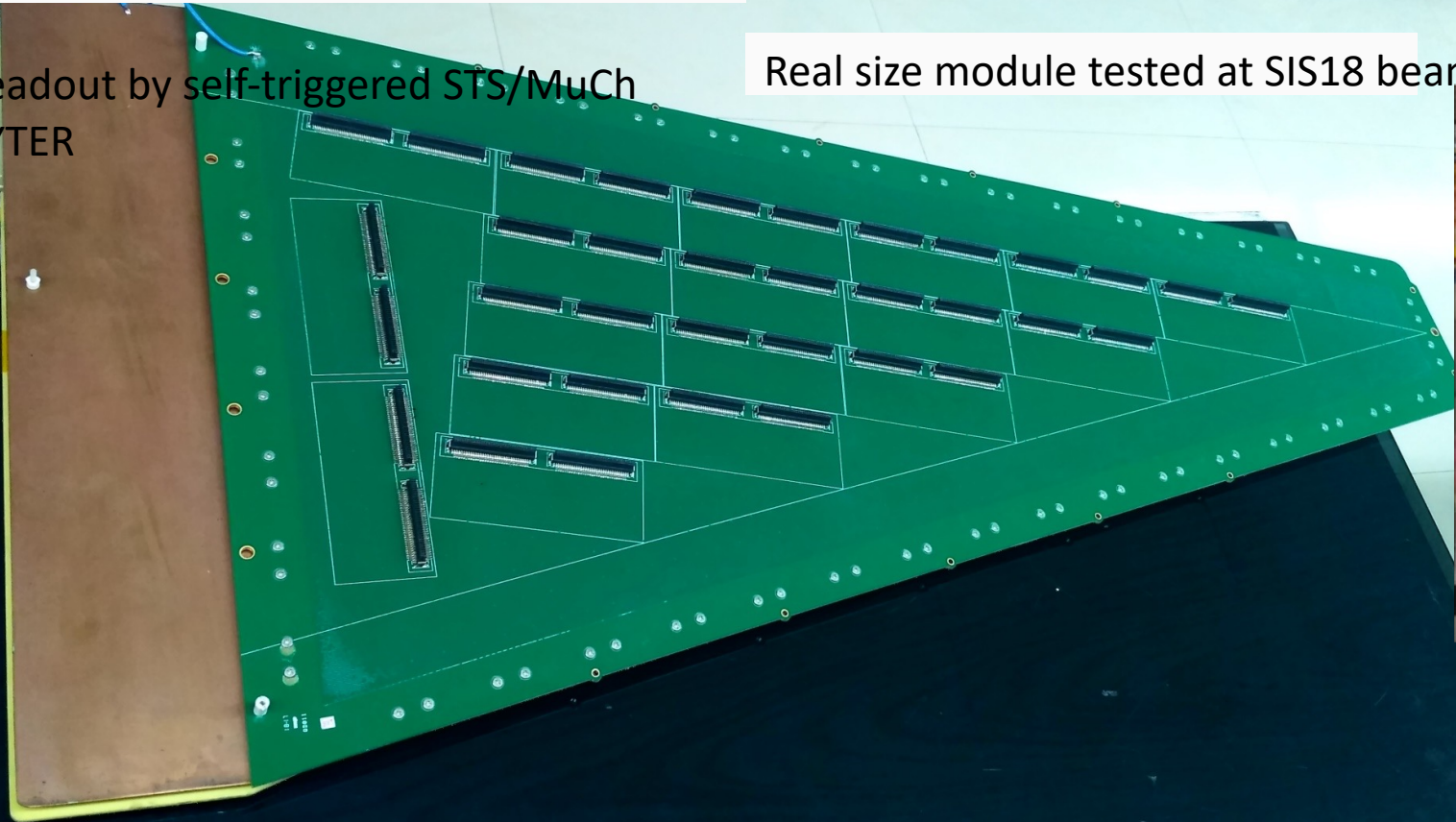
Handles upto $400\text{KHz}/\text{cm}^2$ (SIS100)



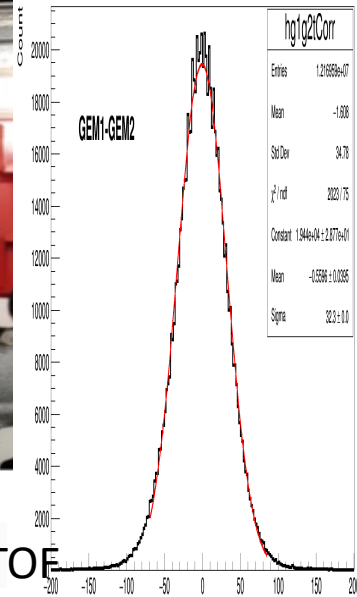
large size GEM foils

Readout by self-triggered STS/MuCh
XYTER

Real size module tested at SIS18 beam

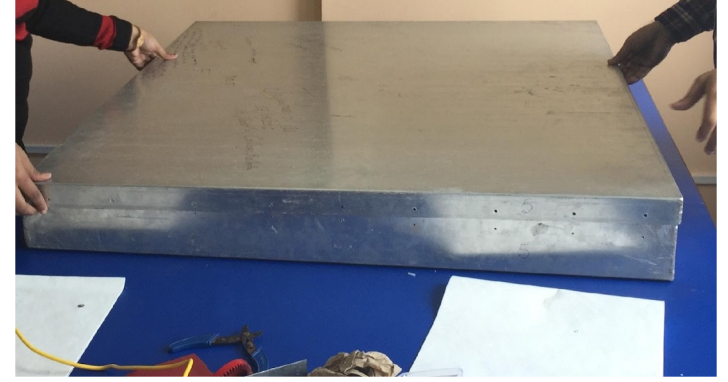
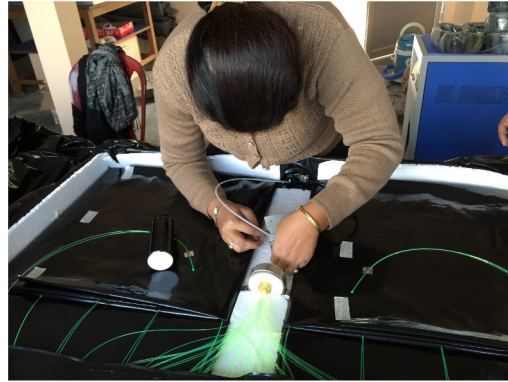


Time correlation with TOF



Samples of large scintillator detector activities

Assembly and testing of the scintillator detectors for cosmic ray shower at Darjeeling hills

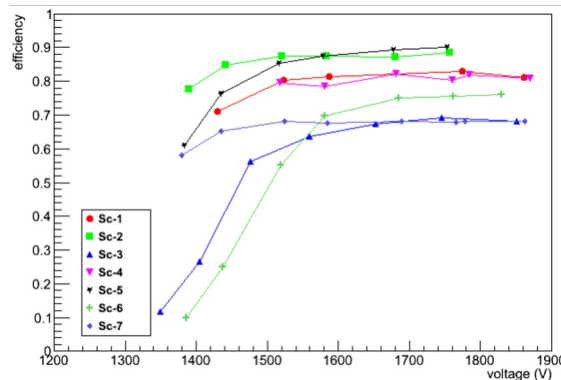


Phase I : Hexagonal array of 7 detectors (Including one at the centre)

- Dimension of each scintillator block: 0.5 m x 0.5 m; One detector consists of 4 such blocks
- 7 plastic scintillator detectors array is commissioned



Stack of Scintillator detectors



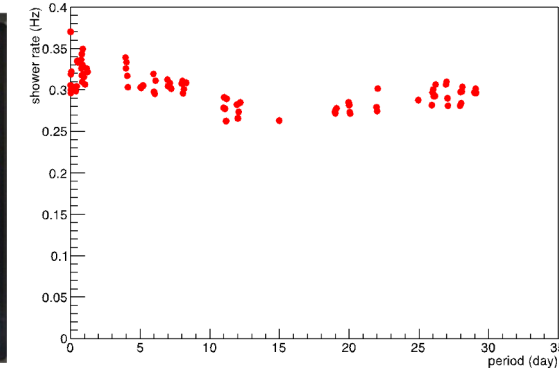
Efficiency as a function of applied voltage



Set-up with 3 detectors



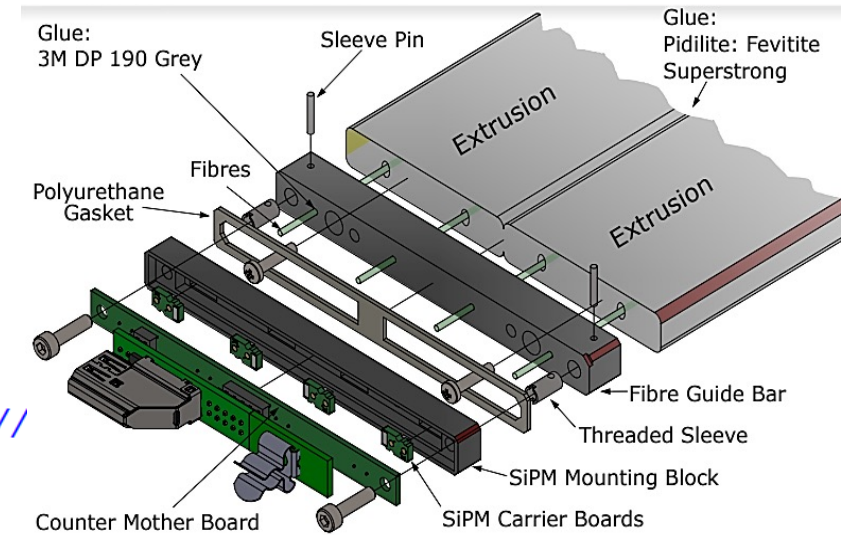
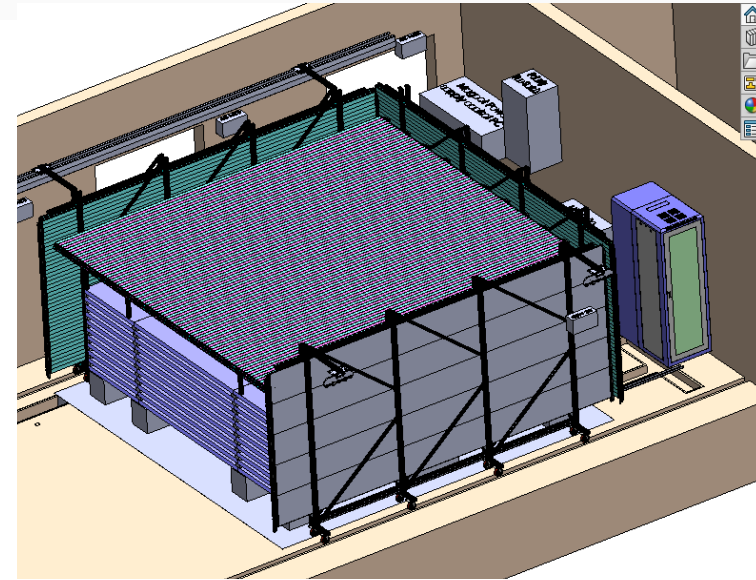
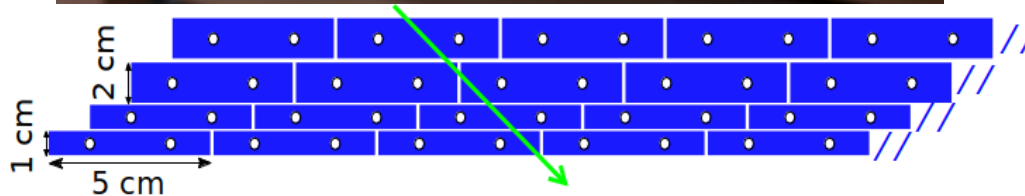
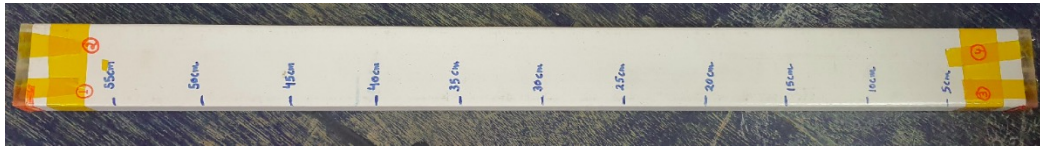
Coincidence signals



3F rate vs. time during mid November - mid December 2016

Scintillator with SiPM readout for Cosmic muon veto detector (CMVD) for INO-ICAL

- Cosmic muon veto detector requires
 - Total 712 extruded scintillator of size $\sim 5 \text{ m} \times 5 \text{ cm} \times 1(1.8) \text{ cm}$
 - Total 2848 SiPM readout

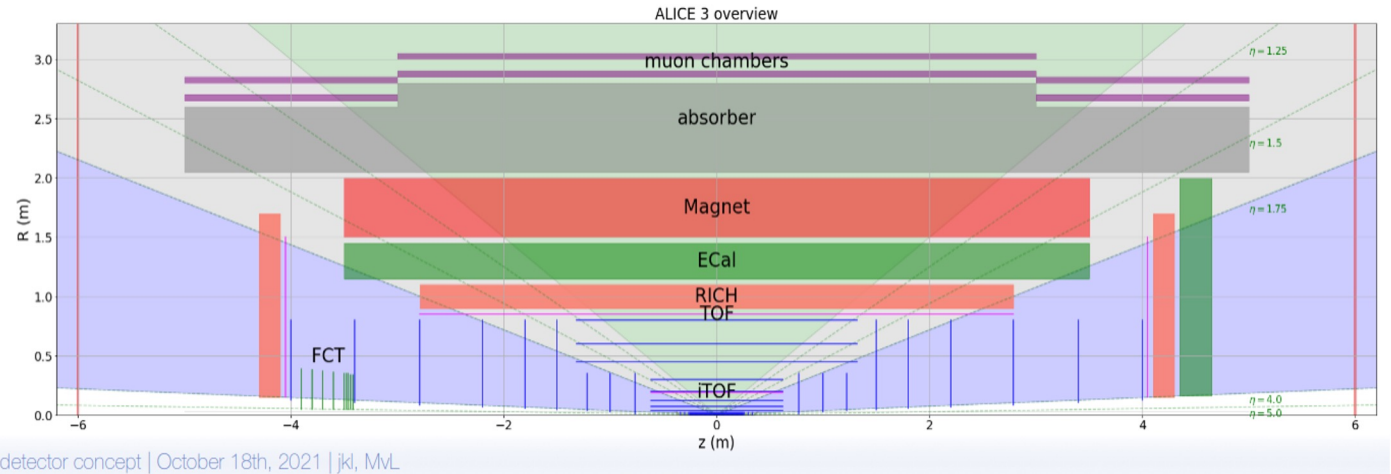


Interests in other detector areas:

- 1) Production of SiPM by Indian industry (good experience)
- 2) R&D (and if successful participation) in LGAD (extension of the Si-pad detector activities)

Time Of Flight (TOF)

- **TOF:** Inner (central barrel) and outer (forward disks)
- **Surface area:**
 - Inner (1.5 m^2),
 - Outer (30 m^2),
 - Forward (14 m^2),
 - Granularity ($1 \times 1 \text{ mm}^2$ to $5 \times 5 \text{ mm}^2$)
- **Large area system:**
not yet built on this scale: R&D is required!
- **Planned system:** Sensor bonded to ASIC (front-end and TDC), clock management and readout
- **Key requirements:**
 - time resolution ($\sim 20 \text{ ps}$),
 - low material budget ($1\text{-}3\%X_0$)

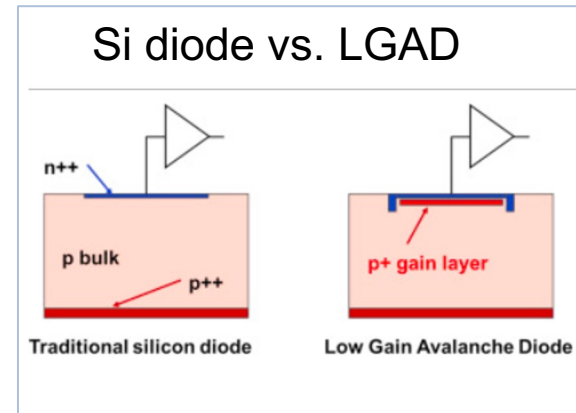


Three solutions are under consideration:

- 1) **Monolithic fully depleted CMOS sensor:**
favored due to integrated electronics, low cost (but R & D required to achieve ps time resolution)
- 2) **LGAD (meets $\sim 30 \text{ ps}$ time resolution):** system level development is needed to achieve 20 ps resolution (costly, needs ASICs for readout)
- 3) **SPADs or SiPM (also used in RICH with aerosols, common readout):**
(dark current, fill factor are issues of concern!)

Ideas for possible contribution – LGAD & SiPM

- Focal like pad design: Develop LGAD and SiPM in India
- LGAD - Modification in Si diode (planned for ALICE FOCAL)
 - Work with BEL Bangalore (6" wafer), and SCL Mohali (8" wafers, 180 nm process)
 - SiPM were successfully produced in India [Ref1] by SITAR*
- Simulations using
 - TCAD (Process and Geometry), MC (Garfield++ and Allpix²) on monolithic detectors with gain as LGAD
- LGADs require dedicated ASIC:
 - Either borrow or purchase such ASIC
 - Explore the possibilities to produce simple ASIC in Ind Si fab and perform electrical qualification studies in lat (with sources, lasers, cosmic rays) and teat beam



SiPM produced on 6" wafers at SITAR, India

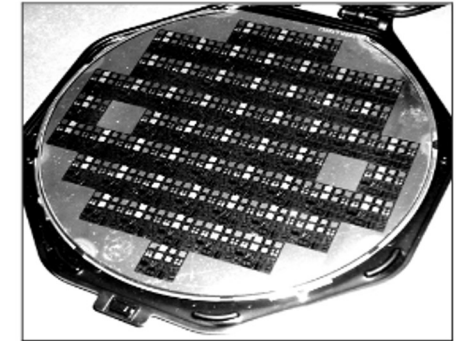
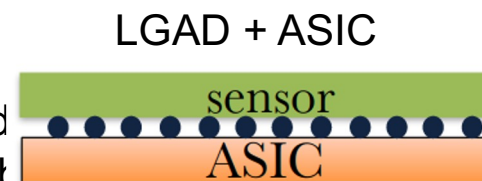
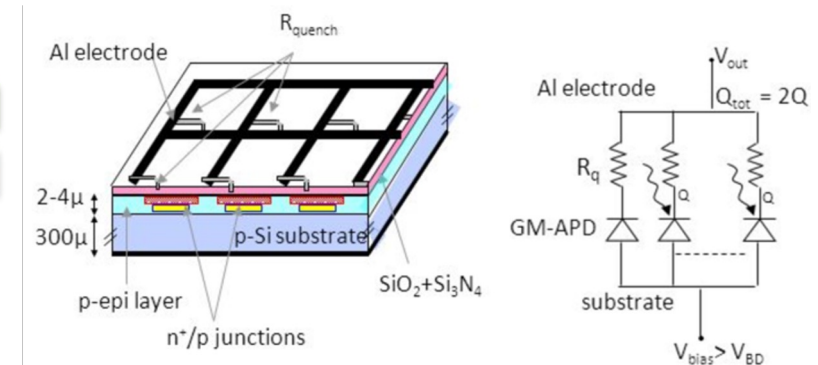


Fig. 1 Fabricated wafer showing SiPMs



SiPM schematic



Ref. Y. Musienko (Iouri.Musienko@cern.ch)

*Society For Integrated Circuit Technology And Applied Research (SITAR)

[Ref1] Anita Topkar et al., Development of SiPM in India using CMOS Technology, <https://inspirehep.net/files/2f05f40e82377fddbcaff41ae24635d1>

Possible contributions from India

- **Muon:**
 - Building of RPC using indigenous materials and delivery
- **TOF:**
 - Explore possibilities to design, fabricate and test LGADs and SiPMs in Indian foundries (India is active contributor in ALICE FOCAL E-PAD array project),
 - Participate in qualification studies of LGAD photosensors developed by collaboration and learn from them and improve our design

SiPM: In various detectors (e.g. EMCal..) by Indian industries



*Thank
you!*

Acknowledgement

- Mr. Sayak Chatterjee
- Mr. Arindam Sen
- Ms. Shreya Roy

1. The **BaBar** experiment uses a big system based on RPC detectors to discriminate muons from pions and to identify neutral hadrons.
2. We constructed glass RPC modules for detecting K_L and muon in BELLE experiment.
3. The **ATLAS** experiment at the large hadron collider LHC employs a trigger system consisting of a first-level hardware trigger (L1) and a software based high-level trigger. the L1 muon trigger system selects muon candidates, assigns them to the correct LHC bunch crossing and classifies them into one of six transverse-momentum threshold classes.
4. The Resistive Plate Chambers (RPCs) are used as **dedicated trigger detector** in the both barrel and endcap regions of the **CMS** experiment together with Drift Tubes and Cathode Strip Chambers. The redundancy of the muon system of CMS is used also to improve the muon identification and reconstruction efficiency.
5. In STAR experiment at RHIC and ALICE at LHC, RPCs are a part of time of flight (TOF) system
6. In **Belle** experiment, RPCs are used for muon identification
7. The **PHENIX** collaboration Resistive Plate Chambers (RPCs) are being installed in the two existing muon spectrometers to allow the muon trigger detector to tag high momentum muons from the decay of W bosons.
8. In **OPERA** the muon spectrometers are composed of a dipole iron magnet, precision drift tubes and resistive plate chambers, *used* as trigger and as tracker
9. The commissioning of the *RPC*-based muon detector in the **BESIII** *experiment* has been carried out.
10. The RPCs **Argo-YBJ** are known as low noise detector usually operated for triggering and tracking purposes.
11. The Resistive Plate Chamber (RPC) detector in the **HARP** experiment at the CERN Proton Synchrotron was designed for the separation of electrons from pions by time of flight.